Title
Transcriptional Mechanisms of Oligodendrocyte Development and Their Response to Hypoxia

Permalink
https://escholarship.org/uc/item/9bv18467

Author
Silbereis, John

Publication Date
2014

Peer reviewed|Thesis/dissertation

Transcriptional Mechanisms of Oligodendrocyte Development and
Their Response to Hypoxia

by

John Christian Silbereis

DISSERTATION

Submitted in partial satisfaction of the requirements for the degree of

DOCTOR OF PHILOSOPHY

in

Neuroscience

in the

GRADUATE DIVISION

of the

UNIVERSITY OF CALIFORNIA, SAN FRANCISCO

For my wife,

Chelsea

Acknowledgements

Portions of this work were reprinted from:

Silbereis et. al. (2014). Olig1 function is required to repress Dlx1/2 and interneuron production in mammalian brain. *Neuron.* 81(3): 574-587.

Silbereis et. al. (2014). Towards Improved models of neonatal white matter injury associated with cerebral palsy. *Disease Models and Mechanisms.* 3(11-12): 678-688.

Abstract

Oligodendrocytes are the myelinating cells of the central nervous system (CNS). By enabling rapid nerve conduction and in turn the dense packing of relatively small-bore axons into white matter tracts, myelination was essential for the evolution of the complex vertebrate brain. Permanent dysmyelination of the CNS is a central component of injuries that cause cerebral palsy and cognitive disabilities, as well as Multiple Sclerosis. The factors that instruct oligodendrocyte specification, proliferation, maturation and their ultimate matching to axonal partners is thus an essential question of both basic and clinical neuroscience.

My dissertation focuses on two distinct transcriptional mechanisms that respectively regulate: (1) the initial allocation oligodendrocytes from multipotent progenitors and (2) the onset of oligodendrocyte maturation and myelination.   I first demonstrate that the bHLH transcription factor *Olig1* is expressed in radial glia of the ventral telencephalon. *Olig1* promotes production of oligodendrocytes and represses production of GABAergic interneurons throughout the mouse brain. *Olig1* deletion in mutant mice results in ectopic expression and upregulation of *Dlx1/2* genes in the ventral medial ganglionic eminences and adjacent regions of the septum resulting in a ~30% increase in adult cortical interneuron numbers with corresponding diminution of oligodendrocyte lineage cells in the embryo and adult. I show that Olig1 directly represses the *Dlx1/2 I12b* intergenic enhancer and that *Dlx1/2* functions genetically downstream of *Olig1*. I find that *Olig1* is likewise responsible for neuron versus oligodendrocyte specification during repair phases of forebrain Hypoxic-ischemic encephalopathy. These findings build on previous studies that suggest there is common origin of oligodendrocytes and interneurons in the telencephalon. They further establish *Olig1* as an essential repressor of *Dlx1/2* and interneuron production in developing mammalian brain.

In a second set of studies, I have investigated roles for Hypoxia Inducible Factors (HIFs) in regulating oligodendrocyte ontogeny. Though, HIFs are largely dispensable for oligodendrocyte specification, they are essential regulators of postnatal oligodendrocyte

maturation. This work has also elucidated a surprising cell intrinsic role for oligodendrocytes in the coordination of myelination and white matter angiogenesis. Here I show that O_2 tension, mediated by OPC-encoded *Hypoxia-inducible factor (HIF)* function, is an essential regulator of postnatal myelination. Constitutive HIF1/2α stabilization resulted in OPC maturation arrest through autocrine activation of canonical *Wnt7a/7b*. Surprisingly, such OPCs also show paracrine activity that induces excessive postnatal white matter angiogenesis in vivo, and directly stimulates endothelial cell proliferation in vitro. Conversely, OPC-specific *HIF1/2α* loss-of-function leads to insufficient angiogenesis in corpus callosum and catastrophic axon loss. These findings establish that OPC-intrinsic HIF signaling is essential for postnatal white matter angiogenesis and for synchronizing vascularization with the onset of myelination in the mammalian brain. Taken together these studies reveal novel transcriptional mechanisms involved in broad aspects of oligodendrocyte ontogeny, which play overlapping roles in the pathophysiology of developmental white matter injury.

Table of Contents

Acknowledgements

Abstract

List of Figures

List of Tables

List of Figures

CHAPTER 4

CHAPTER 5

CHAPTER 6

List of Tables

Chapter 1:

General Introduction

Introduction

Oligodendrocytes are the myelinating cells of the central nervous system (CNS). Myelination enables rapid transmission of action potentials through saltatory conduction (Baumann and Pham-Dinh, 2001; Bradl and Lassmann, 2010), provides trophic support and protection for axons (Funfschilling et al., 2012; Morrison et al., 2013; Paz Soldan and Pirko, 2012; Saab et al., 2013), and allowed for packing of greater axon densities during the evolution of brain complexity (Freeman and Rowitch, 2013). Oligodendrocyte loss and dysfunction is observed in disorders of myelination such as multiple sclerosis and early developmental injuries to the brain white matter tracts leading to cerebral palsy.

Furthering our understanding of oligodendrocyte ontogeny will thus reveal potential therapeutic approaches to treat such disorders. In turn, deciphering the neuropathology that underlies white matter disorders and inhibits myelin regeneration may reveal essential developmental regulatory mechanisms for oligodendrocyte development.

Oligodendrocyte development and neonatal white matter injury

Newborn neurological injuries are the leading cause of intellectual and motor disabilities associated with cerebral palsy. Cerebral white matter injury is a common feature in hypoxic-ischemic encephalopathy (HIE), which affects full term infants, and in periventricular leukomalacia (PVL), which affects preterm infants. This article discusses recent efforts to model neonatal white matter injury using mammalian systems. We emphasize that a comprehensive understanding of oligodendrocyte development and physiology is crucial for obtaining new insights into the pathobiology of HIE and PVL as well as for the generation of more sophisticated and faithful animal models.

Neonatal white matter injury: the clinical problem. In 1861, William John Little reported on a series of 68 cases of difficult birth, which he related to later developments of neurological

deficits, such as spastic diparesis (a movement disorder that primarily affects the lower limbs). This condition, originally known as Little's disease, became generally known as Spasticity or Cerebral Palsy (CP) (Little, 1861). CP denotes a condition of the brain reflected by movement limitation that is often associated with some degree of cognitive impairment. It is generally considered a fixed, non-progressive condition resulting from neurological injury in antenatal or perinatal period (http://www.ninds.nih.gov/disorders/cerebral_palsy/cerebral_palsy.htm). It is now known that in utero hypoxic-ischemic (HI) events (e.g. placental insufficiency, chronic fetal-to-maternal hemorrhage, stroke, infection and inflammation), perinatal events (e.g. placental abruption, respiratory failure) and neonatal disorders (e.g. chronic lung disease) are associated with acquired brain injuries that lead to CP. In recent years, damage to the cerebral white matter has emerged as an increasingly common cause of CP.

Rates of CP in the United States are increasing. In the 1960's, approximately 2.2/1000 live births resulted in CP. With the advent of advanced resuscitation techniques practiced by neonatologists, rates were reduced to 1.3/1000 in the late 1970's and early1980s. More recently, however, rates of CP in the United States are currently >3/1000 births (http://www.cdc.gov/ncbddd/dd/cp3.htm#common), owing to the increasing survival of extremely low birth weight (ELBW) premature infants born at gestational ages <28 weeks, who are at higher risk for cognitive and motor disabilities. Related to this is the notion infants born prematurely are subject to inflammatory conditions that predispose to brain injury (Hagberg and Mallard, 2005).

Common forms of neonatal brain injuries associated with later development of CP. Figure 1 shows associated precursor lesions of CP in full term and preterm infants. Full-term infants (Fig. 1A) can suffer from global hypoxic-ischemic encephalopathy (HIE), resulting in both damage to neuronal populations, such as those in the basal ganglia and cortex, as well as significant cellular necrosis and axonal damage in cerebral white matter injury (WMI). Neonatal stroke

causes HI in focal areas of the brain. (Nelson and Lynch, 2004). Other types of brain injury related to HI or maternal-fetal infection are more common in ELBW infants. Figure 1B shows intraventricular hemorrhage, which is thought to result from rupture of fragile blood vessels in the germinal matrix (also known as the ventricular zone) with resultant hemorrhage into the ventricles, which sometimes extends into the brain parenchyma. We define WMI as a spectrum of pathology that includes (1) the classic lesion of Periventricular leukomalacia (PVL): macroscopic cystic or microscopic non-cystic necrotic lesions with pan-cellular degeneration, and (2) focal and diffuse non-cystic lesions that selectively triggers oligodendrocyte lineage degeneration and later disturbances in myelination (Khwaja and Volpe, 2008). Neuronal loss and axonal damage are often observed in patients with PVL, which can reflect primary injury or arise as a secondary response to WMI (Volpe, 2009). However, evidence is lacking for prominent neuronal loss or axonal degeneration in the non-cystic lesions that predominate in most patients.

WMI as a common component of full term and preterm neonatal brain injuries: implications for oligodendrocyte ontogeny. The development of therapies to prevent neonatal WMI leading to CP, and that promote regeneration and repair, is hindered by a poor understanding of underlying cellular, molecular and genetic mechanisms. For instance, what is the role of inflammatory mediators in enhancing or reducing the risk of injury? Is the risk of injury incremental or non-linear with recurrent insults? Is there a critical window after which normal myelination of injured white matter is not possible due to degeneration or irreversible alterations in oligodendrocyte (OL) lineage cells or axons? Answering these questions requires a more comprehensive understanding of the pathways (both cell intrinsic and extrinsic) that regulate the responses of the oligodendrocyte lineage during the initial and progressive phases of injury and myelination failure. Thus to comprehensively assess effects of WMI on OLs in the neonatal humwan central nervous system (CNS), it is necessary to understand their development.

Conversely, the molecular and cellular pathology of white matter injuries may provide insights into the basic developmental biology of OLs as well. For instance does the high sensitivity of developing oligodendrocytes to hypoxia reflect an essential regulatory role for metabolic processes and O_2 levels in OL development? Do the molecular changes in axons and OLs provide insights into key interactions between neurons and OLs? What are the key inhibitors of myelination in the lesion environment and do they also regulate oligodendrocyte maturation and developmental myelination? Further neuropathological studies and data generated from animal models of neonatal WMI will not only advance our understanding of disorders associated with oligodendrocytes, but also provide important insights into their development and physiology (Johnston et al., 2005).

Oligodendrocyte Specification

In the last decade, a greater understanding of the developmental regulation and ontogeny of the OL lineage in vivo was obtained through the discovery of genes necessary for OL development, such as *Olig1* and *Olig2*, which encode bHLH transcription factors. As shown in Figure 3, OL development can be characterized according to four distinct stages of maturation with unique gene expression profiles. First, neural stem cells (NSCs) give rise to oligodendrocyte precursor cells (OPCs) during embryonic development (beginning E11.5 in mice and gestational age 13 weeks in humans). OPCs proliferate and migrate throughout the brain before differentiating into late oligodendrocyte progenitors (preOLs) (beginning around E16.5 in mice and gestational age 20 weeks in humans), which undergo extensive cellular growth and process elaboration and mature into myelinating OLs (Jakovcevski and Zecevic, 2005; Kessaris et al., 2006) (Jakovcevski et al., 2009; Rowitch, 2004).

Common developmental origins of Oligodendrocytes and neurons. The developmental expansion of the OL population can be further parsed into two distinct stages. Firstly, OLs are

specified from multipotential progenitor cells in developmental niches that produce both neurons

and OLs. Secondly, committed oligodendrocyte precursors, identified by expression of *platelet*

derived growth factor receptor alpha (*PDGFR*) and the proteoglycan NG2 proliferate in order to

sufficiently expand and maintain the OL population. Production of OLs is thus complex,

involving: (1) patterning of spatially discrete progenitor pools for OPC specification, (2) temporal

regulation of multiphase neurogenesis versus gliogenesis (3) mechanisms of neuron versus

oligodendroglial cell fate acquisition from common progenitors and (4) the decision to remain in

a proliferative OPC state or to mature and myelinate axons (Butt et al., 2005; Kessaris et al.,

2006; Marin, 2012; Wonders et al., 2008).   Once an OL enters the myelination phase of

development, it irreversibly loses its mitotic capacity and undergoes robust metamorphic

changes to produce myelin sheaths for multiple axons (Skoff et al., 1994)

All neurons and macroglia are derived from neuroepethilial progenitors that line the

ventricles of the developing cerebrum and spinal cord. Neurogenesis commences before

gliogenesis beginning in caudal regions around E9 and progressing rostrally to the forebrain

though E11 in mice. As stated, OL specification begins at E11 in spinal cord and E13 in the

forebrain. Astrocyte specification commences after the cessation of neurogenesis in the late

fetal period (Freeman and Rowitch, 2013; Rowitch and Kriegstein, 2010; Silbereis et al., 2010).

Patterning mechanisms controlling OL Specification. Distinct neural subtypes are determined

early in development by segmentation of the neuroepithelium into domains that produce distinct

types of neurons (e.g. the P1, P2, P3, and pMN domains of spinal cord); a process termed

neural patterning. Such domains are defined by the spatially discrete expression of patterning

genes regulated by the relative expression of signaling molecules secreted from dorsal-ventral

and rostral-caudal organizing centers. For instance, spinal cord patterning is established by

spatial gradients of Sonic Hedgehog (Shh) secreted ventrally from the floor plate and Bone

Morpgogenic Protein (BMP) secreted dorsally from the roof plate (Briscoe et al., 1999; Liem et al., 1997; Roelink et al., 1995; Rowitch, 2004).

Numerous studies indicate that OLs are similarly produced from spatially distinct progenitor domains. Unlike most neuronal subtypes, however, the regions that derive OPCs change over the course of neural development. For instance, *Shh* dependent expression of the bHLH gene *Olig2* is essential for the establishment of the spinal cord pMN domain, which is required to produce primary motor neurons and majority of spinal cord OLs (Lu et al., 2002; Zhou and Anderson, 2002). At E15, an *Shh* independent domain for OL specification emerges in the dorsal spinal cord following downregulation of BMP expression, a potent inhibitor of OL specification, and upregulation of proOL Fibroblast growth factor (fgf) signaling (Fogarty et al., 2005). In the forebrain (Figure 3), OL production follows a similar ventral to dorsal sequence, where production originates at E12.5 in the ventral regions of the Preoptic area (POA) and medial ganglionic eminences (MGE), then more dorsally in the Lateral Ganglionic Eminences (LGE) by E16, and then in the pallium by P0 (Kessaris et al., 2006).

Neuron versus OL specification from multipotent progenitors. Intriguingly embryonically derived oligodendrogenesis coincides with the latter stages of neurogenesis in the mammalian brain. For example, Cortical inhibitory neurons are produced from E10 to E17 in the medial ganglionic eminence (MGE), and preoptic areas (POA) of the ventral telencephalon; from where they migrate tangentially into the cerebral cortex (Anderson et al., 1997; Corbin et al., 2001; Miyoshi et al., 2007; Wonders and Anderson, 2006). Whereas the adjacent regions of the lateral ganglionic eminence and the telencephalic septum generate neurons of the ventral forebrain and olfactory bulb (He et al., 2001; Kessaris et al., 2006; Petryniak et al., 2007; Rubin et al., 2010).

Though studies elucidating the mechanisms that control OL versus IN fate are few, several key gene regulatory and upstream signaling factors have been identified. At the

transcriptional level, the homoedomain protein *Dlx1/2*, which is necessary for the establishment of IN cell production in the forebrain (Anderson et al., 1997), is required in the MGE and AEP to control the neuron-glial switch by promoting neurogenesis at the expense of OLs through repression of *Olig2* (Petryniak et al., 2007). *Gsx2*, another homeodomain transcription factor, similarly represses OL specification and promotes IN production in the LGE (Chapman et al., 2013).

Several cell-signaling pathways have also been implicated in OL versus IN cell fate decisions. BMP signaling is a well established as a potent inhibitor of OL specification that is also involved in the context dependent promotion of neuron or astrocyte cell fate (Gomes et al., 2003; Le Dreau et al., 2012; Mekki-Dauriac et al., 2002; Samanta et al., 2007; Samanta and Kessler, 2004). In the telencephalon, WNT signaling inhibits OL specification to promote neuronal fate via the RYK receptor (Langseth et al., 2010; Zhong et al., 2011). In contrast transcription factors and signaling pathways that promote OL cell fate and inhibit neurogenesis have not been described. Following specification OLs migrate extensively throughout the brain, where they proliferate locally in response to growth factors including PDGF, IGF and FGF (Fruttiger et al., 1999; Jiang et al., 2001; Naruse et al., 2006; Pringle et al., 1989). A pool of proliferative OPCs persists throughout life, participating in normal myelin turnover and repair following demyelinating injury.

Oligodendrocyte Maturation and Myelination

Myelination is a protracted developmental process beginning in rostral brain regions during late in gestation in humans and rodents, peaks during infancy, and extends into adolescence (Silbereis et al., 2010). As detailed in Figure 2, oligodendrocyte development is characterized by a robust metamorphic as cells undergo a transition from small proliferative OPCs to highly branched mature OLs myelinating as many dozens of myelin segments (Rosenberg et al., 2008). First neural stem cells generate highly proliferative and migratory OPCs, which give rise to

stationary multipolar cells expressing the O4 antigen called pre-oligodendrocytes (preOLs). PreOLs advance to the immature oligodendrocyte (OL) stage, identified by expression of molecules for myelin membrane such as CNPase and Galactoctosylceramidase (GalC). Subsequently, mature OLs are identified the presence of myelinated axons and expression of Myelin Basic Protein (MBP), Proteolipid protein (Plp) and others (Rowitch et al., 2002; Woodruff et al., 2001).

Cell intrinsic regulation of myelination. Initiation of myelination in individual cells is a complex proess that involves intrinsic cell autonomous cues, axon oligodendrocyte communication, and regulation by the cellular microenvironment. At the transcriptional level, downregulation of promitotic factors and the onset of expression of several transcription factors, including *Myelin Regulatory Factor* (*MyRF*), *Olig1*, and *Yin Yang 1* (*YY1*) to drive expression of myelin associated genes initiates OL maturation (Emery et al., 2009; He et al., 2007; Li et al., 2007). Chromatin remodeling over development also represents an important regulatory mechanism. For instance *HDAC1* and *HDAC2* are required to silence the expression of genes in the WNT signaling pathway (Wu et al., 2012; Ye et al., 2009). MicroRNAs are important to promote OL maturation. Most notably *Dicer* expression rises as OLs mature. *Dicer* knockouts exhibit normal OPC specification and proliferation, but later develop a robust dysmyelination phenotype (Shin et al., 2009).

Extrinsic signaling pathways regulating myelination. An important positive trigger of postnatal myelination is thought to be activity-dependent neuronal signaling. It is important to link myelination with neuronal signaling mechanisms, because myelin constrains axon outgrowth and synaptogenesis (Chong et al., 2012; Gyllensten and Malmfors, 1963; Hu and Strittmatter, 2004; Tauber et al., 1980). In this manner, maturing axons are able to coordinate the onset of myelination according the dynamics of their own maturation. Additional mechanisms of Axon-OL

interactions play important roles in myelination (Laursen and Ffrench-Constant, 2007). For instance, Notch mediated communication between axons and OLs can both inhibit and activate myelination depending on the Notch ligands present and differential activation of downstream signaling cascades (Hu et al., 2003; Wang et al., 1998). Lingo-1 and PSA-NCAM are molecules expressed on the extracellular membrane that act as inhibitors of myelination (Charles et al., 2000; Mi et al., 2005). In contrast, axonal expression of neurogulins promotes myelination (Kim et al., 2003; Michailov et al., 2004).

Numerous signaling pathways driven by extracellular ligands and secreted molecules are essential for OL development. Activated canonical WNT signaling is a potent inhibitor of OL differentiation. Through this mechanism WNT acts as a key timer of developmental myelination, which also inhibits remyelination after injury and in MS (Fancy et al., 2009; Fancy et al., 2011). The orphan G protein–coupled receptor (GPCR) *GPCR17* is expressed transiently in immature oligodendrocytes. G*PCR17* knockouts exhibit precocious maturation, while extopic expression of *GPCR17* inhibits maturation. Thus, *GPCR17,* and presumably downstream Adenyl Cyclase / cAMP activity, represents a potent inhibitor of OL maturation, though the ligands responsible and the essential intracellular targets have not been determined (Chen et al., 2009b). Activation of the Akt-mTOR pathways promotes myelination, as evidenced by exuberant myelination in *PTEN* knockout mice (Harrington et al., 2010).

Physical properties of axons and the microenvironment are also important regulators of myelination. Increasing cellular and axonal density promotes myelination. Similarly, larger axon diameters are more frequently myelinated and possess thicker myelin sheaths than do small diameter axons (Lee et al., 2012a; Rosenberg et al., 2008). As discussed below, recent studies further suggest that the cellular nutrient supply and the metabolic microenvironment is also an essential regulator of myelination.

Myelination and brain metabolism: implications for hypoxic brain injury

Developing oligodendrocyte precursor cells (OPCs) undergo as much as a 6500-fold increase in membrane surface area to provide tens, if not hundreds, of myelin segments to multiple axons through extension of protoplasmic processes (Baron and Hoekstra, 2010; Chong et al., 2012; Webster, 1971). This metamorphic change accounts for the extraordinary metabolic demands associated with production of myelin protein and lipids (Chrast et al., 2011; Harris and Attwell, 2012; Nave, 2010). Moreover, mature oligodendrocytes also provide ongoing axonotrophic support in part through functions of the MCT1 transporter (Harris and Attwell, 2013; Lee et al., 2012b). Finally, initiation of myelination and myelin maintenance is regulated by the availability of glycolytic and lipid substrates such as purines, glucose and lactate (Funfschilling et al., 2012; Rinholm et al., 2011). These findings together imply that oligodendrocytes and OPCs require access to a rich vascular supply for nutritive and oxidative substrates. However, oligodendrocytes are not known to regulate angiogenesis and the molecular mechanisms that might synchronize the timing of myelination to adequate blood supply during postnatal brain development are unknown.

Both acute Hypoxia –Ischemic (HI) injury and chronic hypoxic insults have a substantial impact on OL development. Rodents subject to HI during the first 10 postnatal days of life have been reported to show widespread loss of preOLs, maturation blockade, and hypomyelination (Fogal et al., 2010; Ment et al., 1998; Riddle et al., 2006; Segovia et al., 2008). Studies indicate that chronic hypoxic rearing leads to hypomeylination, ventriculomegaly and hypoplasia of the gray and white matter of the forebrain without deficits in the total OL population (Billiards et al., 2008; Ment et al., 1998; Segovia et al., 2008). Taken together these data suggest that hypoxia has profound effects on OL development and survival.

Hypoxia Inducible Factors

Regulation of Hypoxia Inducible Factors. Hypoxia-Inducible Factors (HIFs) are the principal transcriptional mediators of the cellular response to hypoxia and regulate the expression of

genes that control survival, metabolism and angiogenesis (Dunwoodie, 2009; Majmundar et al., 2010; Semenza, 2012). HIFs are heterodimeric proteins comprised of an oxygen-sensitive subunit, HIF1α or HIF2α, and a constitutive subunit, HIF1β or HIF2β (also known as ARNT1/2) (Hirose et al., 1996; Wang et al., 1995). In normoxic conditions, HIF1/2α are hydroxylated by the enzyme prolyl hydroxylase (PHD1-3), and then targeted by von Hippel Lindau (VHL) protein for proteosomal degradation (Ivan et al., 2001; Jaakkola et al., 2001; Kaelin and Ratcliffe, 2008). Conversely, during hypoxia, stabilized HIF1/2α proteins can bind HIF1β and translocate to the nucleus where they bind *cis*-acting motifs called hypoxia response elements (HREs) to induce transcription of HIF targets genes such as *Vascular endothelial growth factor (VEGF)*, *Erythropoietin (EPO)* and members of the Wnt/β-catenin signaling pathway (Beck et al., 1991; Beck et al., 1993; Forsythe et al., 1996; Liu et al., 1995; Mazumdar et al., 2010; Patel and Simon, 2008).

HIFs in neural development. HIFs regulate development in a number of organ systems by: 1.) Sensing naturally occurring oxygen gradients that operate as patterning centers, 2.) Coupling organ development to vascularization, 3.) Regulating developmental cell death, and 4.) Initiating transcription of growth factors such as *VEGF* (Dunwoodie, 2009). Although *HIF* knockouts exhibit potent neural defects, little is known of the function of *HIF* in neural development. *HIF1α* knockouts, which are embryonic lethal, exhibit failure of neural tube closure and defects in brain vascularization (Iyer et al., 1998; Maltepe et al., 1997; Scortegagna et al., 2003). Brain specific *HIF1α* knockouts derived using a neural stem cell specific *Nestin-cre* line are viable, but exhibit increased apoptosis of neural cells, a greater than thirty percent decrease in neural cell number, and severe hydrocephalus (Tomita et al., 2003). Less still is known of the specific role of *HIF2α,* though recent ChIP/Chip studies in neural tissue suggest there transcriptional targets may be largely redundant in the brain (Xia et al., 2009). The neural phenotype of the double knockouts

is yet to be explored. Both proteins are widely expressed under normoxic conditions until at least P7, further suggesting that they may play a role in brain development (Trollmann and Gassmann, 2009). Finally, though HIFs are known to be essential to vasculogensis and angiogenesis in multiple organ systems, roles for cell instrinisc HIF signaling in CNS and angiogenesis and blood brain barrier development are unknown.

How does hypoxia impact neural development?

The work presented here seeks to answer two general questions: (1) How does hypoxia affect important regulatory mechansims in OL development, and, conversely, (2) Are hypoxia and HIFs themselves important developmental regulators of OL development and physiology. To explore the former question, I have studied roles for the transcription factor Olig1, a transcription factor required for repair after demyelination the adult brain, in regulating neuron versus OL fate specification in development and after hypoxic brain injury. To explore the latter, I have explored the roles of HIF signaling OL development, myelination and postnatal white matter angiogenesis.

Figure 1. Common types of injury associated with development of CP in ELBW and term infants. (A, B). Illustration of brain injuries commonly affecting ELBW infants. Panel A shows key characteristics of intraventricular hemorrhage, which results from terminal matrix hemorrhage into the ventricles, sometimes extending into the brain parenchyma. Additionally, there is a high incidence of WMI called periventricular leukomalacia (PVL), which can result in a cystic necrosis of white matter tracts and/or diffuse gliosis. Panel B shows long-term sequelae of brain injury in ELBW infants, including hypomyelination resulting from failure in lesion repair, as well as ventriculomegaly, which represents an ex-vacuo change resulting from significant loss of brain parenchyma. (C, D) Common brain injuries in full term infants include: neonatal stroke in which a focal region of cortex is affected (C) HIE results in global HI injury to the brain to neurons of the cortical plate and basal ganglia, as well as white matter tracts.
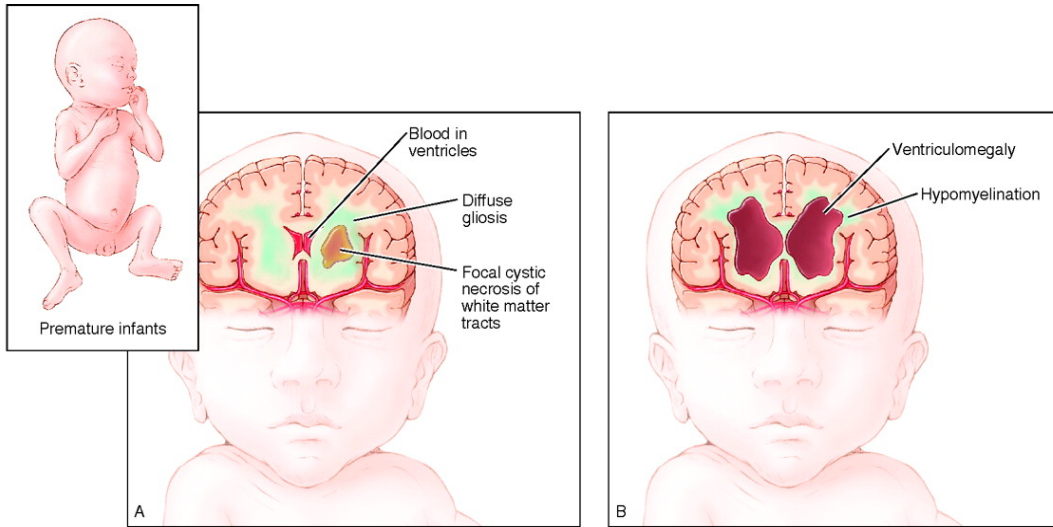
Cerebral palsy and periventricular leukomalacia

Premature infants

A
- Blood in ventricles
- Diffuse gliosis
- Focal cystic necrosis of white matter tracts

B
- Ventriculomegaly
- Hypomyelination

Full-term newborns

Neonatal stroke

C
- Penumbra
- Focal ischema
- Occluded vessels
- Thrombus

Hypoxic ischemic encephalopathy
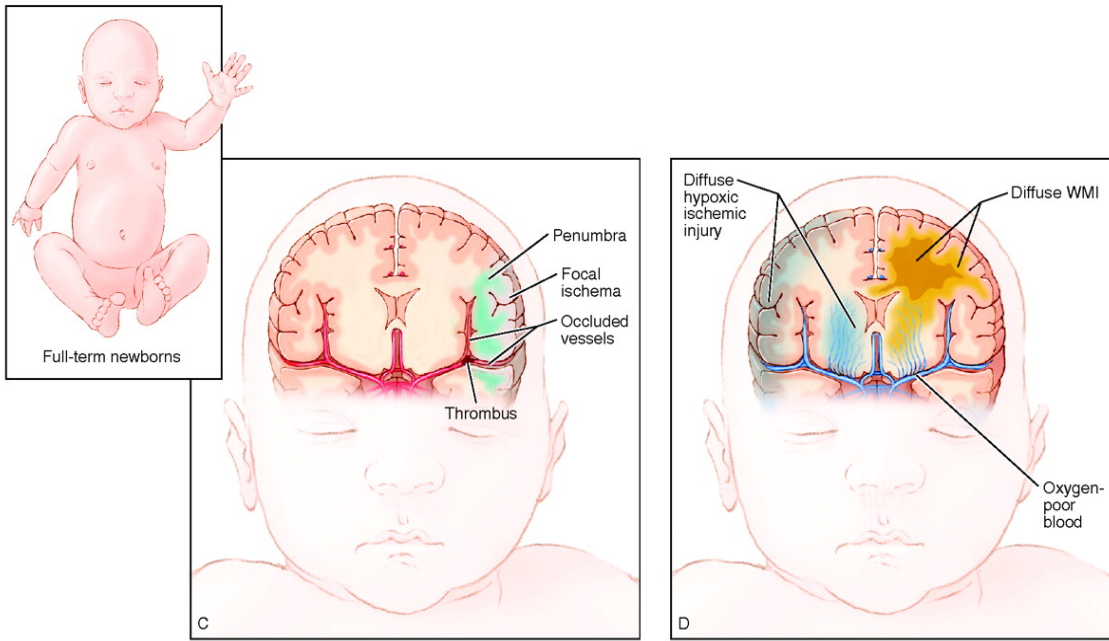
D
- Diffuse hypoxic ischemic injury
- Diffuse WMI
- Oxygen-poor blood

Figure 2. Stages and markers of oligodendrocyte lineage specification and maturation.

The schematic shows oligodendrocyte lineage progression from OPCs to premyelinating oligodendrocytes (preOLs) and then to myelinating oligodendrocytes. In the past decade, various markers have been identified that show lineage- and stage-specific expression (indicated by colored gradients). The markers PDGFRa, Olig2, Nkx2.2, Sox10, NG2 and Olig1 (nuclear) are characteristic of oligodendrocytes precursors (indicated in beige). O4 and O1 (also known as galactocebroside (GalC)) mark intermediate premyelinating oligodendrocytes (indicated in red), whereas APC (also known as CC1), MBP, PLP and Olig1 (cytoplasmic) are typical of mature myelinating oligodendrocytes (indicated in blue). Several laboratories studying MS and PVL have reported abnormal oligodendrocyte differentiation in these conditions, suggesting these abnormalities are associated with a failure to repair demyelinated lesions.

OPC   preOL   Oligodendrocyte

PVL?   PVL?

PDGFRα

Olig2

Sox10

Nkx2.2

NG2

Olig1 (nuclear)

O4

O1 (GalC)

APC (CC1)

MBP

Olig1 (cytoplasmic)

PLP
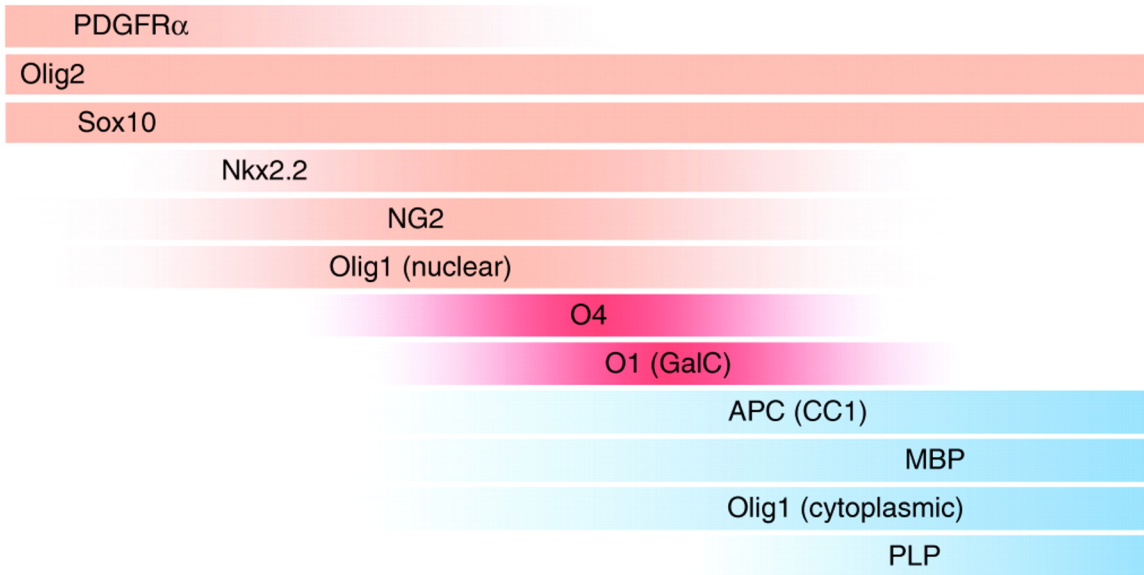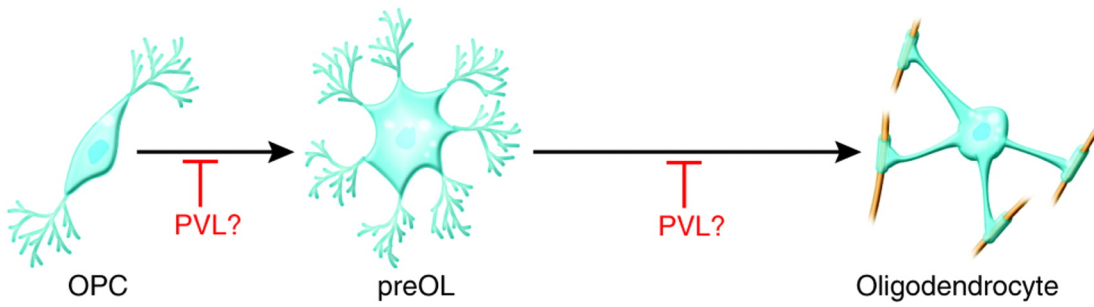
Figure 3. Oligodendrocytes are born in multiple waves and in various locations of the CNS that also produce neurons. Results from the Richardson lab and others have shown that oligodendrocytes of the forebrain are initially specified in ventral regions, such as the Medial Ganglionic Eminence (MGE, corresponding to region 1 in the figure) a ventral domain of embryonic proliferative precursor cells, from which they migrate to more dorsal areas of the brain. At subsequent developmental stages, later waves of oligodendrocytes are produced in successively more dorsal regions, such as the Lateral Ganglionic Eminence (LGE, corresponding to region 2) in late embryonic development and the Cerebral Cortex (CTX, corresponding to region 3) in the early postnatal period. The first three waves of oligodendrocyte production are shown. In addition, NG2-positive precursor cells continue to cycle in the adult brain and are thought to contribute to oligodendrocyte turnover, as well as the response to injury (not shown). Note that these regions also produce neurons throughout the forebrain embryonically.
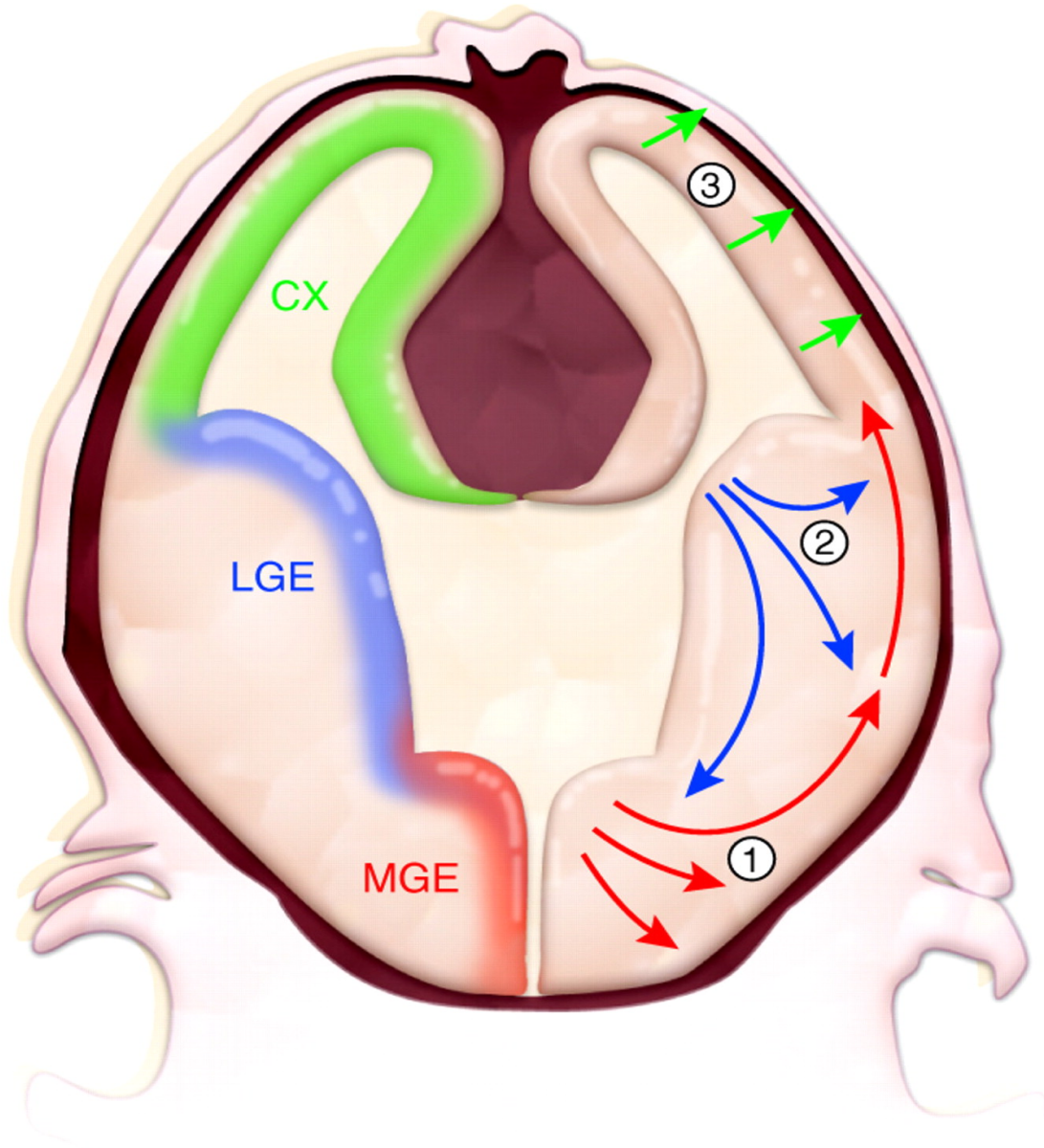
Chapter 2:

Methods

Animals

Animals. All experimental procedures were approved by the Institutional Animal Care and Use Committee and Laboratory Animal Resource Center at the University of California San Francisco (UCSF). Mouse colonies were maintained at UCSF in accordance with National Institutes of Health and UCSF guidelines. The Olig1cre/cre (Lu et al., 2002), The Olig1-cre (Lu et al., 2002), Sox10-cre (Stolt et al., 2006), Plp-CreERT2 (Doerflinger et al., 2003), HIF1α floxed (Ryan et al., 2000), HIF2α floxed (Gruber et al., 2007), and VHL floxed (Rankin et al., 2006) and Caggs-EGFP (Nakamura et al., 2006) reporter mice have been previously described.

Generation of Dlx1/2 floxed mice. Details of the Dlx1/2 floxed conditional knockout targeting construct are shown in Figure 1. The mice were generated by the Gene Targeting and Transgenic Facility and the University of Connecticut Health Center, Farmington, CT. Detailed protocols are available at their website (http://gttf.uchc.edu/index.html). Briefly, the Dlx1/2 floxed conditional knockout targeting vector was introduced into hybrid C57Bl/6 x 129SVEV F1 hybrid mouse embryonic stem cells line and screened for homologous recombination by G148 and Gancyclovir selection. These cells were used to generate chimeric mice. Germline transmission was then tested by outbreeding of chimeras and proper targeting was verified by long arm PCR. The Neomycin cassette was removed by breeding to the R26R-flpe transgenic mouse to excise the Frt sites. Mice were then bred to homozygosity and validated by genotyping PCR for the wild type, 2-lox, and 1-lox allele and crossed to the Olig1-cre knock-in mouse line.

Genotyping. The following primers were used for genotyping: Olig1– cre knock-in: Mutant allele MUT F: 5' CGC TAG AGC CTG TTT TGC ACG TTC ACC GGC 3' and MUT R: 5' CGT TAG TGA AGG GCG CCC CGG GTC GCC CCA 3', Olig1 – cre Wild Type: WT F: 5' AGC CAG

21

CCC TCA CTT GGA GAA CTG GGC CTG 3' and WT R: TGC TGG GTA GCT CGC TGC AGG

AGC TGC GCC, Mutant Band = 550bp, Wild Type Band = 300 bp. Dlx1/2 cKO floxed: 2 – lox

and WT primers: Lox gtF: 5' GGA AAG CGC GGA AGT AGT AG 3', LOX gtR: TTT GCA GGC

GGT AGT TGA GG, Wild Type Band = 291, 2-lox Band = 387 bp. 1 – lox Dlx1/2 cKO PCR:

LoxgtF: 5' GGA AAG CGC CGG AAG TAG TAG 3', FRT gtR: 5' CTG AAC TCT GCC CAA

TCT CC, 1 – LOX BAND = 404 bp. Caggs – GFP: GFP F: AAG TTC ATC TGC ACC ACC G,

GFP R: TCC TTG AAG AAG ATG GTG CG, GFP WT F: GTA GGT GGA AAT TCT AGC ATC

ATC C, GFP WT R: CTA GGC CAC AGA AT GAA AGA TCT, GFP Mutant = 175 bp, GFP Wild

Type: 400 BP. The remaining primers used for genotyping are previously described: *Cre*

(Lu et al., 2002), *HIF1α* floxed (Ryan et al., 2000), *HIF2α* floxed (Gruber et al., 2007),

and VHL floxed (Rankin et al., 2006).

Tissue culture

Neural Progenitor Cultures. Embryonic neurospheres and monolayers were derived from

microdissected medial ganglionic eminences harvested from E14 embryos. Cells were

dissociated by mechanical trituration and plated at 100 cells / ul for neurosphere cultures and

3,000 cells per slide well in 8 well chamber slides (BD Biocoat Poly-D-Lysine / Laminin coated

plates, BD Biosciences). Cells were then expanded in DMEM/F12 supplemented with N-2, B-27,

20 ng/µl EGF and 10 ng/µl bFGF (Life Technologies). Cells were differentiated by removing

growth factors and then culturing the cells for an additional week. Postnatal neurospheres and

monolayers were derived from P3 microdissected subventricular zone. Cells were

disassociated by treatment with Trypsin (Life Technologies) followed by mechanical trituration

and plated at 200 cells / µl and 6,000 cells per slide well in 8 well chamber slides. Conditions

for expansion and differentiation were identical to those for embryonic cultures.

OPC Cultures. Mouse oligodendrocyte precursor cells were isolated by immunopanning P7 mouse cerebral cortices, and then plated and maintained as previously described (Emery et al., 2009; Fancy et al., 2011; Harrington et al., 2010). Cells were allowed to proliferate for 48h with the addition of CNTF, PDGF, and NT-3 (Peprotech) to base medium. Tamoxifen (Sigma) was added to cultures at 24h after plating, and replenished every other day in medium. To assay for differentiation effects, cells were switched to differentiation conditions with the addition of CNTF and T3 (Sigma) to base medium. Once OPCs were put in differentiation conditions, they were either differentiated in the presence of normal conditions, DMOG (0.25mM), or hypoxia (37°C, 2%O$_2$). Factors (IWP2, Stemgent; XAV939, Tocris; Wnt7a, Peprotech) were added in differentiation medium at the time of differentiation. Cells were fixed for 15m in 4% paraformaldehyde at 48h or 60h of differentiation and immunostained for various markers. For PCR or western blot, OPCs were plated and collected at 48h or 60h in trizol or RIPA buffer with protease and phosphatase inhibitors respectively.

OPC-endothelial transwell cultures. Mouse immunopanned OPCs were plated in 0.4μm pore polycarbonate membrane inserts (Corning) coated with PDL (Sigma) and allowed to recover for 24h. Tamoxifen (Sigma) was then added to induce cre-recombination. bEnd.3 cells were maintained in culture medium containing DMEM high glucose supplemented with 10% fetal bovine serum and 1% penicillin-streptomycin (all Invitrogen). The next day, brain endothelial cells (bEnd3. cell line, ATCC CRL-2299) were starved of serum for 5h then trypsinized and plated on PDL-coated glass coverslips, and transwells containing OPCs added. Upon co-culture, growth factors were removed from medium in order to prevent against confounding results. For cultures of endothelial cells alone, bEnd.3 cells were plated on PDL coated glass coverslips. Factors were added at time of plating: Wnt7a (Peprotech) or VEGF (BD Biosciences). For inhibitor studies, XAV939 or SU5416 (both Tocris Bioscience) was added 24h later.

To assay for proliferation, 5-ethynyl-2'-deoxyuridine (10mg/ml) was diluted 1:400 in medium and added to wells for 1h to label dividing cells. Cells were fixed for 15m in 4% paraformaldehyde and imaged using the Click-iT EdU Alexa Fluor 555 Imaging Kit (Invitrogen) followed by immunostaining. Dividing cells labeled by EdU were quantified at the edge of each coverslip.

Cerebellar Slice Cultures. Explant cerebellar slice cultures were cultured according to methods previously described (Fancy et al., 2011; Yuen et al., 2013). For transgenic slice cultures, tamoxifen (Sigma) was added at 1DIV and 3DIV during media changes then withdrawn. Hypoxic cultures were exposed to 24h of hypoxia (37C, 2%O2) between 2-3DIV then returned to normal culture conditions. Dimethyloxalylglycine (DMOG, Sigma) was added at 0.25mM at 2DIV and replenished with each media change every other day until the culture endpoint. IWP2 (Stemgent), XAV939 (Tocris), and Wnt7a (R&D) were added at desired concentrations.

At the culture endpoint, slices were fixed by immersing in 4%PFA for 1h while attached to membranes. Following fixation, slices were then rinsed in PBS, blocked with 3% heat-inactivated horse serum, 2% bovine serum albumin, and 0.25% Triton X-100 in PBS, and then incubated overnight at 4°C in primary antibody diluted in block solution. Primary antibodies used were: chicken polyclonal anti-neurofilament 200kDa (NFH, Encor Biotech), rat monoclonal anti-MBP (Serotec), rabbit polyclonal anti-Caspr (AbCam), Nkx2.2 (DHSB), Cleaved Caspase 3 (rabbit monoclonal, Cell Signaling), and Olig2 (courtesy of Charles Stiles). Secondary fluorescent antibodies from Alexa were then used for immunofluorescent detection. Imaging and quantification was done as previously described (Fancy et al., 2011; Yuen et al., 2013).

Tissue preparation, immunohistochemistry (IHC) and in situ hybridization (ISH).

IHC methods have been described previously (Salmaso et al., 2012). Briefly, following intracardial perfusion of 4% paraformaldehyde, tissue was post-fixed for 2-3h at 4°C,

cryoprotected in 30% sucrose, and embedded in OCT. Frozen sections were then cut on a cryostat (14µm thick) and stored at -80°C. For staining, sections were thawed and then rehydrated in PBS. If needed, antigen retrieval was done with citrate buffer (pH 9.5) or target retrieval solution (Dako) at 95°C for 10m. Tissue was then blocked in 5% normal goat or donkey serum in 0.2% triton-PBS (block solution). Primary antibodies were diluted in block solution, and tissue incubated overnight at 4°C or 2h at room temperature. For primary antibodies, we used antibodies to HIF1α (mouse monoclonal, Abcam; rabbit polyclonal, Cayman Chemical), CC1 (mouse monoclonal, Millipore), Nkx2.2 (mouse monoclonal, DHSB), Olig2 (rabbit or mouse, courtesy of Charles Stiles, Harvard), Olig1 (rabbit, courtesy of Charles Stiles, Harvard), Cleaved Caspase 3 (rabbit monoclonal, Cell Signaling), Iba1 (rabbit polyclonal, Wako), Ki67 (mouse monoclonal, BD), Smi32 (mouse monoclonal, Covance), Neurofilament 200kDa (chicken polyclonal, Encor Biotech), MBP (mouse monoclonal, Covance; rat monoclonal, AbD Serotec), Caspr (rabbit polyclonal, AbCam), Lef1 (rabbit monoclonal, Cell Signaling), VEGF (mouse monoclonal, AbCam), CD31 (rat monoclonal, BD), Fibrinogen (rabbit, courtesy of Jay Degen, Cincinnati Children's), Zic1 (rabbit, courtesy of Rosalind Segal, Dana Farber Cancer Institute), BrdU (mouse monoclonal, BD), DLX2 (rabbit, Abcam), GABA (rabbit, Sigma), GAD67 (mouse monoclonal, Millipore), GalC (mouse, Millipore), Gephyrin (mouse monoclonal, Synaptic Systems), GFAP (rabbit, Dako), GFP (chicken, Aves Labs), Nestin (mouse monoclonal, Millipore), NeuN (mouse monoclonal, Millipore), Nkx2.1 (mouse monoclonal, Zymed), NPY (rabbit, Immunostar), O4 (mouse IgM, gift of Rashmi Bansal, University of Connecticut), Paravlbumin (mouse monoclonal , Sigma & rabbit, Swant), Pax2 (rabbit, Life Technologies), Somatostatin (rabbit, Penninsula Labs), Tuj1 (rabbit, Covance), and VGAT (rabbit, Synaptic Systems). Following incubation with primary antibodies, proper Alexa Fluor secondary antibodies (Invitrogen) were diluted 1:500 in block solution and incubated for 1h at room

temperature. Tissue slices were mounted with flouromount containing 4',6-diamidino-2-phenylindole (DAPI) (Southern Biotech).

Colocalization assays with BrdU required sequential staining. Briefly, IHC for the protein of interest was carried out according to standard protocols, the sections were then fixed in 4% ParaFormaldehyde for 10 minutes at room temperature, after washing slides were incubated in 2N HCl for 45 minutes at 37 ^{o}C and then stained with antibodies for BrdU. The secondary antibodies used were Alexa-flour conjugated species directed antibodies (Invitrogen).

ISH was conducted as previously described (Jeong et al., 2008). ISH probes were as described: Dlx1 and Dlx2 (Bulfone et al., 1993), Lhx6 (Kimura et al., 1999), Olig1 (Lu et al., 2002; Lu et al., 2000), and PDGFRa (Mudhar et al., 1993).

2-Bromodeoxyuridine (BrdU). To assess roles for Olig1 in embryonic interneuron genesis and proliferation, wild type and Olig1-/- pregnant dams were administered a single pulse of BrdU (100 mg/kg) at E16. To assess roles for Olig1 in postnatal interneuron and olfactory bulb interneuron genesis and proliferation, P2 and P16 wild type and Olig1-/- pups were administered a single pulse of BrdU (100 mg/kg) intraperitoneally. All BrdU injected mice were euthanized for analysis at P50.

Cell counting, stereology, synapse quantification and microscopic analysis
In vivo cell counting. For cell counting of immunohistochemistry (IHC), images of anterior to posterior sections of somatosensory and neocortex were taken with a Nikon 80i microscope equipped with a motorized stages using the 10x objective. Images were tiled to a size of 1.32 x 2.56 mm2 taken from 16 μm cryosections and counted by a blinded investigator using the cell counting function on either Nikon Elements (Nikon, Inc) or NIH ImageJ (National Institutes of Health) software. To obtain counts of cortical layers, the estimated width of layers II/III, IV, and V/VI was estimated and measured by assessing Nissl stain of the somatosensory and motor

cortex using the NIH IMageJ software platform. Areas corresponding to these measurements were identified by DAPI staining and then contoured on representative images co-immunostained for PV, CR, SST, or NPY. Cells were then quantified within each contour using the NIH ImageJ cell counting plugin.

For BrdU olfactory bulb tile scans of an entire single olfactory bulb were taken of 3 anterior to posterior cryosections of 16 μm. Counts were then conducted by a blinded investigator. First contours were drawn for the granule and glomerular layers and then the number of BrdU immunopostive cells was determined in each layer using the NIH ImageJ automated cell counting function.

For quantification of PH3 in the mouse embryo, tile scans comprising the aMGE, pMGE, AEP, and posterior septum were obtained from 2 anterior to posterior cryosections. Relevant anatomical regions were identified as previously described (Petryniak et al., 2007). The Ventricular Zone (VZ) and Subventricular Zone (SVZ) boundaries were determined by comparing the relative cell densities of DAPI+ nuclei (VZ being the more dense), countoured and counted by a blinded investigator using NIH ImageJ, as described above. Sox10 quantifications were conducted in the mantle region bordering the AEP, aMGE, pMGE, and Septum in matched sections for each genotype from 0.84 x 0.64 mm2 tile scans.

In vitro cell counting. For cell counting of immunohistochemistry (IHC) from sagittal brain sections of P4, P7, and P11 wildtype and *Sox10-cre, VHL(fl/fl)*, tiled images comprising the entire extent of the corpus callosum and overlying cortex of 2 lateral to medial sections were taken from 14 μm sections with a Nikon 80i microscope equipped with a motorized stages using the 10x objective. The lateral section was identified by the appearance of the internal capsule. The medial section was identified by the emergence of the olfactory bulb fiber tracts. For counts of E18 and P4 coronal sections *Sox10-cre, HIF1/2α(fl/fl)* and *Olig1-cre, HIF1/2α(fl/fl)* mutants,

tiled images of corpus callosum and overlying cortex were taken from two anterior to posterior

sections beginning at the medial edge of the lateral ventricle and extending to the lateral edge of

the corpus callosum. The anterior section was identified by the emergence of the anterior

commissure just inferior to the lateral subventricular zone.   The posterior section was identified

by the appearance of both blades of the dentate gyrus of the hippocampus. The numbers of

immunopositive or double-immunopositive cells were then quantified by a blinded investigator

using the cell counting function on either Nikon Elements (Nikon, Inc) or NIH ImageJ (National

Institutes of Health) software.

Counts of immunocytochemistry in neural stem cell and OPC cultures were obtained by

sampling three defined locations within each slide well (central focus, corner, and slide) of an 8

well chamber slide (BD Biosciences) using the 20x objective. The bottom left corner was used

as reference point and the sites were sampled at defined locations using Nikon Elements

software to control a motorized stage. Images of a field size of 840 x 640 um2 were obtained at

each site and counted as detailed above.

Synaptic counts. Images for synaptic counts were taken from confocal images of sections

stained for NeuN, Parvalbumin, Gephyrin and vGAT. Single optical images were taken from

somatosensory cortex by a Leica SP5 confocal microscope using the 63x objective. Merged

images were analyzed for colocalized puncta with a custom plug-in (written by Barry Wark;

provided by Dr. Ben Barres, Stanford University for the NIH image-processing package

ImageJ.)

Stereologic analysis. To estimate the volume of the cortex and total number and density of

GABAergic interneurons within the cortex, stereological analysis was conducted using the

Steroinvestigator software platform (Microbrightfield, Inc. Williston, VT). Immunohistochemistry

for GAD67 (mouse monoclonal, Millipore, Inc) was performed and detected by treatment with a

horseraddish peroxidase (HRP) conjugated antibody followed by treatment with diaminobenzidine (DAB) using the DAKO HRP/DAB Envision Detection System according to manufacturers instructions. Contours of cerebral cortex were drawn of 1 and every 16 cryosections of 16 μm coronal sections beginning at the first appearance of the internal capsule. Cells were counted using the optical fractionator method in a 3-dimensional counting frame of 100 × 100 × 10 μm and a sampling grid of, 750 × 750. 4 coronal sections were sampled per brain. All analyses had a Schaeffer Error of below 0.10.

Quantification of blood vessel density Immunohistochemistry for CD31 was used to identify endothelial cells. Images of CD31 IHC were obtained from *Sox10-cre, HIF1/2α(fl/fl)* and *Olig1-cre, HIF1/2α(fl/fl)* mutants as described above. Regions of interest (cortex, corpus callosum and cerebellum) were then countoured and the density of vessel coverage was determined by quantifying the percent of the contoured area covered by CD31 staining using the Measure and Analyze Particles functions on NIH ImageJ software (National Institutes of Health).

Electrophysiology

Whole cell electrophysiological recordings were made in acute cortical slices made from wild type and mutant mice at P40-44. Mice were anesthetized with a lethal dose of a ketamine/xylazine cocktail, brains were removed into ice-cold sucrose solution containing (in mM): 150 sucrose, 50 NaCl, 25 NaHCO3, 10 dextrose, 2.5 KCl, 1 NaH2PO4, 0.5 CaCl2, 7 MgCl2. 300 mm coronal sections were made on a vibratome. Slices were incubated in oxygenated artificial cerebrospinal fluid (ACSF) containing (in mM): 124 NaCl, 3 KCl, 1.25 NaH2PO4, 2 MgSO4, 26 NaHCO3, 10 dextrose, 2 CaCl2. For recording, slices were submerged and continuously perfused (2-3 ml/min) with room temperature ACSF in a recording chamber mounted to a microscope (Olympus BX50WI; Center Valley, PA) equipped for

29

differential interference contrast (DIC) optics. Whole cell recordings were made from visually identified Layer 5 pyramidal neurons with borosilicate patch pipettes (3-5 GW resistance) using a Multiclamp 700B and pClamp8 software (Molecular Devices; Sunnyvale, CA). High chloride internal solution contained (in mM): 140 CsCl, 1 MgCl2, 10 HEPES, 11 EGTA, 2 ATP-Mg, 0.5 GTP-Na. After obtaining whole-cell configuration, spontaneous inhibitory synaptic currents (sIPSCs) were recorded for a period of 5 minutes, followed by a 5 minute epoch in which slices were perfused with ACSF containing tetrodotoxin (TTX; 2 mM; Alomone Labs, Jerusalem) and kynurenic acid (3 mM; Sigma, St. Louis) to pharmacologically isolate miniature IPSCs (mIPSCs). mIPSCs were recorded during a third 5-minute recording epoch in the presence of these drugs. Only recordings in which input resistance and holding current were steady across the entire recording period were used for analysis. mIPSC frequency, amplitude, and rise and decay kinetics were measured using Mini Analysis v.6 (Synaptosoft; Fort Lee, NJ), with experimenter blinded to genotype. Statistical differences between genotypes were analyzed using paired t-tests.

Western blotting

Preparation of protein extracts and immunoblot analysis was done as previously described (Kenney and Rowitch, 2000). Fluorescent detection of proteins was carried out using the LiCor Odyssey system (LiCor, Lincoln NE) according to manufacturers instructions. Antibodies used include: Tuj1 (Millipore), Olig2 (a gift of Charles D stiles), Dlx2 (Abcam), DCX (Cell Signalling), HIF1α (mouse monoclonal, Novus Biologicals), HIF2α (rabbit polyclonal, Abcam), VEGF (mouse monoclonal, Abcam), activated β-catenin (mouse monoclonal, Millipore), Notum (rabbit polyclonal, Sigma), Naked1 (rabbit polyclonal, Cell Signaling), Axin2 (rabbit polyclonal, Cell Signaling), β-tubulin (mouse monoclonal, Sigma), and β-actin (rabbit polyclonal, Cell Signaling).

Quantitative PCR

Quantitative PCR (qPCR) was carried using cDNA from Olig1 -/- and Wild Type tissue made using a Reverse Transcripts cDNA kit according to manufacturers instructions (Applied Biosystems). Relative expression analysis was performed by the 2nd derivative Ct method and fold changes for genes of interest were referenced against the average of two housekeeping genes beta-Actin and GAPDH. Primer sequences for WNT ligands are provided in Table 1. Primer sequences for WNT targets (Notum & Naked1), Myelin genes (MBP, MOG, CNPase), and housekeeping genes have been previously described (Fancy et al., 2011). Additional Primer sequences are as follows:

Vax1

F – GCCTCACCCAAACTCAGGT

R – AGGCACAAGGAGGAGAAGC

DLX2

F – GCTTCGGAAGARTTGTAACAAAAG

R – GGATAGACCCCTTGGCATC

Sp8

F – CCTGCTATGGCCACGTCTAT

R - GCCGATCTTGTTGCAGGT

Electromobility Shift Assays (EMSA) and Luciferase Assays

EMSA. Olig1 protein (OriGene Technologies) was quantified by silver stain against known concentrations of BSA protein. Oligonucleotides were annealed in annealing buffer (10mM Tris HCl pH7.5, 50mM NaCl, 1mM EDTA) using a thermocycler for 5 min at 95°C, and allowed to cool down for approximately 1 hour. Annealed probe was labeled with [α-32p] 6000 Ci/mmol dCTP (PerkinElmer) using Klenow (New England Biolabs). Radioactive DNA probe was

incubated with Olig1 protein in binding buffer (20mM Tris-HCl pH7.5, 5mM MgCl2, 0.1% NP40, 0.5mM DTT, 10% glycerol) for 30 min at 4°C. Protein:DNA complex was analyzed on 4% non-denaturing poly-acrylamide gel electrophoresis (PAGE) for 30 min at 4°C. Oligoducleotide sequences, including mutated E-Box sequences are detailed in supplemental figure 3.

Transfection and Luciferase Assays. Dual luciferase assays and transfections were conducted in P19 cells as previously described (McKinsey et al., 2013). The I12b enhancer was cloned into the pGL4.23 luciferase construct (Promega) and the pCAGGS plasmid was used to drive expression of Olig1 (pCAGGS-Olig1) and Dlx2 (pCAGGS-Dlx2).

Chronic Hypoxia and Hypoxia-Ischemic encepholopathy.

Chronic hypoxia. Chronic hypoxic rearing was performed as previously described (Fagel et al., 2006; Turner et al., 2003; Weiss et al., 2004). Briefly, litters of the C57BL/6 strain were culled to a size of 8 pups and co-fostered with CD1 or Swiss Webster strain dams then reared at 10% O2 in an hypoxic chamber (Biospherix, Inc. Laconia, NY). Tissue from P3 to P4, P7 or P11 was then harvested acutely for analysis.

Hypoxia-Ischemia Encephalopthy (HIE). HIE was induced in WT and *Olig1-/-* P9 pups according to the procedure of Rice and Vannuci. Briefly, mice anestitihized in isoflourane, the right carotid artery was isolated and closed with an electric cauterizer. Pups were then exposed to 8.5% O_2, returned their mother and reared as normal. BrdU was administered at P16 (7 days postinjury) and mice were perfused for histological analysis at P23 and P37 (14 and 28 days post injury, respectively). This procedure results in a variable extent of brain injury. Subjects were selected that had moderate brain injury ipsilateral to the manipulated hemisphere

as defined by ventriculomegaly with astrogliosis in the affected hemisphere but the absence of macroscopic necrotic cysts.

Chromatin Immunoprecipitation.

Mouse embryonic fibroblasts (wild-type and HIF knockout courtesy of Emin Maltepe) were cultured in RPMI-1640 supplemented with 10% fetal bovine serum, 1% sodium pyruvate, 1% penicillin streptomycin, and 1% fungizone (all from UCSF cell culture facility but FBS, Invitrogen). Once confluent, plates were either exposed to DMOG (0.25mM, Sigma) or vehicle for 16h. Cells were then rinsed once with DPBS (Invitrogen) and trypsinized, spun down and crosslinked with 4% paraformaldehyde for 10m at room temperature. 1M glycine was then added for 5m to quench the PFA reaction. Crosslinked cells were then spun down, rinsed with ice cold PBS (with protease inhibitor, Roche), and frozen at -80°C. Cell pellets were sonicated on ice for 30 cycles (30sec on, 30sec off) using the Bioruptor. The Human/Mouse HIF-1 alpha ExactaChIP Chromatin IP kit (R&D systems), magnetic dynabeads protein G (Invitrogen) and QIAquick PCR purification kit (Qiagen) were used according to manufacturer's directions. IgG pulldown was used as a negative control. Quantitative PCR was then carried out using the Roche LightCycler 480 with LightCycler 480 SYBR Green I Master (Roche). Primers for Wnt7a, Wnt7b, GAPDH, 1kb upstream (negative control), and Epo enhancer regions (positive control) were used.

Primers were as follows: Wnt7a – F: 5' – CTTCTGCCCCACCGTTTTTC – 3', R: 5' – GCAATGTCCTGTCTTCGTGG – 3'; Wnt7bA – F: 5' – AGCAGCAGAAGGTTTGATGG – 3', R: 5' – CAAGGCTCCAGTGACACGTAA – 3'; Wnt7bB – F: 5' – CATTTACATCGCAGCGTCTGG – 3', R: 5' – GTGGTCACCCGATACACACG – 3'; 1kb upstream – F: 5' – CATGAGGGATTCTGCTGGAGG – 3', R: 5' – CAGCCACCACCTAGACTCAAA – 3'; Epo – F: 5' – TACCTCACCCCATCTGGTCG – 3', R: 5' – GCTTATTGACTAGCGTGGGC – 3'. 5% input controls were added, and reactions were run in triplicate.

Table 1: Primer sequences and qPCR expression of WNT ligands in OPCs

WNT Ligand	OPC Expression	Hypoxia Regulated	Primer Sequences
Wnt1	ND	N/A	F: 5' - CCT CAC CCC ACC TCA CTG – 3' R: 5' - AGA TAC TAC ATT GGT GGG GGC – 3'
Wnt2	ND	N/A	F: 5' - CGG CCT TTG TTT ACG CCA TC – 3' R: 5' - TGA ATA CAG TAG TCT GGA GAA – 3'
Wnt2b	ND	N/A	F: 5' - CAC CCG GAC TGA TCT TGT CT – 3' R: 5' - GCC ACA ACA CAT GAT TTC ACA -3'
Wnt3	ND	N/A	F: 5'- GGG GCG TAT TCA AGT AGC TG – 3' R: 5' - GTA GGG ACC TCC CAT TGG AT – 3'
Wnt3a	ND	N/A	F: 5' - CAT ACA GCC CAT CTG CCA C – 3' R: 5' - AAT CCA GTG GTG GGT GGA TA – 3'
Wnt4	Y	N	F: 5' - GAG AAG TGT GGC TGT GAC CGG – 3' R: 5' - ATG TTG TCC GAG CAT CCT GAC C – 3'
Wnt5a	ND	N/A	F: 5' - CCC AGT CCG GAC TAC TGT GT – 3' R: 5' - TTT GAC ATA GCA GCA CCA GTG – 3'
Wnt5b	ND	N/A	F: 5' - TCT CCG CCT CAC AAA AGT CT – 3' R: 5' - CAC AGA CAC TCT CAA GCC CA – 3'
Wnt6	ND	N/A	F: 5' - TGC CCG AGG CGC AAG ACT G – 3' R: 3' - ATT GCA AAC ACG AAA GCT GTC TCT C – 3'
Wnt7a	Y	Y	F: 5' - GAC AAA TAC AAC GAG GCC GT – 3' R: 5' - GGC TGT CTT ATT GCA GGC TC – 3'
Wnt7b	Y	Y	F: 5' - TCT CTG CTT TGG CGT CCT CTA C – 3' R: 5' - GCC AGG CCA GGA ATC TTG TTG – 3
Wnt8	ND	N/A	F: 5' - ACG GTG GAA TTG TCC TGA GCA TG – 3' R: 5' - GAT GGC AGC AGA GCG GAT GG – 3'
Wnt8b	ND	N/A	F: 5' - TTG GGA CCG TTG GAA TTG CG – 3' R: 5' - AGT CAT CAC AGC CAC AGT TGT C – 3'
Wnt9a	ND	N/A	F: 5' - CGG CAA GAT GCT GGA TGG GTC – 3' R: 5' - CTG CTT GCG CTC CAG CTT CAG – 3'
Wnt9b	ND	N/A	F: 5' - CAT GGA GCG CTG TAC TTG TGA C – 3' R: 5' - CAT GGA GCG CTG TAC TTG TGA C – 3'
Wnt10a	ND	N/A	F: 5' - CCT GTT CTT CCT ACT GCT GCT GG – 3' R: 5' - CGA TCT GGA TGC CCT GGA TAG C – 3'
Wnt10b	ND	N/A	F: 5' - GGG CTT CGA CAT GCT GGA GGA GCC CC – 3' R: 5' - AGC CGC CGC CGC CCT CCA GT – 3'
Wnt11	ND	N/A	F: 5' - GAC ACC ACA CCA GGA GGC – 3' R: 5' - ATT CCA GAA AGC CGG TCT TT – 3'
Wnt16	ND	N/A	F: 5' - AGT AGC GGC ACC AAG GAG AC – 3' R: 5' - GAA ACT TTC TGC TGA ACC ACA TGC – 3'

Figure 1: Targeting construct and generation of the *Dlx1/2* floxed mouse
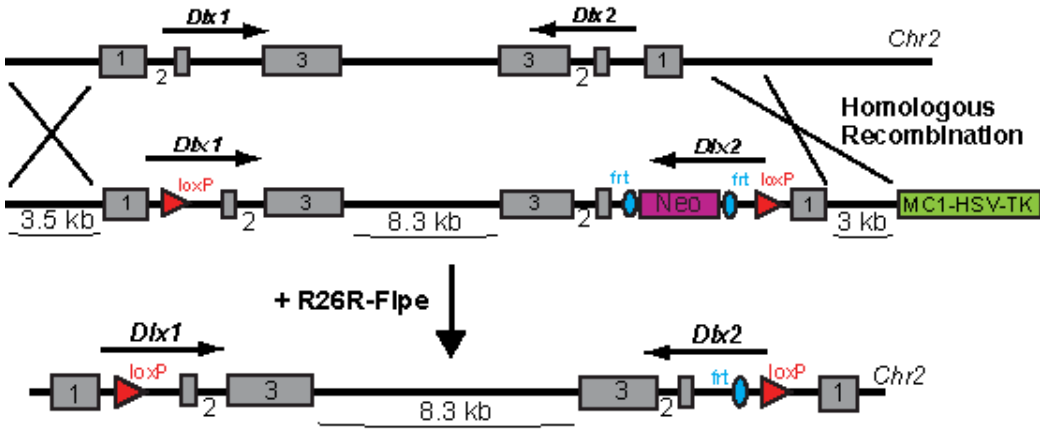
Chapter 3:

Olig1 determines oligodendrocyte versus interneuron

population size through repression of Dlx1/2

Introduction: Common Developmental Origins for Interneurons and Oligodendrocytes

Embryonically Oligodendrocytes are derived from common progenitor domains for interneurons throughout the brain. Specification of these two cell types in the embryonic brain is complex, involving: (1) patterning of spatially discrete progenitor pools for specific subtypes, (2) temporal regulation of multiphase neurogenesis and gliogenesis (3) mechanisms of neuron versus oligodendroglial (OL) cell fate acquisition (Butt et al., 2005; Kessaris et al., 2006; Marin, 2012; Wonders et al., 2008). For instance, cortical inhibitory neurons are produced from E10 to E17 in the medial ganglionic eminence (MGE), anterior entopeduncular area (AEP; a ventral region of the MGE), caudal ganglionic eminence (CGE), and preoptic areas (POA) of the ventral telencephalon; they then migrate tangentially into the cerebral cortex (Anderson et al., 1997; Corbin et al., 2001; Miyoshi et al., 2007; Wonders and Anderson, 2006). Parvalbumin (PV) and calretinin (CR) positive cells are derived relatively late in embryogenesis from progenitor domains that produce both OLs and INs, whereas neuropeptide-Y (NPY) and somatostatin (SST) subtypes are born prior to the onset of OL specification (Kessaris et al., 2006; Miyoshi et al., 2007; Taniguchi et al., 2013; Wonders et al., 2008). In contrast, the adjacent regions of the lateral ganglionic eminence and the telencephalic septum generate neurons of the ventral forebrain and olfactory bulb, but are not thought to give rise to cortical INs (He et al., 2001; Kessaris et al., 2006; Petryniak et al., 2007; Rubin et al., 2010). Dlx1/2 function is necessary for the establishment of IN cell production within these regions and differentiation into GABAergic INs (Anderson et al., 1997). In late embryonic development, OPCs are produced from these regions as well.

Thus establishing the appropriate number of OPCs and INs during development requires precise regulation of neuron glial fate choice from multipotent progenitors. A recent study suggests that the size of the cortical IN population is determined primarily in the early embryo at time of specification, rather than by neurotrophic competition, and programmed cell death later in development (Southwell et al., 2012). Transplanted IN precursors are capable of functional

integration into the adult brain (Alvarez-Dolado et al., 2006; Southwell et al., 2010) and can

attenuate seizures in rodent models of epilepsy (Baraban et al., 2009; Hunt et al., 2013).

Increased IN population size also induces and extends critical periods for ocular dominance

plasticity (Southwell et al., 2010). Thus, generating the appropriate number of cortical neurons

during development is crucial. However, the factors that normally limit the size of the IN

progenitor pool are poorly understood and essential repressors of IN developmental programs

have not been described. In contrast OPCs are generated throughout life and OL density is

tightly controlled by both programmed cell death and mechanisms to limit OPC proliferation.

(REF)

Though the mechanisms that control OL versus IN fate are poorly understood, we have

shown that Dlx1/2 function is required in the MGE and AEP to control the neuron-glial switch,

promoting neurogenesis at the expense of OLs through repression of Olig2 (Petryniak et al.,

2007). In contrast, Olig2-null animals show no abnormalities in early IN development (Petryniak

et al., 2007, (Furusho et al., 2006; Ono et al., 2008) Olig1 is expressed in the embryonic

neuroepithelium of the ventral forebrain (Petryniak et al., 2007), which can give rise to INs and

OLs (Mukhopadhyay et al., 2009; Samanta et al., 2007). However, Olig1 function is generally

thought to be limited to late stages of OL development to promote differentiation (Lu et al., 2002;

Xin et al., 2005) and remyelination (Arnett et al., 2004). Here I show a surprising role for Olig1

as an upstream repressor of Dlx1/2 and GABAergic IN production in the embryonic brain,

establishing that Olig1 functions in the regulation of the neuron-glial switch. Loss of Olig1 de-

represses production of late CR and PV IN subtypes in ventral MGE, AEP, and regions of the

MGE connected to the septum, resulting in a 30% excess of INs in adult cortex. Postnatally,

Olig1-null neural progenitors produced excessive numbers of INs and are deficient in OL

production. I show Olig1 directly binds and represses the I12b enhancer element, a known

Dlx1/2 intergenic cis-acting DNA regulatory sequence, and using a newly generated floxed

conditional Dlx1/2 knockout allele, we show that Dlx1/2 lies genetically downstream of Olig1.

Together, these findings demonstrate that Olig1 is an essential repressor of GABAergic neuron production in the mammalian brain.

Inhibitory IN numbers are increased in the cortex of Olig1-null animals

To assess Olig1-dependent regulation of IN production, I first analyzed IN markers in the adult (P50) motor and somatosensory cortex of Olig1-null and controls by immunohistochemistry (IHC) (Figure 1a). Evaluation of IN subtypes in motor and somatosensory cortex demonstrated that there was a ~35% increase in parvalbumin+ (PV) and calretinin+ (CR) IN subtypes, but not somatostatin+ (SST) or neuropeptide Y+ (NPY) subtypes (Figure 1 b, i-k and m). I also observed an ~ 30% increase in cells expressing the pan-IN lineage markers GABA and GAD67 (Figure 1 g-h & Figure S1 k-l). We next determined if the laminar distribution of INs was abnormal. Increased numbers of PV+ and CR+ INs were present throughout the cortical layers. We did not find any difference in the laminar distribution of SST+ and NPY+ cells (Figure 1 n-q). SST+ and NPY+ neurons are generated early in telencephalic neurogenesis before E13. In contrast, CR+ neurons are generated at later stages and the PV+ subtype is generated throughout embryogenesis coinciding with the onset of OL specification (Kessaris et al., 2006; Miyoshi et al., 2007; Taniguchi et al., 2013; Wonders et al., 2008). Thus, Olig1 acts to limit late born INs generated simultaneously with OLs, but not early born INs. Normal numbers of glutamatergic and cholinergic neurons were observed in Olig1-null animals (data not shown).

To confirm our findings, we conducted unbiased stereological analysis of the number of GAD67+ cells throughout the cortex and determined that the density and estimated total number of GAD67+ cells was increased by ~25% throughout the cortex (Figure 2 k-l). Cortical volume was unchanged in Olig1-null mice (Figure 1b & Figure S1m). To ensure that our results are not due to misexpression of IN markers with other cell types, we performed IHC for PV and GAD67 with markers of pyramidal cells (Tbr1), OLs (Olig2), microglia (Iba1) and astrocytes

(GFAP). As shown (Figure 2 g-j), we found no instance of abnormal IN marker expression in Olig1 -/- brains.

Inhibitory PV+ INs synapse on the soma of cortical pyramidal cells, whereas CR+ neurons synapse mainly on the soma of other INs (Caputi et al., 2009; Freund and Buzsaki, 1996; Gonchar and Burkhalter, 1999). In keeping with the counts described above, we found a ~30% increase of PV+ puncta on the soma of layer 2/3 and 5/6 pyramidal neurons of somatosensory and motor cortex (Figure 1 c-d). Moreover, such puncta also expressed vesicular GABA transporter (VGAT) (Figure 1e), a marker of inhibitory synapses (Bragina et al., 2007). Quantification of VGAT+ puncta in dendritic fields revealed no differences in the number of inhibitory synapses on dendrites, consistent with our finding that SST+ cell numbers are not affected in Olig1-/- mice (Figure 1 e-f).

Increased IN number does not alter inhibitory events on cortical pyramidal cells: Evidence of postsynaptic Gephyrin mediated compensation

There are a myriad of cell intrinsic and synaptic homeostatic mechanisms that control inhibition in cortical circuits (Pozo and Goda, 2010; Turrigiano, 2011). Olig1 -/- mice provide a here-to-fore unique system to determine if increases in endogenously derived INs are sufficient to enhance inhibition in the adult cortex. To test this possibility we performed voltage-clamp analysis of inhibitory postsynaptic currents in layer 5 pyramidal cells in acute cortical slices derived from P35 mice. As a functional measure of inhibitory tone we analyzed both spontaneous and miniature inhibitory postsynaptic potentials (sIPSPs & mIPSPs). We found no significant increase in inhibitory activity onto pyramidal cells in terms of event frequency, amplitude or kinetics (Figure 3 a-b and data not shown). Because, we observed more presynaptic vGAT puncta, expressed at the soma of cortical neurons, we hypothesized that a postsynaptic compensatory mechanism might regulate inhibition in Olig1-/- mice. Gephyrin, a scaffolding protein that regulates recruitment, stability and clustering of GABA receptors at the

postsynapse is downregulated in response to increased GABAergic activity (Langosch et al., 1992; Poulopoulos et al., 2009; Prior et al., 1992; Saiepour et al., 2010; Tretter et al., 2008; Tretter et al., 2012). As demonstrated (Figure 3 c), we observed normal numbers of Gephyrin puncta identified by IHC at the postsynapse. We also noted that some CR+ interneurons make inhibitory connections with other interneurons, and thus excess CR+ may also limit the activity of other IN subtypes in Olig1 -/- mice (Caputi et al., 2009; Freund and Buzsaki, 1996; Gonchar and Burkhalter, 1999).

Olig1 represses neurogenesis in the cerebellum and olfactory bulb

We next assessed Olig1 function in the cerebellum (CB) and olfactory bulb (OB), brain areas that exhibit protracted neurogenesis (Maricich and Herrup, 1999; Schuller et al., 2006). As shown (Figure 4 a-c & d), we observed a ~30% surplus of AP2Beta+ and Pax2+ cerebellar INs at P7 and P21, respectively. Robust neurogenesis and neural cell turnover persists in the olfactory bulb (OB) throughout life and is regulated by Dlx1/2 (Alvarez-Buylla et al., 2002; Long et al., 2007). To assess neurogenesis in the OB, we conducted birth dating assays by injecting the thymidine analogue Bromodeoxyuridine (BrdU) intraperitoneally into P2 pups and analyzing olfactory bulbs in tissue harvested by perfusion at P50. These mice exhibited approximately 2-fold increases in the numbers of BrdU+ cells in the granule layer and glomerular layer (Figure 4 f-j). In summary, these findings provide evidence that Olig1 has a general role in repressing IN production, including in the neocortex (PV+ and CR+ subtypes), cerebellum (Pax2+ / AP2Beta+), and perinatal olfactory bulb.

Olig1-/- mice produce fewer numbers of oligodendrocytes

Given previous evidence for common precursor domains for INs and OLs in the embryonic telencephalon, perinatal cerebellum and olfactory bulb throughout life (Goldman et al., 1997; Menn et al., 2006; Petryniak et al., 2007; Silbereis et al., 2009; Zhang and Goldman, 1996), we

assessed the impact of Olig1 loss-of-function on the OL population in the adult cerebral cortex and cerebellum by histological analysis. The numbers of cells expressing the pan-OL marker Olig2, as well as the mature OL markers PLP and APC are all reduced in the corpus callosum, motor cortex, and cerebellar white matter of the P21 and P50 mouse brain (Figure 2 a-f).

Olig1 is expressed in multipotent telencephalic progenitors that produce cortical IN.

GABAergic INs of somatosensory and motor cortex develop from the ventral embryonic telencephalon under control of Dlx1/2 and other transcriptional programs (Anderson et al., 1997; Wonders and Anderson, 2006). As shown (Figure 5 a-d), we detected Olig1 mRNA transcripts in the AEP and ventral MGE telencephalic regions that express Dlx1/2 (Petryniak et al., 2007), as well as caudal/dorsal regions of embryonic septum, which produces OLs but is not thought to produce cortical INs (Rubin et al., 2010). Nkx2.1 is a hedgehog responsive gene critical for establishing progenitors of ventral identity that derive both forebrain OLs and INs (Butt et al., 2008; Elias et al., 2008; Kessaris et al., 2006; Maricich and Herrup, 1999). As shown (Figure 5 e-f), we found that Olig1+ cells co-labeled with Nestin and Nkx2.1.

A second line of evidence assigning Olig1 expression to IN progenitors was provided by fate mapping with Olig1-cre. Our analysis in the adult (P50) neocortex, consistent with previous studies (Mukhopadhyay et al., 2009; Samanta et al., 2007), showed that Olig1-cre precursors fate mapped to ~35% of GABAergic cells and ~45% of PV+ INs, but fewer INs of other subtypes. In contrast, we found no labeling of glutamatergic cortical neurons (Figure 5 g-h, data not shown). Together, these findings indicate Olig1 is expressed in multipotent precursor cells for GABAergic INs, particularly the PV+ subtype.

Olig1 represses telencephalic IN genetic programs

We next used in situ hybridization (ISH) to assess expression of Lhx6, Dlx1 and Dlx2, genes necessary for the genesis of INs from MGE, AEP, CGE and preoptic area (POA) of wild type

and Olig1-/- E15 embryonic brain. Olig1 mutants showed expansion of Lhx6, Dlx1 and Dlx2 expression into the ventral MGE, the AEP and the caudal septum (Figure 6 a-h). To quantify this upregulation and assess the expression of Vax1 and Sp8 (two additional genes associated with IN production in the telencephalon), we dissected the caudal septum, AEP and ventral MGE from wild type and Olig1-null embryos and performed qPCR (Anderson et al., 1997; Taglialatela et al., 2004; Waclaw et al., 2006). We observed 2-4-fold increased expression of Dlx2, Vax1 and Sp8 (Figure 6i). These data indicate that loss of Olig1 function results in upregulated expression of key transcription factors that drive IN cell fate acquisition.

Previous, gain-of-function studies have shown that Olig1 promotes OL specification from neural progenitors (Kim et al., 2011; Lu et al., 2001; Lu et al., 2000; Maire et al., 2010). To assess potential changes in embryonic OPC production, we assessed PDGFRa+ cells by ISH and quantified Sox10+ OPCs by IHC in Olig1-/- mutant and wild type E15 embryos in the mantle of the ventral telencephalon. This showed a reduction in OPC number (Figure 7 a-c). In contrast, we observed no significant change in levels of the mitotic cell marker phospho-Histone3 (PH3) in the septum, MGE, and AEP (Figure 7 d–f). Together, these findings suggest that Olig1 function is required to promote OPC production at the expense of INs in the ventral telencephalon, but that it does not regulate IN precursor proliferation. Further, this shows a unique function of Olig1 as a repressor of IN development, because Olig2-null mice, which lack OPCs, show normal expression of Dlx2 (Petryniak et al., 2007) and IN precursor numbers identified by expression of GAD67 mRNA in the ventral telencephalon (Figure 8)(Furusho et al., 2006; Ono et al., 2008).

To confirm the birthdate of ectopic cortical INs in the Olig1 mutant embryonic forebrain we injected Bromodeoxyuridine (BrdU) into pregnant dams at E16. BrdU co-labeling analyses with PV and GABA revealed an approximately 30% increase in the number of INs generated at these ages (Figure 6 j-o). Interestingly, at P0 we observed enhanced expression of Dlx2 in the subventricular zone (SVZ) of Olig1-null animals (Figure 9 a-d), raising the possibility of

persistent IN production. However, BrdU birth dating at P2 ruled this out (Figure 9 e-f). Together, these findings indicate that Olig1 regulates neuron-glial fate choice in the embryonic telencephalon.

Postnatal roles for Olig1 in suppression of IN production

The finding of increased olfactory bulb neurogenesis perinatally and ectopic Dlx2 expression in Olig1–null dorsal SVZ at P0 suggested there may be persistent roles for Olig1 in neural stem cells. To test if Olig1 regulates cell fate in defined culture conditions, we harvested progenitors from P3 anterior SVZ and then cultured progenitor cells as neurospheres or adherent monolayers of neural stem cells (NSCs). Neurospheres were expanded in EGF and FGF and then transferred to factor-free medium overnight to induce differentiation markers. Western blot analysis of total proteins demonstrated increased levels of neuron-specific Tuj1 and Dlx2 expression in Olig1-null neurospheres compared to wild type; in contrast, Olig2 levels were dramatically reduced (Figure 10a). In keeping with these findings, Olig1-null spheres showed enhanced capacity to produce young doublecortin (DCX)+ neurons (Figure 10b). As shown (Figure 10c-e), Olig1 loss-of-function enhanced GABAergic IN production from NSC monolayer cultures. By contrast, monolayers derived from Olig1-null progenitors were deficient in production of NG2+, O4+ and GalC+ OL lineage cells (Figure 5f-i), which respectively label OPCs, premyelinating OLs and myelinating OLs. GFAP+ astroglial production was unaffected (data not shown). Thus, Olig1 function is required in cultured postnatal neural progenitors to repress IN production and preserve oligodendrogenesis.

Evidence that Olig1 is a direct repressor of the Dlx1/2 I12b intergenic enhancer

Olig1 acts as a transcriptional repressor (Lee et al., 2005; Novitch et al., 2001; Sun et al., 2003). Thus, we hypothesized that Olig1 may directly repress Dlx1 and/or Dlx2, which colocalize within 10 kb of each other on mouse chromosome 2. This potential hierarchy is consistent with the

observations that (1) Olig1-cre fate mapping labels 30% of cortical GABAergic neurons, (2) Olig1 protein shows segregated expression from Dlx2 in ventral telencephalon (Figure 11a), and (3) the previous finding that Dlx1/2-cre fate mapping fails to label Olig1-positive cells (Potter et al., 2009).

We tested whether Olig1 might regulate cis-acting DNA regulatory sequences in the intergenic region of Dlx1/2. Activity of the I12b enhancer drives expression of Dlx1/2 in the embryonic ventral telencephalon (Ghanem et al., 2007; Park et al., 2004; Poitras et al., 2007). We determined that the I12b enhancer contains three E-box sites, the canonical binding sequences for bHLH transcription factors including Olig1 (Figure 11 b, Figure 12 a-b). We then used electrophoretic mobility shift assays (EMSA) to test Olig1 binding to Dlx1/2 I12b E-box sites in vitro. As shown in Figure 11 c-d, purified Olig1 proteins shifted E-boxes 1 and 3, with the highest affinity for E-Box 1. Binding to E-box 1 was dose-dependent and was abrogated by DNA mutation of E-box sites within the I12b enhancer (Figure 11 c-d, Figure 12 b). Specificity of Olig1 binding was further tested by supershift assays, which demonstrated that treatment of an antibody against Olig1, but not treatment with a control IgG antibody, inhibits binding of Olig1 protein to enhancer DNA sequences (Figure 11 e-f).

To confirm that Olig1 acts as a repressor of Dlx1/2, we next used a luciferase assay by cloning the I12b enhancer into the pGL4 luciferase construct (Promega) and transfecting it into P19 cells. Because Dlx1/2 are positive feedback regulators of their own expression via the I12b locus (Potter et al., 2009), we transfected a Dlx2 expression construct to induce I12b-dependent luciferase activity. When an Olig1 expression construct was transfected into these cells it induced a nearly three-fold reduction in luciferase activity (Figure 11 g). Together, these data provide biochemical evidence that Olig1 functions upstream of Dlx1/2 as a transcriptional repressor of the Dlx1/2-I12b enhancer.

Genetic functions of Dlx1/2 downstream of Olig1

We next tested whether Dlx1/2 function lies genetically downstream of Olig1. We generated a conditional floxed allele that removes Dlx1 exons 2 and 3, the intergenic region and Dlx2 exons 2 and 3 upon exposure to cre recombinase (Figure 13 a). Targeted ES cells produced chimeras that passed the allele through the germline (Figure 13 b-c).

We first sought to determine whether the increase in cortical IN density in Olig1-null mice was Dlx1/2-dependent in vivo. To test specific requirements of Dlx1/2 in the Olig1 lineage, we crossed our Olig1-null cre knockin mice (Olig1cre(KI)/cre(KI)), in which the Olig1 coding sequence has been replaced with a cre recombinase gene (Lu et al., 2002), to the Dlx1/2 floxed mice. By using these cre knockin mice, we are able to confine Dlx gene excision in Olig1-null animals to the Olig1 expression domain. Olig1cre(KI)/cre(KI) x Dlx1/2fl/fl animals failed to thrive, typically died in the neonatal period and never survived past P21, precluding analysis of PV populations in the adult cortex. However, Olig1cre(KI)/cre(KI) x Dlx1/2fl/+ animals were viable into adulthood, at which point analysis of the cortices showed normalization of INs identified by IHC for GAD67 and PV (Figure 13 d-g).

To further establish Dlx1/2 functions downstream of Olig1, we derived NSC monolayers from the ventral telencephalon of E14 Olig1cre(KI)/cre(KI) x Dlx1/2fl/fl, Olig1cre(KI)/cre(KI) x Dlx1/2+/+ and wild type mice. As shown (Figure 13 h-i & k-l), we observed that the increased IN production characteristic of Olig1cre(KI)/cre(KI) NSCs was normalized in Olig1cre(KI)/cre(KI) x Dlx1/2fl/fl NSCs. Conversely, we observed complete rescue of OL specification in Olig1cre(KI)/cre(KI); Dlx1/2fl/fl NSCs (Figure 13 j & m). Taken together, these genetic findings support a model in which Olig1 acts as an essential repressor of Dlx1/2 to limit IN pool size and promote oligodendrogliogenesis (Figure 14 a).

Figure 1. Increase in interneuron numbers in the cerebral cortex of adult *Olig1*-null mutant mice

(a) Representation of regions of secondary somatosensory cortex (S2) and primary motor cortex (M1) in which INs were quantified. (b) Representative images of parvalbumin (PV) in wild type (WT) versus *Olig1*-null (*Olig1-/-*) motor cortex. Note the increased number of PV+ cell bodies. (c) Representative image showing increases in PV+ (red) synaptic puncta localized to NeuN+ (blue) soma in *Olig1-/-* vs. WT M1. Arrowheads point to soma localized PV+ puncta, asterisks denote non soma localized puncta. (d) Quantification of PV+ synaptic puncta colocalizing NeuN positive soma in M1 (e) Representative image showing VGAT (green), PV (red), and NeuN (blue). As shown in the boxed region VGAT+ (green) / PV- (red) synaptic puncta in dendritic fields (DF) are identical in *Olig1-/-* vs. WT M1. (f) Quantification of the number of VGAT+ puncta in dendritic fields demonstrating that there is not a significant increase in the number of VGAT+ neuronal synapses in dendritic fields of *Olig1-/-* cortex vs. WT.

(g -k) Representative images of INs in *Olig1-/-* and WT cortex. Arrows point to cell bodies of cell types for which significant differences were observed. (g-h) 2 μm confocal projections of pan IN markers GAD67 (g) and GABA (h). (i-k) 2 μm confocal projections of IN subtype markers Somatostatin (SST) (i), Calretinin (CR) (j), and Neuropeptide Y (NPY) (k). (l-m) Quantification of the number of cells expressing the pan IN markers (l) and IN subtypes (m). (n-q) Quantification of the number of cells expressing IN subtypes within distinct lamina of the cortex (II/III, IV, V/VI) as in panel (b). Cell counts were taken from micrographs of S2 and primary M1 (For all quantifications: mean +/- SEM, n = 3-4; *p<.05, **p<.01, ***p<.005; 2 tailed unpaired student's t test). (b',e',k") Scale bar = 50 μm, (c') scale bar = 5 μm (k"), (e') scale bar = 15 μm.

Abbreviations: AC, anterior commissure; DF, dendritic field; IN, interneuron; M1, primary motor cortex; MSN, medial septal nucleus; S2, secondary somatosensory cortex.
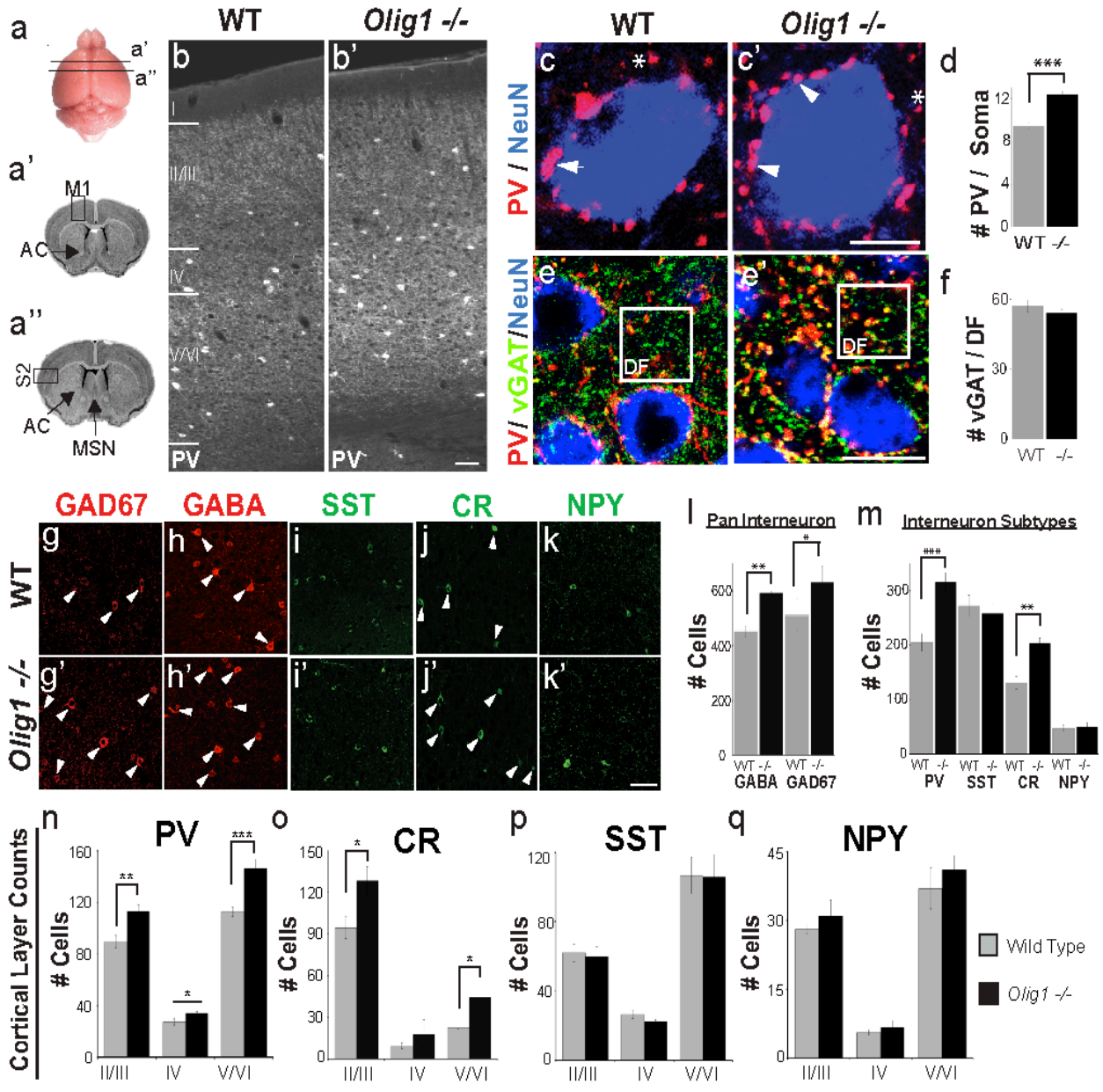
Figure 2. Diminution of the oligodendrocyte population not misexpression of interneuron markers explains cortical volume stability in *Olig1-/-* mice

(a-b) Representative images (a) and quantification (b) of Olig2+ cells, showing the total number of OL lineage cells is reduced in the adult cortex of *Olig1-/-* mice. (c) Representative image of *in situ* hybridization for *Plp*, a marker of mature oligodendrocytes, showing a reduction in the number OLs in the adult corpus collossum. (d) Quantification showing reduced numbers of Olig2+ cells in corpus collossum. (e-f) Representative images (e) and quantification (f) of Olig2+/APC+ cells, showing the total number of OL lineage cells is reduced in the P21 cerebellum of *Olig1-/-* mice. (g-j) Representative images showing no colocalization of the interneuron markers GAD67 and PV (both in red) with the pyramidal cell marker Tbr1, Olig2, Iba1, and GFAP (all in green). (k-m) Stereologic analysis of GAD67 immunohistochemistry in the cortex demonstrating a significant increase in the estimated total number of GAD67+ cells (k) and the density of GAD67+ cells (m), but no change in the volume of the cortex (l) (For all quantifications: mean +/- SEM, n = 3-4; *p<.05, **p<.01, ***p<.005; 2 tailed unpaired student's t test). (a') scale bar = 500 μm, (j) scale bar = 50 μm.

a

a'

Olig2

CTX
CC
ST

CTX
CC
ST

b

**

Olig2 / CTX

WT   Olig1-/-

c

c'

Plp (P50)

cc

cc

d

*

Olig2 / CC

WT   Olig1-/-

e

e'

Olig2/APC

P21

P21

f

***

Olig2+ / CB

WT   Olig1-/-

g

PV / Tbr1

h

PV/Olig2

i

GAD67/Iba1

j

GAD67/GFAP/DAPI

k

Estimated Cell #

*

Olig2+ Cells

WT   Olig1-/-

l

CTX Density

*

Olig2+ Cells / mm²

WT   Olig1-/-

m

CTX Volume

Area mm²

WT   Olig1-/-
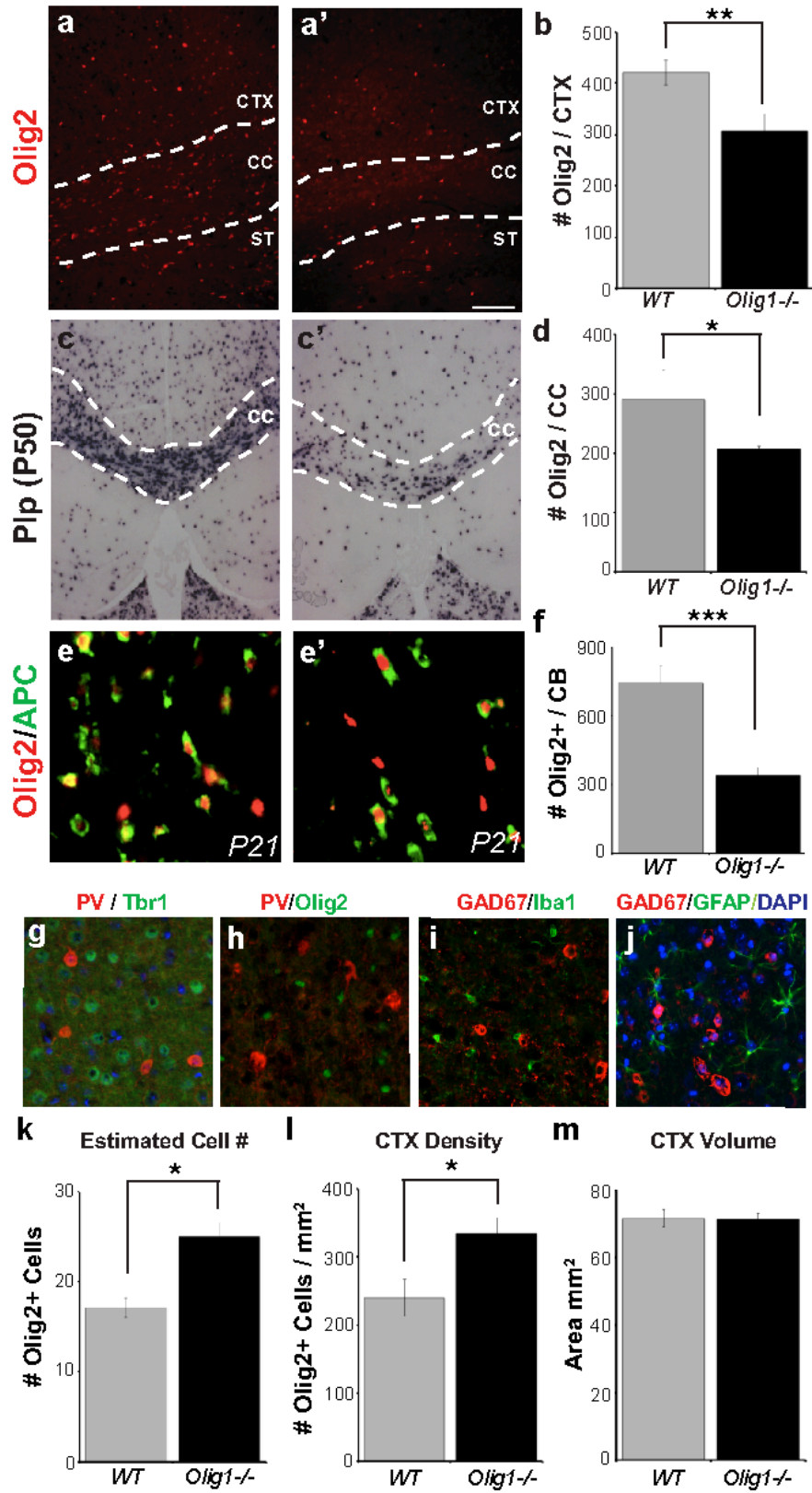
Figure 3. No change in inhibitory events on cortical pyramidal cells and normal expression of the postsynaptic protein Gephyrin in *Olig1-/-* mice

(a) Representative traces (left) and graphs (right) showing no difference in the frequency or amplitude of spontaneous inhibitory postsynaptic potential (sIPSPs) in *Olig1-/-* cortical pyramidal cells. (b) Representative traces (left) and graphs (right) showing no difference in the frequency or amplitude of mini inhibitory postsynaptic potential (mIPSPs) in *Olig1-/-* cortical pyramidal cells. (c) Representative images and quantification of Gephyrin+ (red) puncta colocalizing the presynaptic protein VGAT (green) and DAPI (blue). There is not a significant increase in the number of Gephyrin+ puncta. Note Gephyrin is expressed at the postsynapse and is necessary to make active inhibitory synapses. Images in the bottom panel are higher magnification images of the staining shown in the top panel. (For all quantifications: mean +/- SEM, p-values derived from a 2-tailed unpaired student's t test). Scale bars = 5 µm.

a

sIPSCs

WIld Type

Olig1 -/-

100 ms | 50 pA

Frequency (Hz) — p=0.99 — WT, -/-

Amplitude (pA) — p=0.76 — WT, -/-

b

mIPSCs

WIld Type

Olig1 -/-

Frequency (Hz) — p=0.62 — WT, -/-

Amplitude (pA) — p=0.09 — WT, -/-

c

Wild Type   *Olig1 -/-*

vGAT / Gephyrin / DAPI

WT   *Olig1 -/-*   WT   *Olig1 -/-*

VGAT / Gephryn — n.s. — WT, -/-
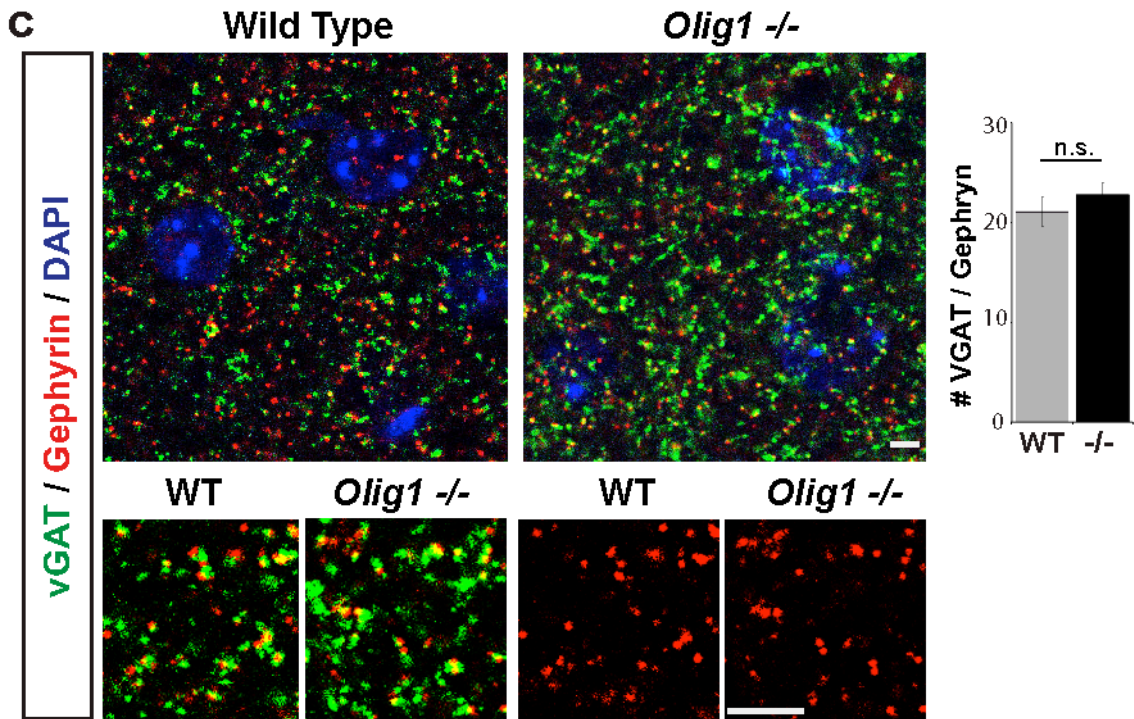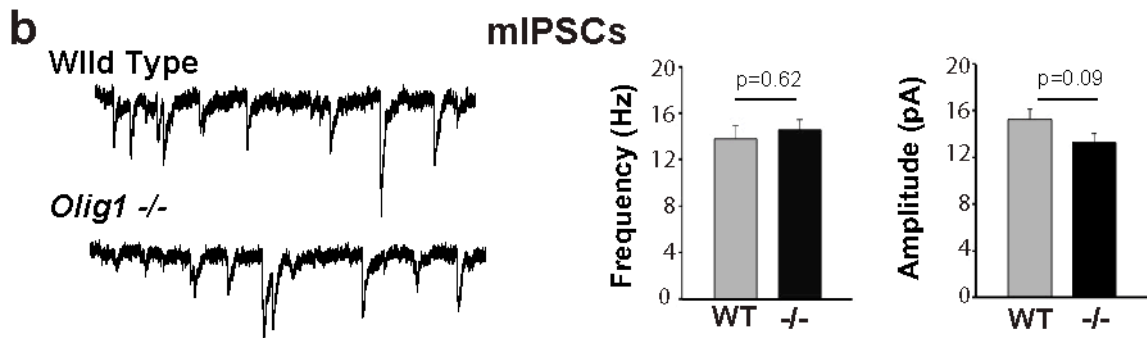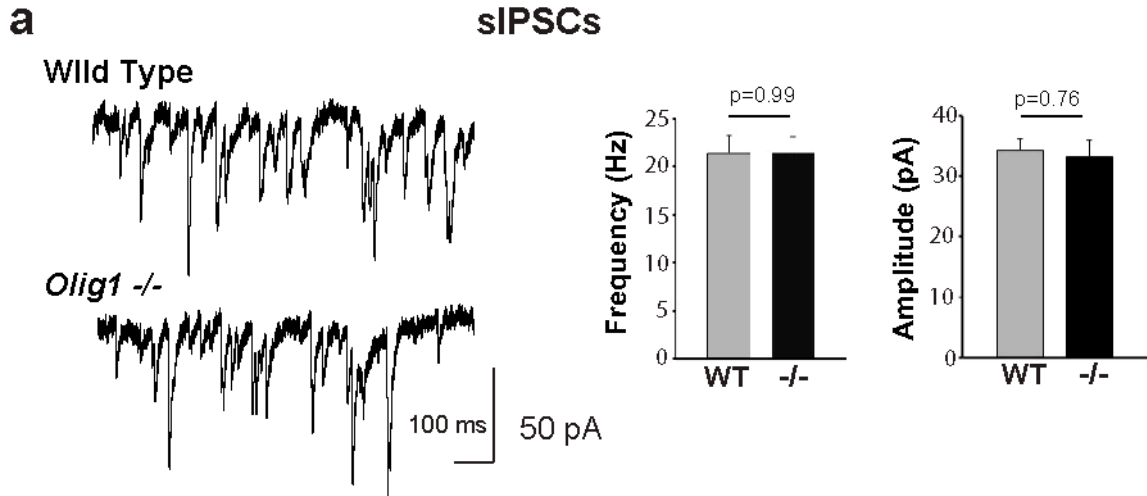
Figure 4. Increase in the number of interneurons in *Olig1-/-* cerebellum and olfactory bulb

(a) Low magnification imagea of MBP (green) and DAPI (blue) of juvenile cerebellum. The box represents the region where the images in b-d were taken. (b) Image taken of P21 cerebellum showing Pax2+ INs (red) and anatomy of cerebellar lobules with white matter defined by dense MBP immunoreactivity (green) and the granule layer defined by dense DAPI staining (blue). Note the ectopic presence of Pax2+ INs in the white matter (arrows) in the *Olig1-/-* mice. (c) Single channel image of Pax2 (red) staining in panel a demonstrating increased numbers of Pax2+ INs in *Olig1-/-* mice. (d) Representative images of immunohistochemistry showing increased numbers of cerebellar IN precursor cells expressing AP-2ß in *Olig1-/-* versus WT mice at P7. (e) Quantification of Pax2+ cells in the P21 cererbellum demonstrating a statistically significant increase in Pax2+ cells *Olig1-/-* versus WT mice. (f) Low magnification image of the olfactory bulbs of WT (f) vs *Olig1-/-* (f') mice injected with BrdU at P2 stained for BrdU (red) and DAPI (blue). (g) Higher magnification images of the granule cell layer corresponding to the box inset labeled (g & g') in panel (f). (h) Higher magnification images of the glomerular layer corresponding to the box inset labeled (h & h') in panel (f). (i-j) Quantification of the number of BrdU+ cells in the P50 granule cell layer (GRL) and glomerular layer (GL) respectively, following BrdU injection at P2 demonstrating a statistically significant increase in BrdU+ cells in *Olig1-/-* versus WT mice. (c') scale bar = 50 μm, (f) scale bar = 500 μm, (g) scale bar = 50 μm. (For all quantifications: mean +/- SEM, n = 3; *p<.05, **p<.01, 2 tailed unpaired student's t test. Abbreviation: GRL = Granule layer, GL = Glomerular layer.

Cerebellum

Olfactory Bulb

A MBP/DAPI

A' B-D

WT   ***Olig1-/-***

B Pax2/MBP/DAPI *P21*   **B'** *P21*

C Pax2 *P21*   **C'** *P21*

D AP-2-ß+ *P7*   **D'** *P7*

E # Pax2+ Cells (x 10²)
*
WT   Olig1-/-

P2 (BrdU) ➝ P50 (Sac)

WT   ***Olig1-/-***

F BrdU/DAPI   G   H   **F'** G'   H'

G BrdU/DAPI *GRL*   **G'** *GRL*

H BrdU/DAPI *GL*   **H'** *GL*

I GRL
BrdU+ Cells (x 10²)
**
WT   Olig1-/-

J GL
BrdU+ Cells (x 10²)
**
WT   Olig1-/-
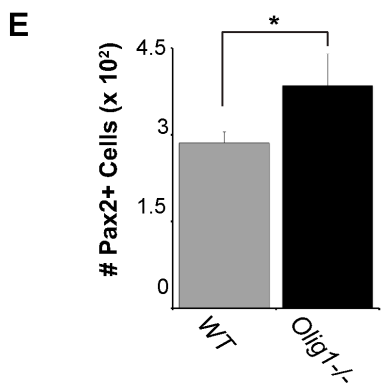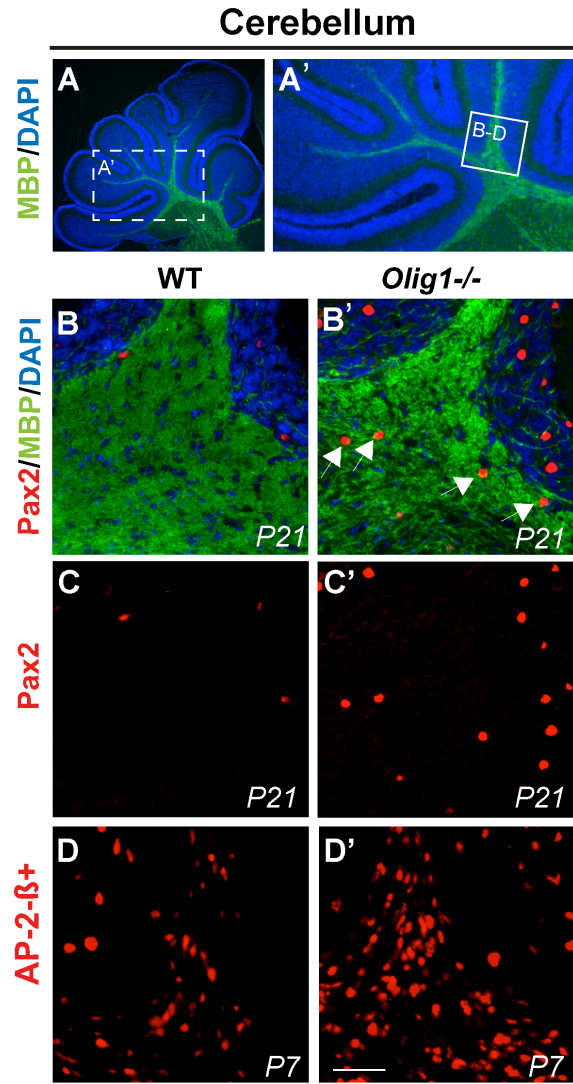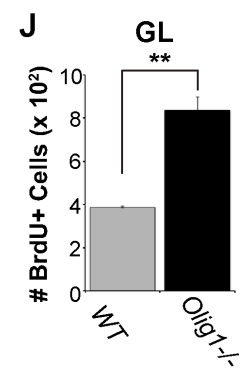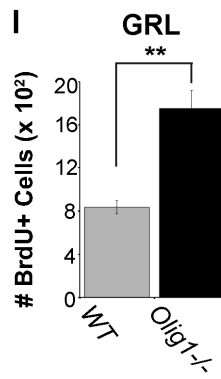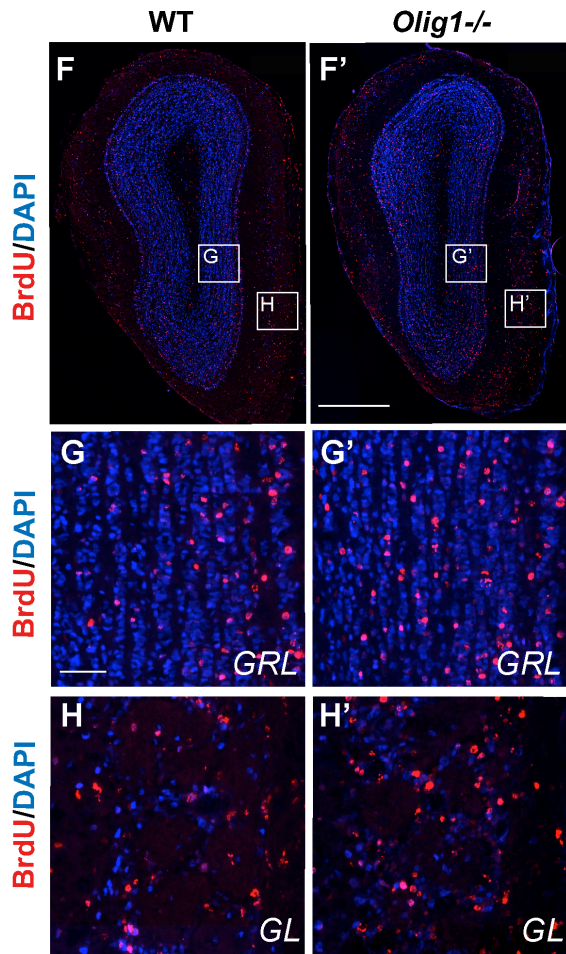
Figure 5. *Olig1* **is expressed in ventral telencephalic progenitors for interneurons**

(a-c) Anterior to posterior serial sections of *in situ* hybridization for *Olig1* demonstrating expression in the ventricular zone (VZ) of dorsal embryonic septum (sep), ventral medial ganglionic eminence (vMGE) and anterior enteropeduncular area (AEP). (d) A cartoon of the domain in which *Olig1* is expressed in the ventricular zone. (a'-c') Higher magnification view of the regions expressing *Olig1*. These regions are denoted by the boxes and arrows in panels a-c. The bracket labeled e-f in image b' defines the regions shown in panels e-f. (e) Confocal projections showing that Olig1 (green, e) colocalizes the radial glia protein Nestin (red, e'; merged image e"). (f) Confocal projections showing that Olig1 (green, f) colocalizes Nkx2.1+ progenitors (red, f'; merged image f") which are known to give rise to both INs and OLs. (g) Representative image of fate mapping in cerebral cortex from *Olig1$^{cre/+}$* mice crossed to the *Caggs-Gfp* reporter mouse, showing approximately ~35% of GABA+ INs (red) are derived from *Olig1+* progenitors as defined by the expression of the GFP+ (green) reporter protein. (h) Quantification of the proportion of a panel of IN markers (GABA, PV, SST, CR, or NPY) colabeling GFP (percentage +/- SEM). Note the preferential labeling of PV+ subtypes. (c) scale bar = 500 µm, (c') scale bar = 200 µm, (e",f") scale bar = 20 µm. Additional abbreviations: lge, lateral ganglionic eminence; cge, caudal ganglionic eminence.

Olig1 ISH (E15)

a

MGE
Sep

b

MGE
Sep

c

MGE
AEP

d

IGE
CGE
MGE
SEP
AEP

Olig1 expression in NSCs

a'

MGE
Sep

b'

e - f

MGE
Sep

c'

MGE
AEP

e Olig1   e' Nestin   e" Merge

f Olig1   f' Nkx2.1   f" Merge
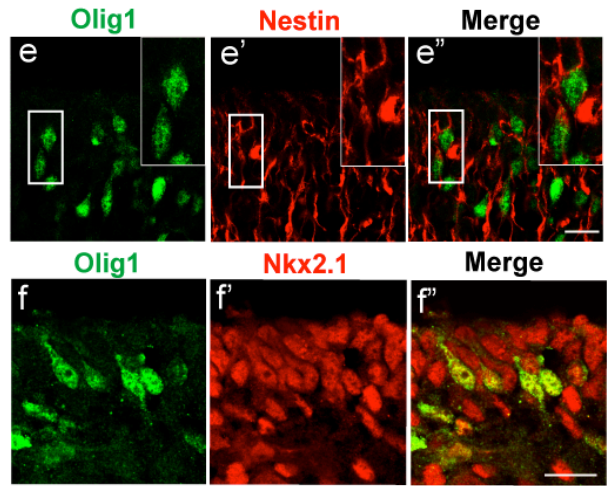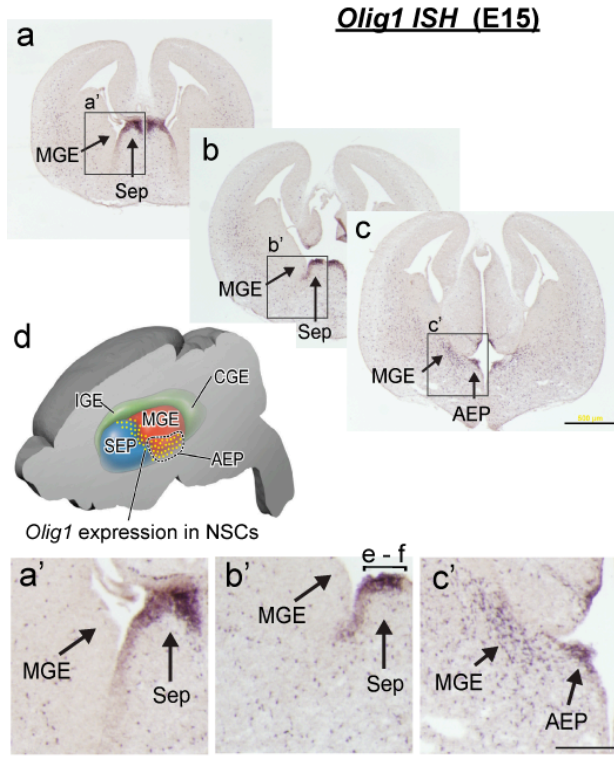
Olig1^cre/+ x *Caggs-GFP* fate map (P50)

g GFP / GABA

h

% GFP+

GABA SST PV CR NPY

57
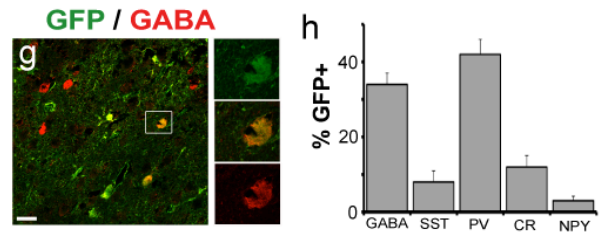
Figure 6. *Olig1* **represses prointerneuron genetic programs in embryonic brain**

(a-b) Representative images of *In situ* hybridization for *Dlx2* in two anterior to posterior sections

of E15.5 forebrain showing upregulation of *Dlx2* in the AEP and ventral MGE (a' and b'

respectively) denoted by the box and arrowheads respectively. (c-d) High magnification of *Dlx2*

expression delineated in the boxed region (a-b). The brackets in (c) emphasize the expansion

of the domain expressing *Dlx2* in the AEP and the arrowheads denote increased expression in

ventral MGE. (e-f) High magnification images showing similar upregulated expression of *Dlx1*

and (g-h) the proneural gene *Lhx6.* (i) Graph showing quantitative PCR results of cDNA

samples derived from RNA samples taken from the E15 ventral forebrain of *Olig1*-null and WT

mice. Note upregulation of the proneural genes *Dlx2*, *Vax1* and *Sp8*. (j-k) Representative

images of GABA (green) and BrdU (red) birth dating analysis in P50 cortex demonstrating that

more GABA+ INs are labeled by BrdU injected at E16. Higher magnification images

demonstrating colabeling are shown in j'-k'. (l-m) Representative images of PV (green) and

BrdU (red) birth dating analysis in P50 cortex demonstrating that more PV+ INs are labeled by

BrdU injected at E16. Higher magnification images demonstrating colabeling are shown in l'-m'.

(n-o) Quantification of GABA+ (n) or PV+(o) cells colocalizing BrdU. BrdU was injected at E16.

(mean +/- SEM, n = 3; *p<.05, 2 tailed unpaired student's t test). (b') scale bar = 500 µm, (d')

scale bar = 200 µm, (m,m') scale bar = 50 µm.

Embryonic Forebrain (E15)

WT   *Olig1 -/-*   WT   *Olig1-/-*

Dlx2

Dlx2

Dlx1

Lhx6

i.

Primary Motor Cortex (P50)

WT   *Olig1 -/-*   WT   *Olig1 -/-*

GABA / BrdU

PV / BrdU
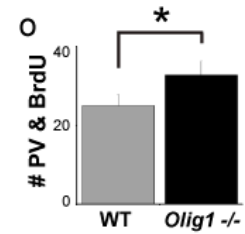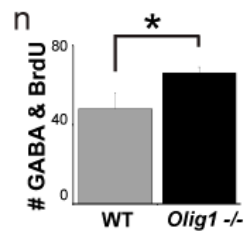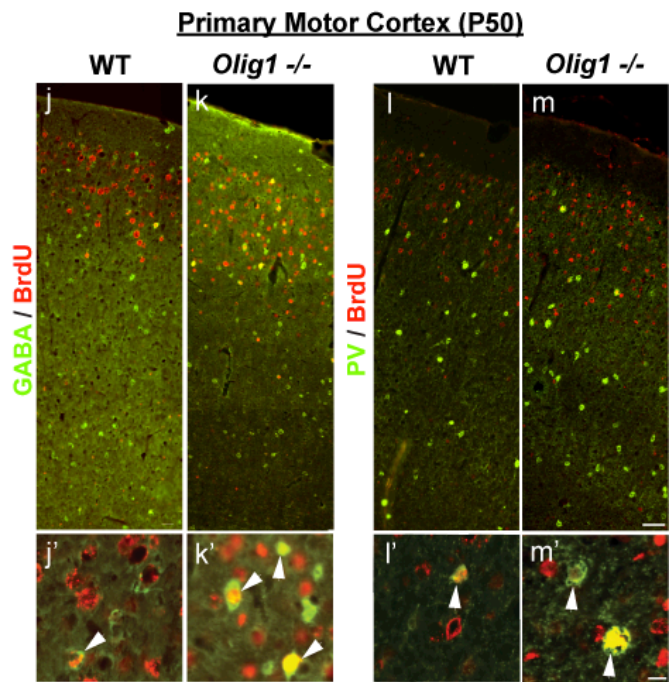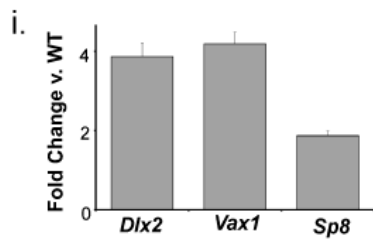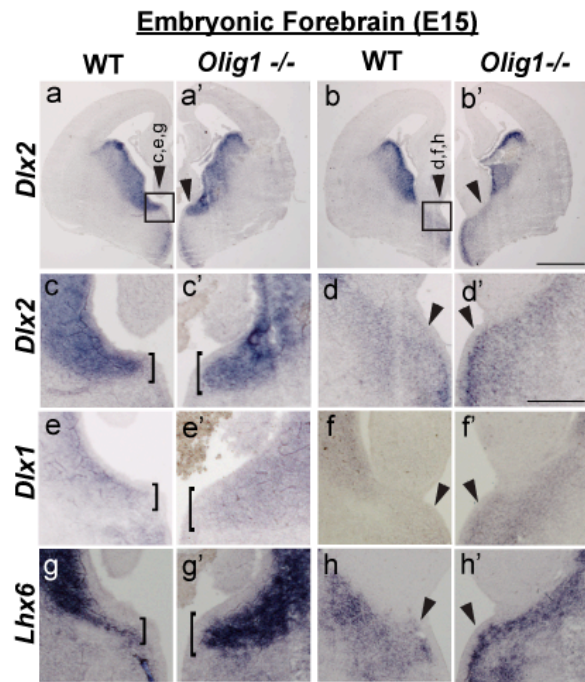
Figure 7. Reduced OPC numbers, but no change in proliferation in E15 *Olig1-/-* embryos

(a-b) Representative images of *in situ* hybridization for *Plp*, a marker of oligodendrocyte precursors showing a reduction in the number OPCs in the E15 mouse forebrain. (b-c) Representative images (b) and quantification (c) of Sox10+ OPCs showing the total number of OPCs is reduced in the forebrain of E15 *Olig1-/-* mice. (d-f) Representative images (d-e) and quantification (f) of PH3 immunohistochemistry showing the number of PH3+ mitotic cells is unchanged in the MGE, AEP, and Septum of E15 *Olig1-/-* mice. (For all quantifications: mean +/- SEM, n = 3; *p<.05; 2 tailed unpaired student's t test). (a') scale bar = 500 μm. Abbreviations: aMGE = anterior medial ganglionic eminence, pMGE = posterior medial ganglionic eminence, AEP = anterior enteropeduncular area, VZ = ventricular zone, SVZ = subventricular zone.
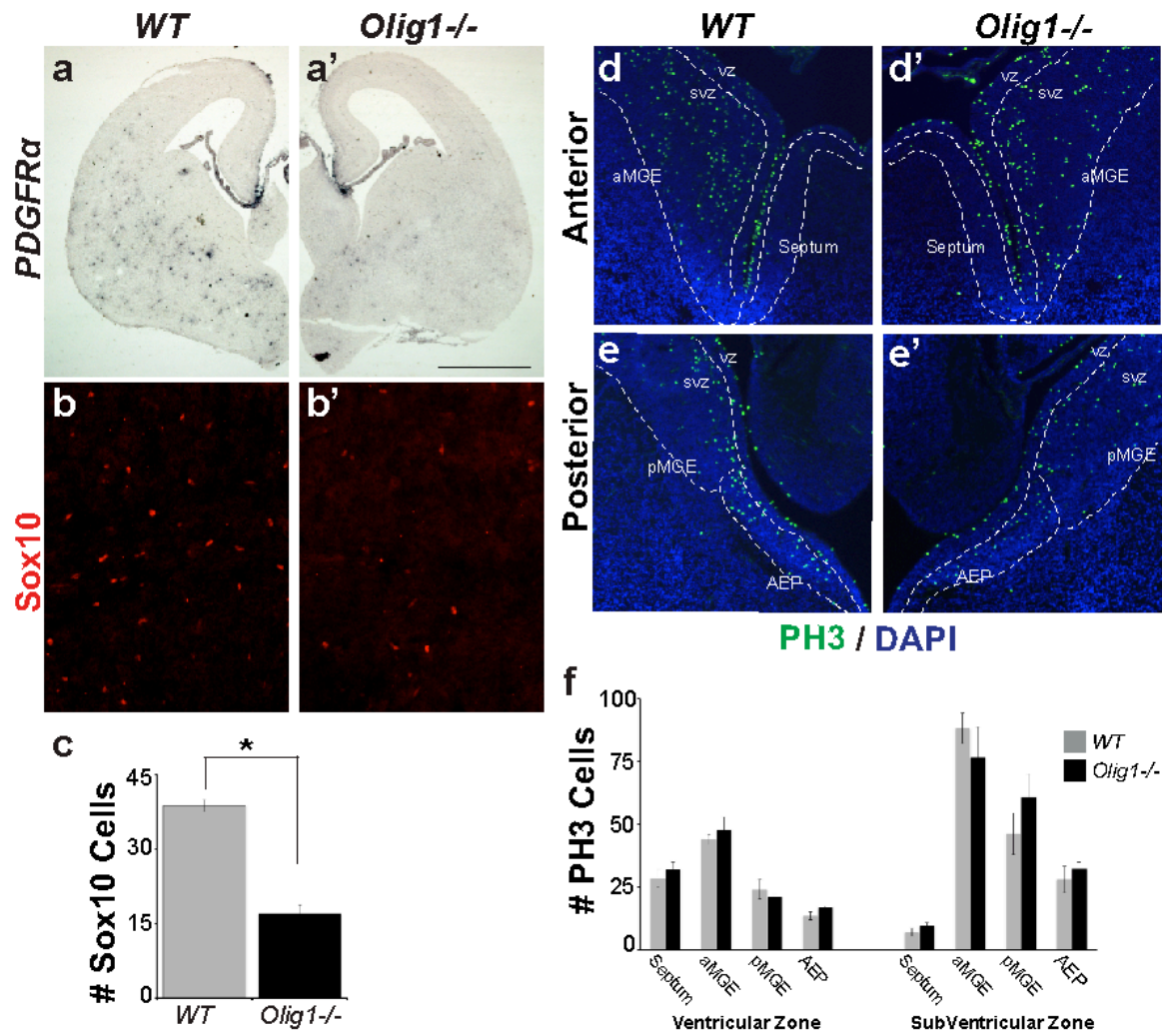
Figure 8. GAD67 mRNA expression is normal in *Olig2 -/-* E15 embryos

Images of *in situ* hybridization of GAD67 in *Olig2 -/-* mice demonstrating that interneuron

precursor number is not regulated by *Olig2*. Scale bar = 500 µm.

WT | Olig1 -/-

GAD67

a

a'

500 µm
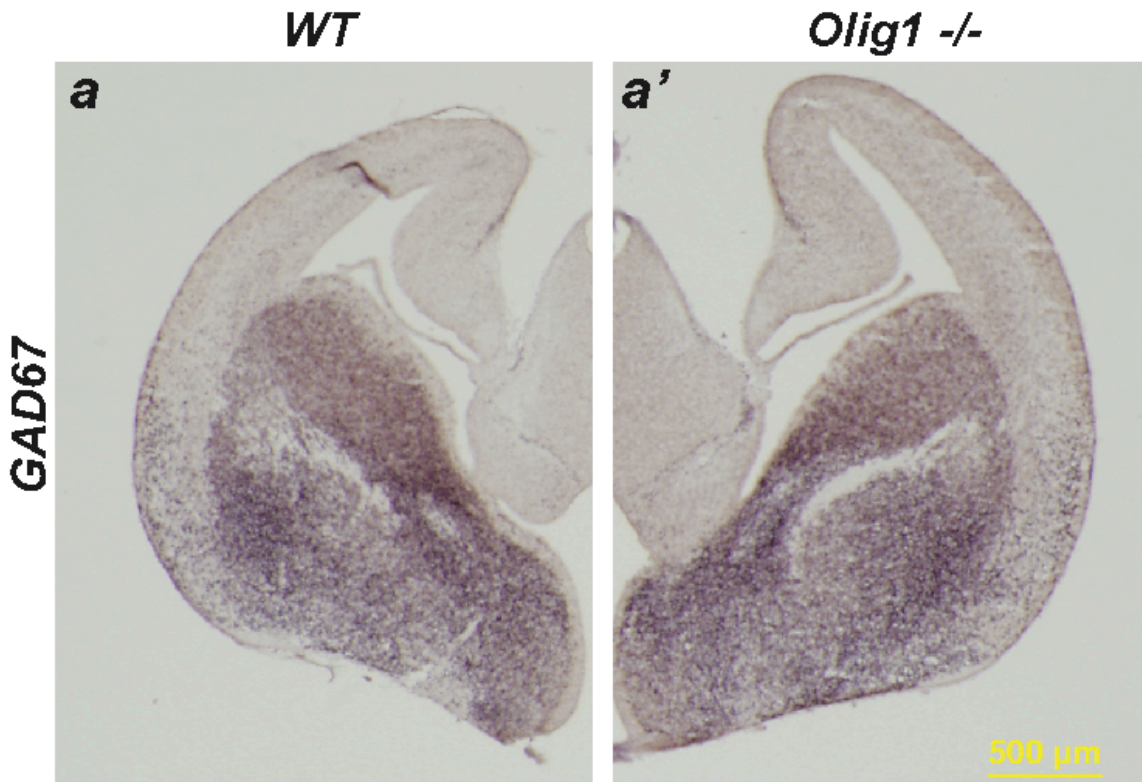
Figure 9. *Olig1* **deletion causes expansion of** *Dlx2* **expression in neonatal SVZ, but does not extend the period of cortical interneuron genesis.**

(a-d) Representative images of *Dlx2* expression at P0 in an anterior (a-b) to posterior (c-d) serial coronal sections demonstrating upregulation of *Dlx2* expression in anterior sub ventricular zone and ectopic expression of *Dlx2* in dorsal SVZ of *Olig1-/-* mice. (a'-d') Higher magnification images of the boxed region in (a-d). (e-f) Representative images of Parvalbumin (PV, green, top panel a'), GABA (green, bottom panel e') and BrdU(red, e'' & f'') of P50 *Olig1-/-* cortex after injection with BrdU (red) at P2. Note there is no colocalization of BrdU with IN markers (arrows) suggesting that IN neurogenesis does not extend past its normal developmental epoch in *Olig1-/-* mice. (d') scale bar = 500 µm (b') scale bar = 50 µm.
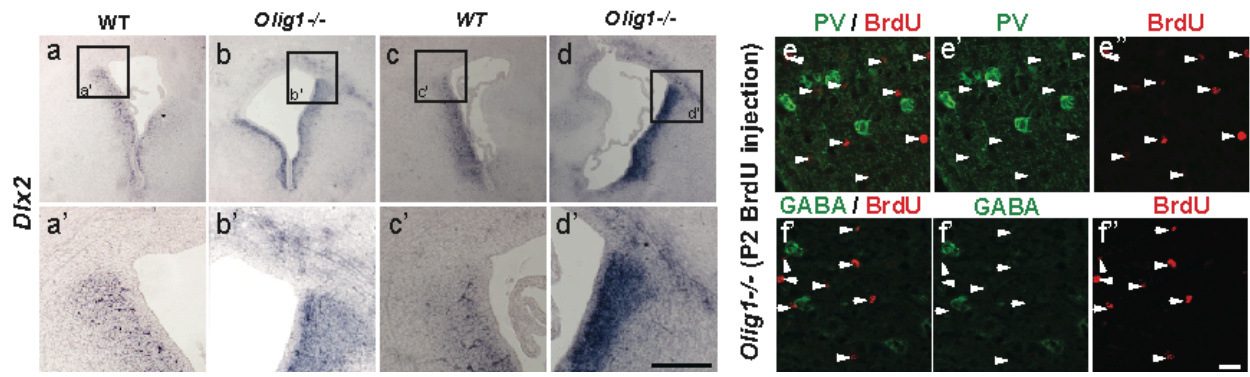
Figure 10. *Olig1* **regulates interneuron versus oligodendrocyte cell fate in neural stem cell cultures**

(a) Western blots from WT and *Olig1-/-* neurospheres for the neuronal protein Tuj1, Dlx2, and Olig2 showing increased expression of neuronal proteins and decreased expression of Olig2.

(b) Quantification of number of DCX+ cells per neurosphere identified by immunohistochemistry

(c-d) Representative images of neural progenitor monoloyer cultures derived from P3 WT and *Olig1-/-* SVZ, differentiated for 1 week and stained for DCX (c) and GABA (d). (e) Quantification of the number of DCX and GABA cells captured at 3 defined coordinates in chamber slide wells reveals increased numbers of DCX and GABA+ cells in *Olig1-/-* versus wild type. (f-h) Representative images of neural progenitor monolayer cultures derived from P3 WT and *Olig1--/-* SVZ, differentiated for 1 week and stained for NG2 (g), O4 (h) and GalC. (i) Quantification of the number of NG2, O4 and GalC cells captured at 3 defined coordinates in chamber slide wells reveals decreased numbers of O4 and GalC+ cells in *Olig1-/-* versus wild type. (For all quantifications: mean +/- SEM, n = 3 experiments, 4 slide wells per experiment; *p<.05, **p<.01, ***p<.005, 2 tailed unpaired student's t test). (h) scale bar = 50 µm.

Neurosphere Cultures

a
Tuj1
Dlx2
Olig2
β- Actin

WT -/-

b
DCX+ / Sphere
**
WT -/-

Adherent Cultures - Neuronal Lineage

GABA   DCX

WT
c   d

Olig1-/-
c'   d'

e
cells / field
***   **
WT -/- WT -/-
DCX   GABA

Adherent Cultures - Oligodendrocyte Lineage

NG2   O4   GalC

WT
f   g   h

Olig1-/-
f'   g'   h'

i
cells / field
***   ***
WT -/- WT -/- WT -/-
NG2   O4   GalC

Figure 11: *Olig1* is a direct repressor of *Dlx1/2* at the *I12B* intergenic enhancer.

(a) 1 μm confocal projection demonstrating that Olig1 (green, a') and Dlx2 (red, a'') does not

colocalize Olig1 in VZ. (b) Schematic of the *Dlx1/2* bigenic region showing location of *I12B*

intergenic enhancer and 3 E-box sites. (c) Images of gels from electrophoretic mobility shift

assays (EMSA) for the 3 *I12B* E-boxes (WT, wildtype and MUT, mutated) in presence or

absence of *Olig1* protein. Note the strongest and most specific affinity for E-box site 1. (d)

Increasing concentrations of *Olig1* protein show dose-dependent affinity of *Olig1* for E-box 1 WT,

but not for E-box 1 MUT. (e) Supershift assay demonstrates that Olig1 antibody, but not control

IgG antibody inhibits binding of *Olig1* protein to E-box site 1. (f) Quantification by densiometry

of inhibition of DNA binding by incubation of Olig1 protein with Olig1 or control antibody (student

T test * $p < 0.05$) (g) Luciferase assays demonstrate that Olig1 is a transcriptional repressor

capable of reducing *Dlx2* induced *I12B* luciferase activity to 40% control levels (student's t test

***$p < 0.001$). (a'') scale bar = 50 μm.

a Olig1 / Dlx2

a' Olig1

a" Dlx2

b

8.3 kb

Dlx1 I12b *Dlx2*

1   2   3   I12b   3   2   1   *Chr2*

1   I12b   2   3

E-box sites

c

| 1-WT | 1-MUT | 2-WT | 2-MUT | 3-WT | 3-MUT |
| − + | − + | − + | − + | − + | − + | Olig1

d

1-WT   1-MUT   Olig1

e

− + + + +   Olig1
− − + − −   Olig1 ab
− − − − +   control IgG

f

Relative Shift (AU)

*   n.s.

no antibody
with antibody

g

Relative I12/b Luciferase Activity (AU)

***

pCAGGS-Dlx2	+	+
pCAGGS-Olig1	−	+
pCAGGS-eGFP	+	+

69
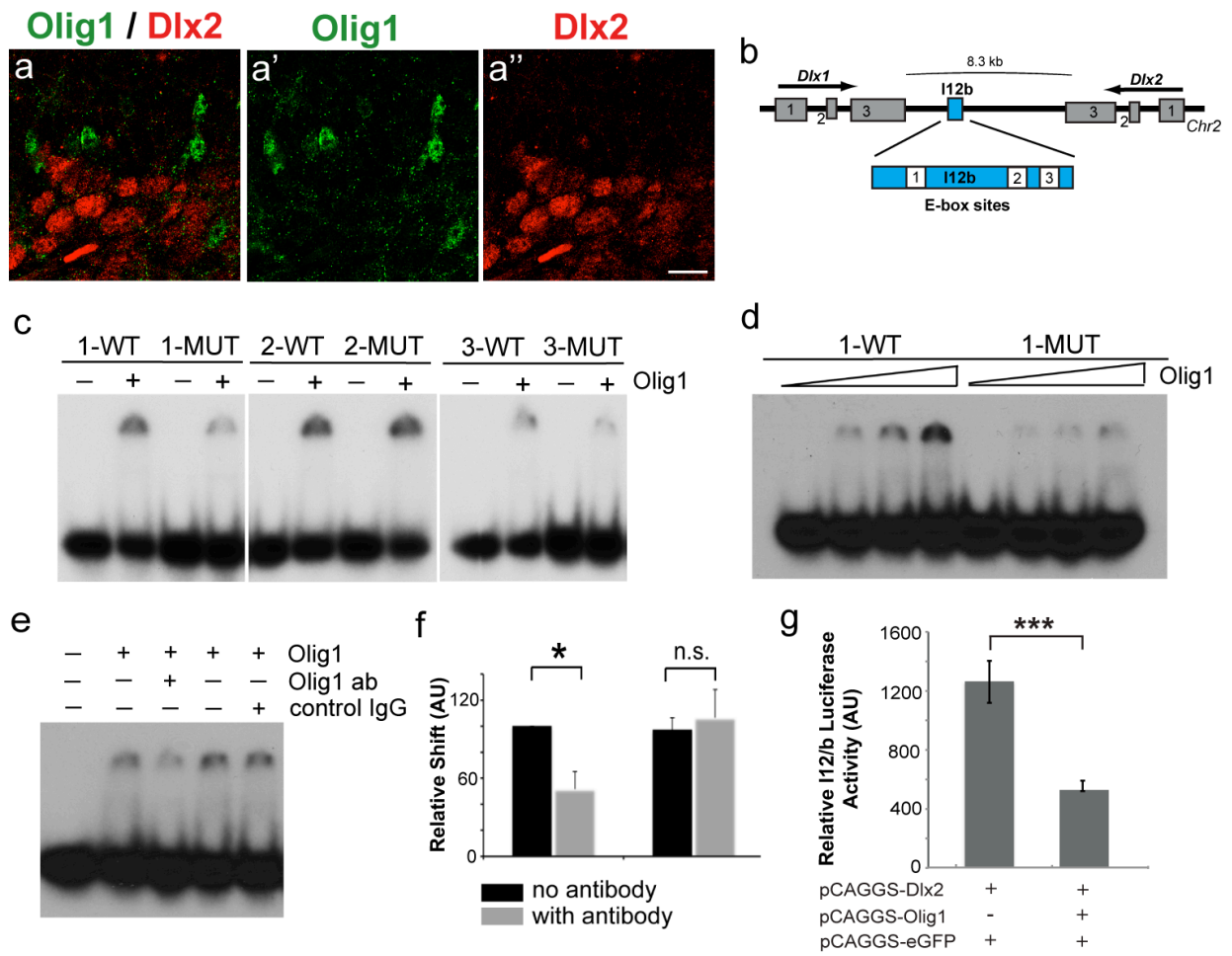
Figure 12. E-box sites in the *I12b* enhancer. (a) Nucleotide sequence of the *I12b* enhancer with nucleotide sequences highlighted. (yellow = E-box site 1, green = EBox site 2, red = E-box site 3). (b) Table listing WT and Mutant (MUT) DNA sequences used for EMSA assays.

(a)

E-boxes in *I12b* enhancer:

CACAGCTTAATGATTATCAAAATGACTCTTTTCTGCAAAAAAAAGACCCCAAA
GTGCGCGTA<mark>CAGCTG</mark>CAAACCCAAGAGGGTCAGCATCATTTCACTGTATTCT
CTTCTTGATTACAAGCCGGGCCCATCAAACACAACATAATTACAGTAATTTCA
GGTTTATTTATTCTAATGCAGTTTCCCCATCTCTCTGGTAATTATGAGCAATTT
TTTCGCCCAGGGAATCTTTTTGCATTAACAAAAGAGATAACGCACTGAAAGC
CAAATTTGCTGCGCATTGAGAAAAGGGAAAAAAAAATCAAATAGGTGCGAGC
TGCCATCTCTGCAATTCTCCGGTACCGGAGCCCGCAAATTGCTTG<mark style="background-color:#00ff00">CAGGTG</mark>T
ATGGAGCAAGCTTGTCAATGGCCGGGCCTCCAAATTAG<mark style="background-color:red">CAAATG</mark>CACAGCA
GCGAAGTAATGAAGACAGACTTAGCAAAATTGCTAAACAACAGATACCTCTT
TAATATCCTCTCTCTCACACACGAGCTCTAAAGG

(b)

Wild type and mutated Ebox nucleotide sequences for *Olig1* EMSA

E-box 1 WT	I12b-1 AGCTGTGCGCGTACAGCTGCAA I12b-2 AGCTTTGCAGCTGTACGCGCAC
E-box 2 WT	I12b-3 AGCTTGCTTGCAGGTGTATGGAGC I12b-4 AGCTGCTCCATACACCTGCAAGCA
E-box 3 WT	I12b-5 AGCTATTAGCAAATGCACAGC I12b-6 AGCT GCTGTGCATTTGCTAAT
E-box 1 MUT	I12b-9 AGCTGTGCGCGTATAGCCTCAA I12b-10 AGCTTTGAGGCTATACGCGCAC
E-box 2 MUT	I12b-11 AGCTTGCTTGTAGGCTTATGGAGC I12b-12 AGCTGCTCCATAAGCCTACAAGCA
E-box 3 MUT	I12b-13 AGCTATTAGTAAACTCACAGC I12b-14 AGCT GCTGTGAGTTTACTAAT

71

Figure 13. Increased interneuron production in *Olig1*-null animals requires *Dlx1/2* function *in vitro* and *in vivo*

(a) Schema illustrating the *Dlx1/2* flox targeting vector and strategy to knockout *Dlx1/2* within the *Olig1* lineage by generating *Dlx1/2* floxed mice (*Dlx1/2$^{fl/fl}$*) and crossing them to *Olig1-cre* knockin mice (*Olig1$^{cre(KI)/cre(KI)}$*). (b) Long range PCR for the *Dlx1/2* floxed allele confirming successful homologous recombination and integration of the full targeting construct into founder (F1) mice. (c) Representative image of PCR for the wild type and *Dlx1/2* floxed alleles demonstrating successful derivation of floxed homozygous mice. (d) Representative images of PV+ cells in cerebral cortex of P60 WT, *Olig1$^{cre(KI)/cre(KI)}$*, and *Olig1$^{cre/cre}$* x *Dlx1/2$^{fl/+}$* mice demonstrating that heterozygosity for *Dlx1/2* in the *Olig1* lineage is sufficient to rescue the increase in PV INs in *Olig1*-null mutants *in vivo*. (e) Representative images of GAD67+ cells in cerebral cortex of P60 WT, *Olig1$^{cre(KI)/cre(KI)}$*, and *Olig1$^{cre(KI)/cre(KI)}$* x *Dlx1/2$^{fl/+}$* mice demonstrating that heterozygosity for *Dlx1/2* in the *Olig1* lineage is sufficient to rescue the increase in GAD67 INs in *Olig1*-null mutants *in vivo.* (f-g) Quantification of the number of PV and GAD67 expressing cells, respectively, in combined counts of motor and somatosensory cortex. (mean +/- SEM, n = 3, *p<.05, 2 tailed unpaired student's t test). Representative images (h-i) of GABA+ and Tuj1+ cells, respectively, generated by neural stem cell monolayer cultures derived from MGE of E14 WT, *Olig1$^{cre/cre}$* and *Olig1$^{cre(KI)/cre(KI)}$* x *Dlx1/2$^{fl/fl}$* mice, demonstrating that genetic ablation of *Dlx1/2* in the *Olig1* lineage is sufficient to rescue the increase in GABAergic INs in *Olig1*-null mutants *in vitro*). (j) Representative images of PDGFRa+ OPCs, demonstrating that *Dlx1/2* deletion in *Olig1* lineage cells rescues the diminution of the OL population observed in *Olig1* knockouts. (k-m) Quantification of the number of GABA+, Tuj1+, and PDGFRa+ cells respectively in NSC monolayer cultures (mean +/- SEM, n = 3 experiments, 2 slide wells per experiment; *p<.05, **p<.01, 2 tailed unpaired student's t test). (e") scale bar = 50 µm.

a

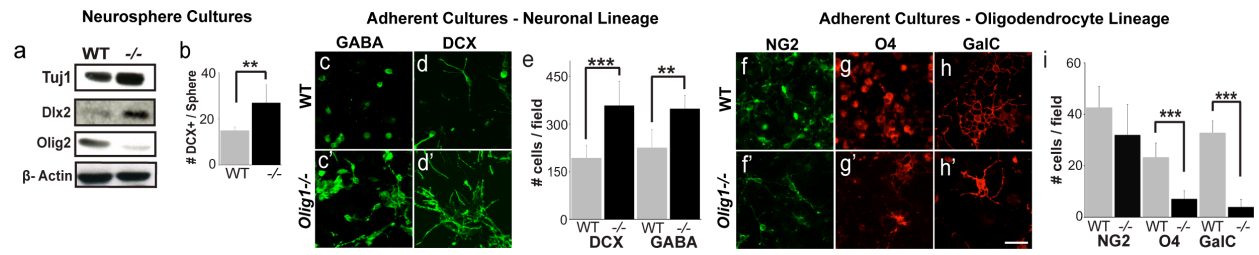Dlx1   Dlx2   Chr2

Homologous Recombination

Dlx1   loxP   8.3 kb   frt NEO frt   loxP   3 kb   MC1-HSV-TK

3.5 kb

+ R26R-Flpe

Dlx1   loxP   8.3 kb   Dlx2   frt loxP   Chr2

+ Olig1 creKI/creKI

Dlx1   loxP   Dlx2   Chr2

b long range PCR
short arm   long arm

c Dlx flox PCR
fl/+   fl/fl   fl/+   +/+

NSC Monolayers - Neuron & OL Lineage

WT   *Olig1^{creKI/creKI}*   *Olig1^{creKI/creKI} x Dlx^{fl/fl}*

GABA   h   h'   h"

Tuj1   i   i'   i"

PDGFRα   j   j'   j"

WT   *Olig1^{creKI/creKI}*   *Olig1^{creKI/creKI} x Dlx^{fl/+}*

PV   d   d'   d"

GAD67   e   e'   e"

f
PV

* *

WT   Olig1^{-/-}   Olig1^{-/-} x Dlx 1/2^{fl/+}

g
GAD67

* *

WT   Olig1^{-/-}   Olig1^{-/-} x Dlx 1/2^{fl/+}

k GABA - INs
GABA / field

* *

WT   Olig1^{-/-}   Olig1^{-/-} x Dlx 1/2^{fl/fl}

l Tuj1 - Neurons
Tuj1 / field

*

WT   Olig1^{-/-}   Olig1^{-/-} x Dlx 1/2^{fl/fl}

m PDGFRα - OPCs
PDGFRα / field

* **

WT   Olig1^{-/-}   Olig1^{-/-} x Dlx 1/2^{fl/fl}

73

Figure 14. Model of the mechanism of *Olig1* function in the ventral telencephalon

(a) Schematic demonstrating genetic interaction between *Olig1* and *Dlx1/2* control specification of INs versus OLs. *Olig1* inhibits *Dlx1/2*, which are necessary for the production of interneurons and inhibit OL specification. (b) *Olig1* inhibits production of INs from the vMGE, AEP & septum.

a

Olig1 ———⊣ Dlx1/2 ⟶ INs

Olig1 ⟶ OPCs

Dlx1/2 ———⊣ OPCs

b

Wild Type

CTX

LGE

MGE

Sep & AEP

Interneurons (INs)

Olig1 -/-

CTX

LGE

MGE

Sep & AEP

Increased IN Production
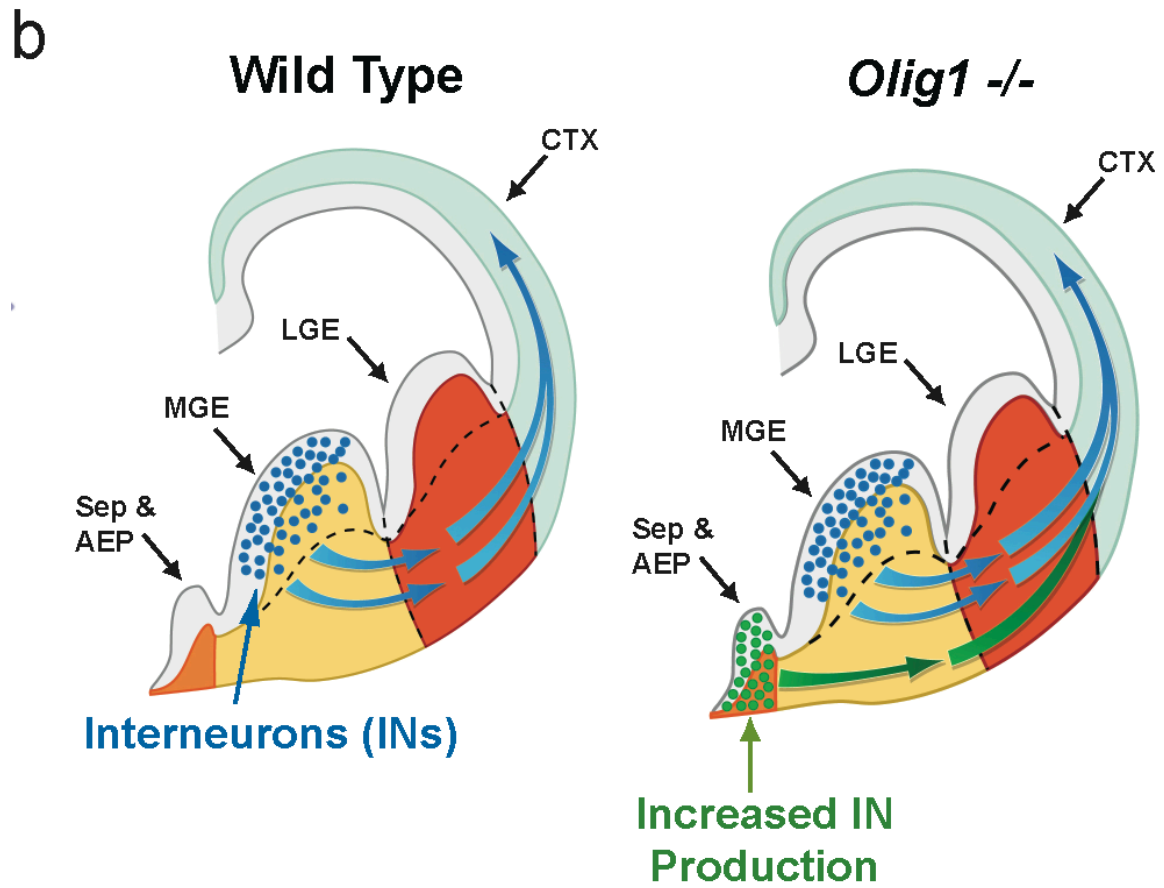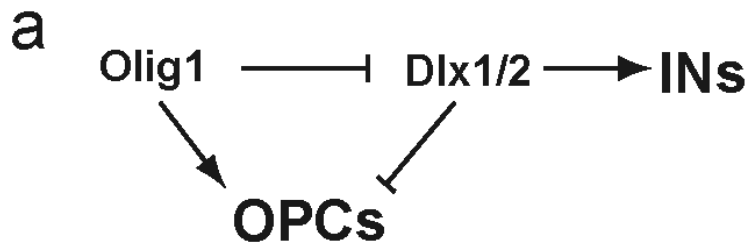
Chapter 4:

Olig1 promotes OPC specification and remyelination after

forebrain neonatal hypoxic-ischemia

Introduction: Roles for Olig1 in white matter repair after demyelinating injury

A previous study from our lab demonstrates *Olig1* is required for remyelination following toxin induce demyelination of the spinal cord. Upon demyelination Olig1 expression transitions from the cytoplasm and the nucleus in OPCs and is subsequently regulates genetic programs for remyelination. *Olig1* in this context is not however required for OPC recruitment (Arnett et al., 2004)

Demyelination and hypoxic-ischemic damage activate both locally proliferating OPCs in the white matter, as well as astroglial like subventricular zone (SVZ) progenitors that produce neurons and OPCs that migrate into the lesion site. Selective damage to the white matter biases SVZ progenitor fate towards the OL lineage (Jablonska et al., 2010; Menn et al., 2006). We hypothesized that *Olig1* might play a role in both directing neural progenitors towards the OL fate and subsequently directing OPCs to remyelinate the damaged white matter.

Olig1 is necessary for myelin repair after forebrain HIE

To evaluate functions for *Olig1* in the injury response, we subjected *Olig1*-null and wild type neonatal animals to hypoxic-ischemia using the procedure of Rice and Vannucci and animals were sacrificed two or four weeks post injury. As shown in Figure 1, *Olig1*-/- animals demonstrated deficient myelination following injury compared to controls, as demonstrated by a reduction in MBP in the corpus callosum, striatum and cerebral cortex. Unlike in lysolethicin of the adult spinal cord, the reduction was associated with a marked reduction in the number of PDGFRa+ and Olig2+ OPCs recruited to the lesion site in Olig1-/- animals 2 weeks post injury (Figure 1).

Olig1 regulates neuron versus glial cell fate specification after forebrain HIE

We next sought to determine if the reduction in OPC number caused by a decrease in OPC proliferation alone or if it was also associated with an increase in neurogenesis. To label cells

that proliferated in response to HIE, BrdU was administered one-week post injury. We observed a decrease in proliferation of Olig2-positive cells labeled with BrdU in *Olig1*-null animals compared to wild type and a corresponding increase in the number of DCX-positive neuroblasts labeled by BrdU in the subcortical white matter of *Olig1-null* animals. Taken together these data imply that *Olig1* is required to inhibit neurogenesis and promote OL fate during repair of injured white matter.

Figure 1. *Olig1* **required for OPC recruitment and myelin repair after neonatal HIE**

(A) Image (A) with boxed inset representing (A') demonstrating demyelinated forebrain region by MBP (green) IHC with recruitment of Olig2+ (red) OPCs into the lesion 2 weeks post injury in wild type mice. (B) Same analysis as in (A) now in 4 weeks post injury demonstrating failure of OPC recruitment in Olig1 -/- mice. (C-D) Images of Olig2 (red) and MBP (green) demonstrating myelin repair in wild type control (C), but failure of remyelination in Olig1 -/- mice (D).

2 Weeks Post Injury

A — Control — LV

A' — OPC recruitment

B — Olig1-/- — LV

B' — No OPC recruitment
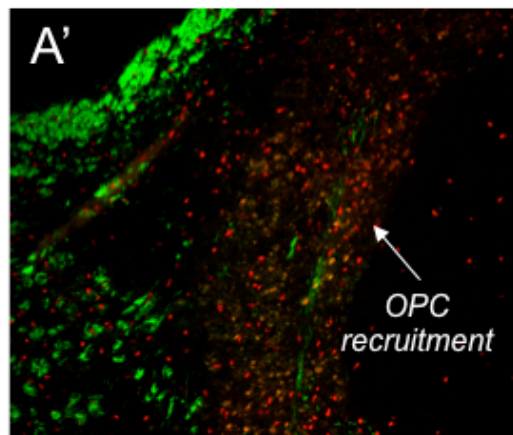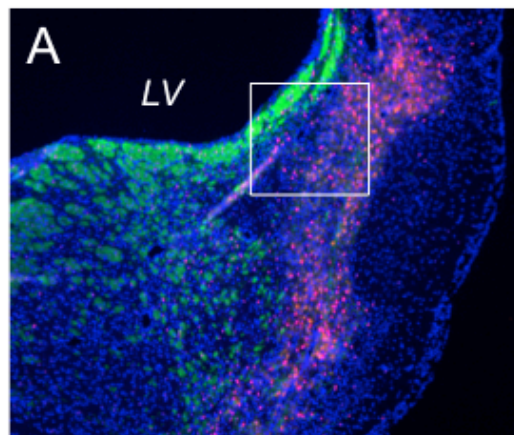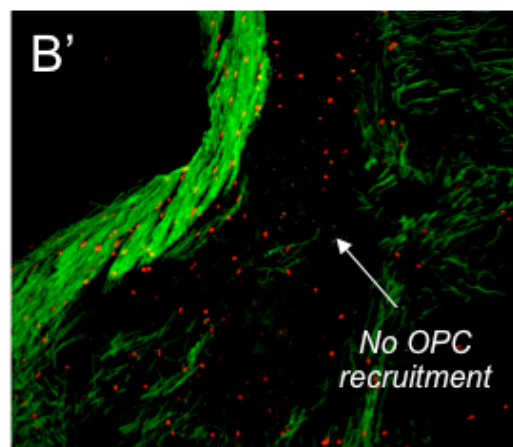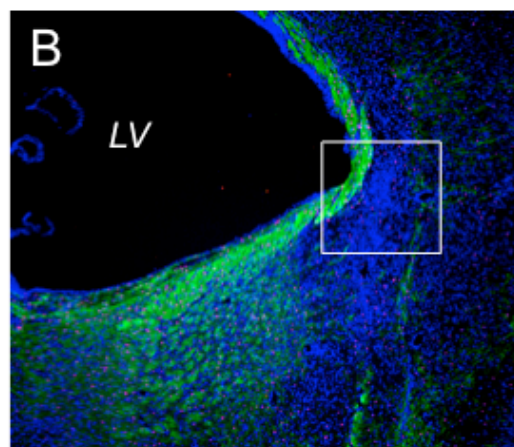
4 Weeks Post Injury

C — Control — LV

C'

D — Olig1-/- — LV

D'
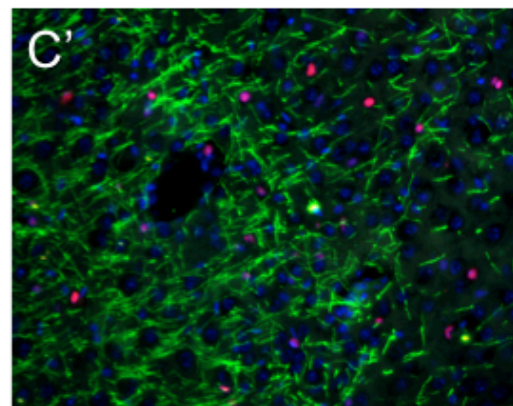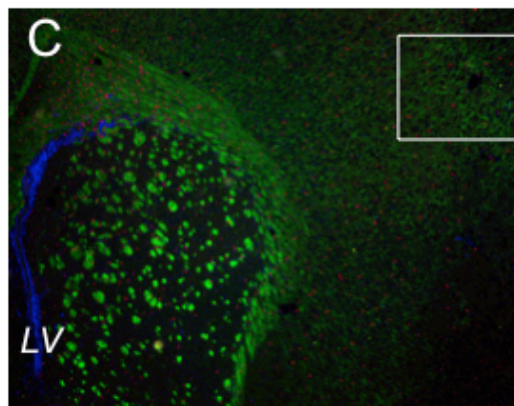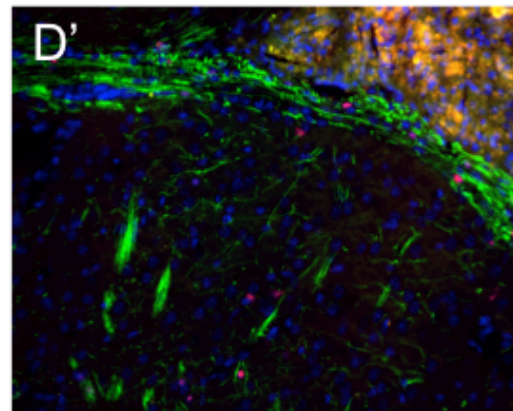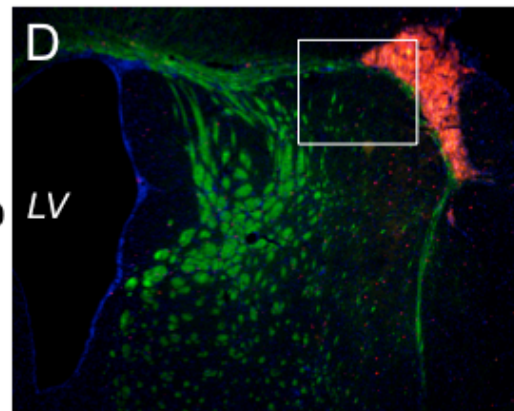
Olig2 MBP

Figure 2. Increased neuroblast proliferation in Olig1-/- mice after neonatal HIE

(A) Staining of BrdU (red) to mark cells in S-Phase and Olig2 (green). BrdU was injected 1 week post injury and animals were harvest at 2 weeks post injury. Note the decrease in BrdU/Olig2 double positive cells in *Olig1 -/-* mice (A') versus control (A). (B) Staining of BrdU (red) to mark cells in S-Phase and DCX (green). Note the increase in BrdU/DCX double positive cells in *Olig1 -/-* mice (B') versus control (B). (C) Quantification of the results shown in (A & B). * = $p < 0.05$, n = 3, error bars represent s.e.m.
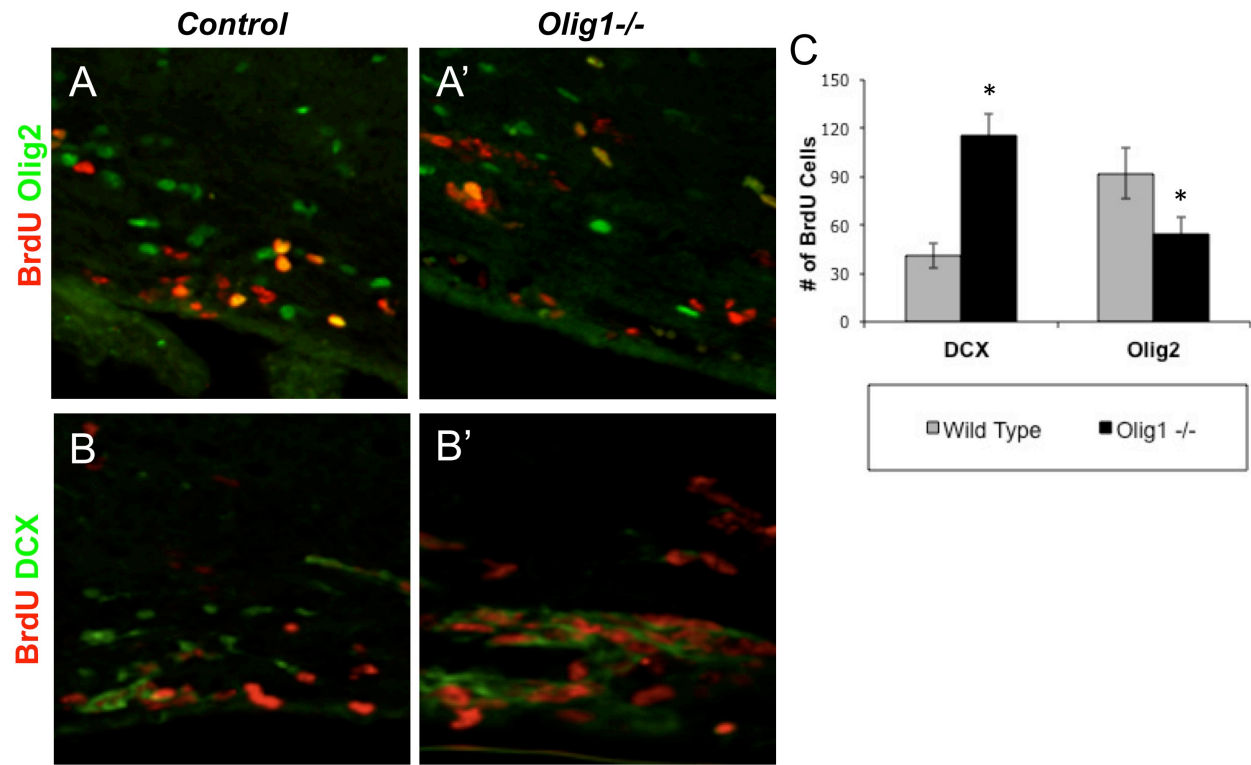
Chapter 5:

HIF mediated oxygen sensing regulates myelination

upstream of WNT signaling

Introduction: Potential roles for developmental hypoxia and HIFs in OL ontogeny

While severe hypoxia-ischemic insults lead to OL cell death and destruction of white matter tracts, chronic moderate hypoxia and inflammation events also lead to hypomyelination. Studies from animals and pathologic specimens of moderate / diffuse white matter injuries suggest that maturation block rather than hypomyelination is likely responsible. Intuitively, adequate tissue oxygenation, nutrient supply, and thus blood flow is likely essential for both developmental myelination and remyelination given the high metabolic demands of oligodendrocytes and the axons they invest. I therefore hypothesized that Hypoxia Inducible Factors (HIFs), the principle transcriptional mediators of the cellular hypoxia response, play an essential role in regulating OL development and white matter repair through regulation of key regulatory pathways in OL development.

Indeed, a previous study showed *HIF1*α function is required for Wnt pathway activation by hypoxia in neural stem cells (Mazumdar et al., 2010). In OPCs, canonical Wnt signaling functions as a potent inhibitor of maturation (Fancy et al., 2009). We have further reported that hypoxia-induced hypomyelination can be rescued by XAV939 (Fancy et al., 2011; Huang et al., 2009), a small molecule canonical Wnt pathway inhibitor that stabilizes Axin2 proteins, thus promoting β-catenin degradation (Figure 3A). I thus determined if HIF plays an important role in OL ontogeny though induction of downstream WNT activity.

Oxygen levels and cell-intrinsic *VHL* function regulate OPC differentiation and myelination.

In mice, postnatal myelination in the corpus callosum and cerebellar white matter is initiated about postnatal day (P) 7-9 and peaks at P15-21 (Tessitore and Brunjes, 1988). As shown (Figure 1 A-B, Figure 2 A-C), chronic exposure of neonatal mice to mild hypoxia (10% FiO2) from P3-11 resulted in hypomyelination and delayed OPC differentiation, without altering total

oligodendrocyte lineage numbers (Olig2+). This was indicated by reduced expression of myelin basic protein (MBP) and cells expressing the mature lineage-specific marker CC1 (a.k.a., adenomatous polyposis coli, APC), consistent with previous findings (Weiss et al., 2004). Under such hypoxic conditions, we observed stabilized HIF1α proteins in white matter lysates and Olig2+ OPCs (Figure 1B, Figure 2E).

We next tested effects of cell-intrinsic HIF stabilization in OPCs of the corpus callosum and cerebellar white matter. We targeted conditional knockout of a floxed *VHL* allele (Rankin et al., 2005) through intercrosses with *Sox10-cre (*Stolt et al., 2006), *Olig1-cre* (Lu et al., 2002) or tamoxifen-inducible *PLP-creERT2* (Doerflinger et al., 2003) transgenic mice. As shown (Figure 1B, Figure 2C), OPC-specific *VHL* conditional knockout by *Sox10-cre* resulted in HIF1α stabilization and severe OPC maturation arrest. We observed global hypomyelination throughout the brain of *Sox10-cre, VHL(fl/fl)* mice (Figure 1B, Figure 2C), which displayed tremor, ataxia and failure to survive past weaning age (P21). It is possible that lethality resulted from *VHL* loss of function in the peripheral nervous system, which is also targeted by *Sox10-cre* (Stolt et al., 2006). However, *Olig1-cre, VHL(fl/fl)* mice showed a similar phenotype of hypomyelination and reduced viability past P10 (Figure 2D, data not shown). Together, these findings indicate that cell-intrinsic *VHL* function phenocopies the effects of hypoxia and is required for OPC maturation and myelination.

To further verify that effects of hypoxia on the OL lineage were direct, we purified OPCs by immunopanning from the neonatal brain for *in vitro* studies (Emery and Dugas, 2013). As shown (Figure 1C, Figure 2F-I), exposure to 2% oxygen or treatment with the HIF-stabilizing agent dimethyloxaloylglycine (DMOG) inhibited OPC maturation and myelin gene expression (*MAG, MBP, CNPase*). We found similar results in OPCs isolated from *Plp-creERT2, VHL(fl/fl)* mice following treatment with tamoxifen (Figure 1C). These findings show direct effects of oxygen levels on OPCs, and indicate that cell-autonomous HIF signaling causes maturation arrest.

Hypoxic effects on OPCs are mediated by *HIF1/2α* function. We next determined whether

HIF1/2α function is required for hypoxia-induced hypomyelination. We crossed conditional

HIF1α(fl/fl) and *HIF2α(fl/fl)* mutants to compound homozygosity (hereafter called *HIF1/2α(fl/fl)*)

with *PLP-creERT2,* a tamoxifen inducible Cre recombinase expressed specifically in

oligodendrocytes (Doerflinger et al., 2003). Given dramatic hypomyelination observed in the

cerebellar white matter of *Sox10-cre, VHL(fl/fl)* and *Olig1-cre, VHL(fl/fl)* mice (Figure 2C), we

utilized a cerebellar explant culture assay suitable to quantify changes in postnatal myelination

and compact myelin paranode formation after hypoxia and pharmacologic manipulations (Fancy

et al., 2011; Yuen et al., 2013). We generated cerebellar explants from P0-P1 transgenic mice

and added tamoxifen 24h later (which did not affect survival) to induce acute Cre-mediated

excision of *HIF1/2α* in oligodendrocytes (Figures 3A, 4A). Subsequently, cultures were exposed

to hypoxia (2% FiO2) for 24h and maintained for 12 days prior to analysis. As shown (Figure 3

B-C, Figure 4B), hypoxia, and subsequent *HIF* activation, inhibited myelination and OPC

differentiation in wild type cerebella, as shown by MBP staining as well as the ratio of Caspr

paranode staining to NFH+ axons and the increased ratio of Nkx2.2 (immature OPCs)/Olig2

(total OLs) double-positive cells (Fancy et al., 2011). However, these effects were rescued by

deletion of *HIF1/2α* (Figure 3 B-C, Figure 4B). Thus, hypoxia-induced hypomyelination and OPC

maturation arrest require intact *HIF* function within OPCs (Figure 3D).

HIF stabilization in OPCs activates canonical Wnt signaling.

To determine whether HIF signaling activates the Wnt pathway in white matter, we performed

Western blot analysis of P11 corpus callosum lysates taken from wild type mice exposed to

chronic hypoxia and normoxic *Sox10-cre, VHL(fl/fl)* conditional knockouts. As shown (Figure 5B,

Figure 6A), both experimental conditions resulted in upregulation of the activated form of β-

catenin, and the Wnt transcriptional targets Axin2, Notum and Naked1 compared to controls *in vivo.* Similar findings were obtained in DMOG-treated immunopurified OPC cultures (Figure 6B), indicating HIF stabilization activates canonical Wnt signaling in OPCs. As we used purified OPC cultures, these results suggest production of Wnt ligands by OPCs that act in autocrine fashion. To test this, we used IWP2, an inhibitor of porcupine function and Wnt ligand secretion (Figure 5A) (Chen et al., 2009a). As shown (Figure 5 C-D, Figure 6C), IWP2 was sufficient to rescue both hypomyelination and OPC maturation arrest after hypoxia or *VHL* loss-of-function in OPCs. As a control for canonical Wnt pathway activity, we confirmed effects using XAV939 (Figure 5 C-D, Figure 6 C-E). Together, these findings indicate HIF pathway activation in OPCs promotes the secretion of canonical Wnt ligand(s) that act in an autocrine manner to inhibit OPC differentiation and subsequent myelination.

Evidence that *Wnt7a* and *Wnt7b* are direct HIF-inducible targets.

Prospective analysis of a database of genes expressed during OL development (Cahoy et al., 2008) revealed that, amongst the approximately 20 Wnt vertebrate genes that have been identified (Willert and Nusse, 2012), *Wnt4, Wnt7a* and *Wnt7b* are expressed at high levels in OPCs but down-regulated in mature OLs (Figure 8). To validate relevant gene targets of HIF, we performed qRT-PCR with primers for each mammalian Wnt gene (Table 1 of Chapter 2) against mRNA from OPCs treated with DMOG or exposed to hypoxia. This analysis indicated robust HIF-mediated upregulation of *Wnt7a* and *Wnt7b* (Figure 7A, Table 1 of Chapter 2)*,* but none of the other Wnt genes tested. These data identify *Wnt7a/7b* as candidate loci activated by HIF in OPCs.

To investigate whether *Wnt7a* and/or *Wnt7b* are direct targets of HIF, we first identified HRE (A/GTCTG) motifs proximal to the core promoter of the gene loci (Figure 8B, Chapter 2), and then performed chromatin immunoprecipitation (ChIP) in the presence/absence of DMOG to regulate HIF protein stability. HREs for *Epo* served as a positive control (Figure 8B). As

shown (Figure 7B), anti-HIF1α antibody-mediated precipitation resulted in significant signal from putative *Wnt7a* or *Wnt7b* HREs and a known *Epo* HRE in WT MEFs treated with DMOG, but not *HIF1/2α* double KO MEFs. These findings indicate HIF proteins bind the identified *Wnt7a* and *Wnt7b* HREs, suggesting they are targets directly regulated by stabilized HIF1α.

Wnt7a and *Wnt7b* have redundant functions in CNS development (Stenman et al., 2008). As shown (Figure 7C; Figure 8C-D), Wnt7a exposure resulted in inhibition of OPC differentiation (increase in ratio of immature Nkx2.2/Olig2 cells) and hypomyelination that was rescued by XAV939. Thus, Wnt7a proteins directly activate canonical Wnt signaling in OPCs.

Figure 1: Oligodendrocyte-specific *VHL* deletion inhibits OPC differentiation and myelination.

(A) Schematic showing anatomical regions of the corpus callosum (CC) and cerebral cortex (CTX) presented in (B) and experimental timeline for chronic hypoxic rearing analyses. (B) Representative images showing hypomyelination, oligodendrocyte-lineage HIF1α expression, and OPC maturation arrest in CC of P11 mice exposed to chronic hypoxia from P3-P11 or in *Sox10-cre, VHL(fl/fl)* mice. Arrowheads denote double-positive cells. Data were analyzed by one-way ANOVA with Dunnett's multiple comparison test, and significant differences (**$p<0.01$) are indicated.(C) Immunopurified OPCs exposed to hypoxia or isolated from *Plp-creERT2, VHL(fl/fl)* mice and treated with tamoxifen show differentiation block. Data were analyzed by one-way ANOVA with Dunnett's multiple comparison test, and significant differences (**$p<0.01$, ***$p<0.001$) are shown. Scale bar: 100μm.

A

Corpus Callosum

Chronic hypoxic rearing

10% O$_2$ rearing

P0   P3   P11   Sac

B

MBP   Olig2 HIF1α   Olig2 CC1

WT

CTX
CC   V

WT Hypoxia

Sox10-cre, VHL(fl/fl)

CC1/Olig2

** **

Nx   Hx   VHL

Olig2

Nx   Hx   VHL

C

OPC cultures

WT   WT Hypoxia   Plp-creERT2, VHL(fl/fl)

MBP Olig2

MBP/Olig2

*** ***   **

Nx   Hx   DMOG   WT   VHL
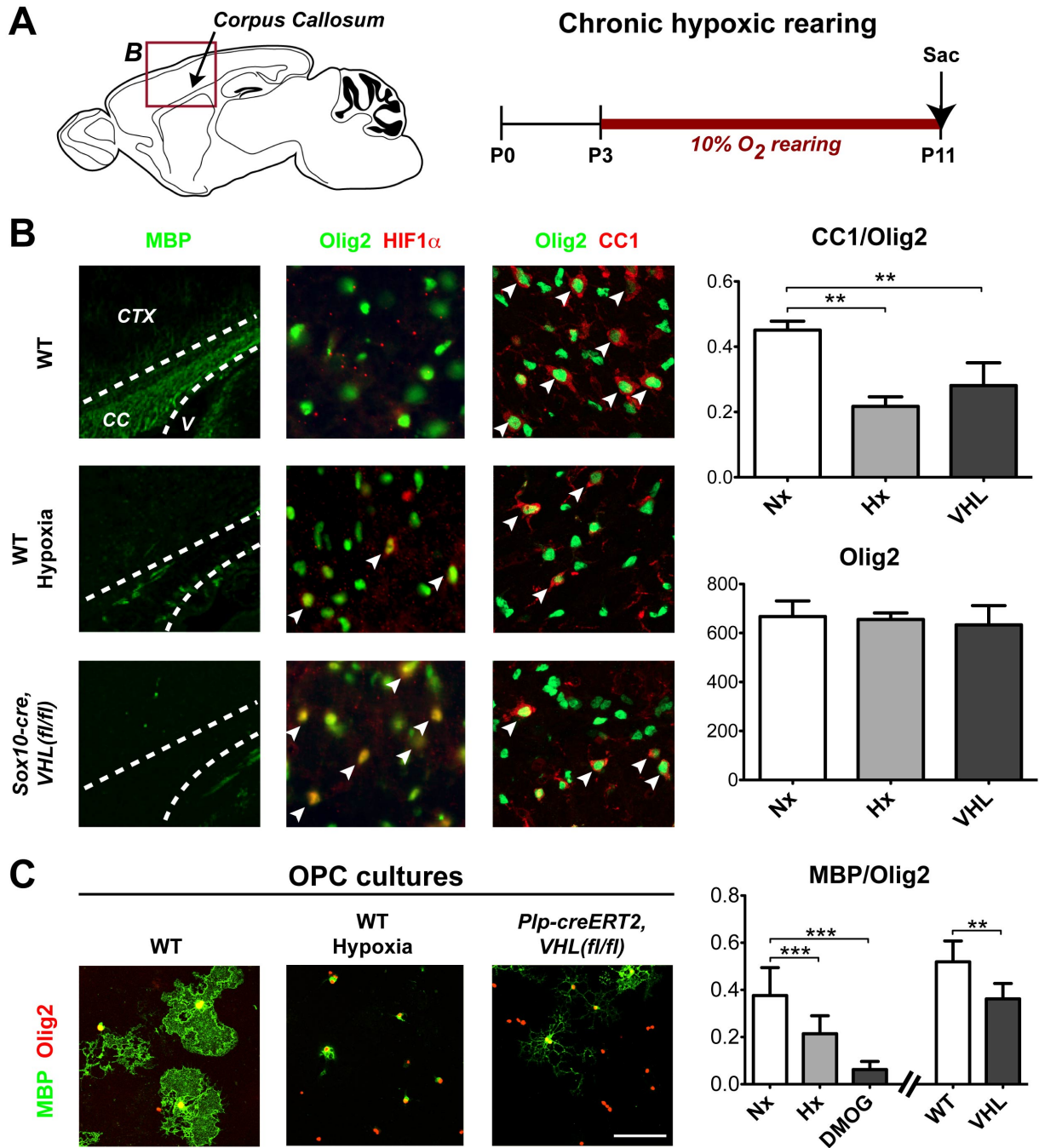
Figure 2: Additional analyses of proliferation, survival, myelination, and HIF/myelin gene expression.

(A) Proliferation of oligodendrocyte lineage cells is not affected after rearing in hypoxia. Cell counts were done in P11 corpus callosum (Ki67/Olig2) and data were analyzed by t-test. (B) Survival of oligodendrocyte lineage cells is not affected after rearing in hypoxia. Cell counts were done in P11 corpus callosum (Casp3/Olig2) and data were analyzed by t-test. (C) Severe hypomyelination in P11 cerebellum in mice reared in hypoxia and *Sox10-cre, VHL(fl/fl)* mice. (D) Severe hypomyelination in P7 corpus callosum in *Olig1-cre, VHL(fl/fl)* mice. (E) Western blots of white matter isolates showing increase in HIF1α and HIF2α in mice reared in hypoxic conditions. (F) Schematic of immunopurification of OPC cultures. (G) Western blots of OPC lysates showing increase in HIF1α and HIF2α in OPCs cultured in hypoxic conditions (2%O2). (H) qRT-PCR data showing decrease in expression of myelin genes *Mag, Mbp,* and *CNPase* in OPCs following hypoxia or DMOG treatment. (I) OPC survival is not affected after culturing in hypoxic conditions for 48h. Casp3+ cells were counted and data were analyzed by t-test

A P11 Corpus Callosum

Normoxia

Olig2 Ki67

Hypoxia

Ki67/Olig2

ns

B P11 Corpus Callosum

Normoxia

Olig2 Casp3

Hypoxia

Casp3/Olig2

ns

C P11 Cerebellum

WT - Normoxia   WT - Hypoxia   *Sox10-cre, VHL(fl/fl)*

MBP DAPI

D WT   *Olig1-cre, VHL(fl/fl)*

MBP Olig2 DAPI

P7

E WM isolates:

Hypoxia   Normoxia

HIF1α

HIF2α

Tubulin

F OPC cultures

Dissociate

BSL1   PDGFRα

Remove microglia   *Immunopurify for OPCs*

G OPC lysates:

Hx   Nx

HIF1α

Tubulin

HIF2α

Tubulin

H

Mag   Mbp   CNPase

Fold Change

Hypoxia DMOG Hypoxia DMOG Hypoxia DMOG

I 48h OPC Casp3+

ns

Nx   Hx

Figure 3: OPC-encoded *HIF1/2α* function mediates hypoxia-induced hypomyelination.

(A) Schematic and timeline for cerebellar slice cultures (CSC) exposed to hypoxia. (B) *HIF1/2α* function in oligodendrocytes is required for hypoxia-induced hypomyelination in CSC. Scale bars: 25μm (Caspr), 50μm (MBP/NFH). (C) Quantification of myelination in CSC. Data were analyzed by one-way ANOVA with Dunnett's multiple comparison test, and significant differences (***p<0.001) are shown. (D) Model for hypoxia-induced OPC differentiation block.

A Cerebellar slice cultures

B

	WT		Plp-creERT2, HIF1/2α(fl/fl)	
	MBP NFH	Caspr	MBP NFH	Caspr
Normoxia				
Hypoxia				
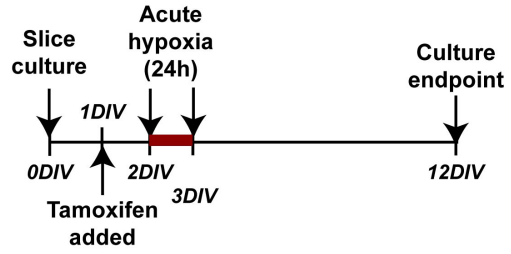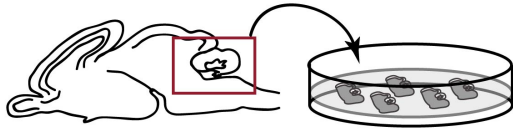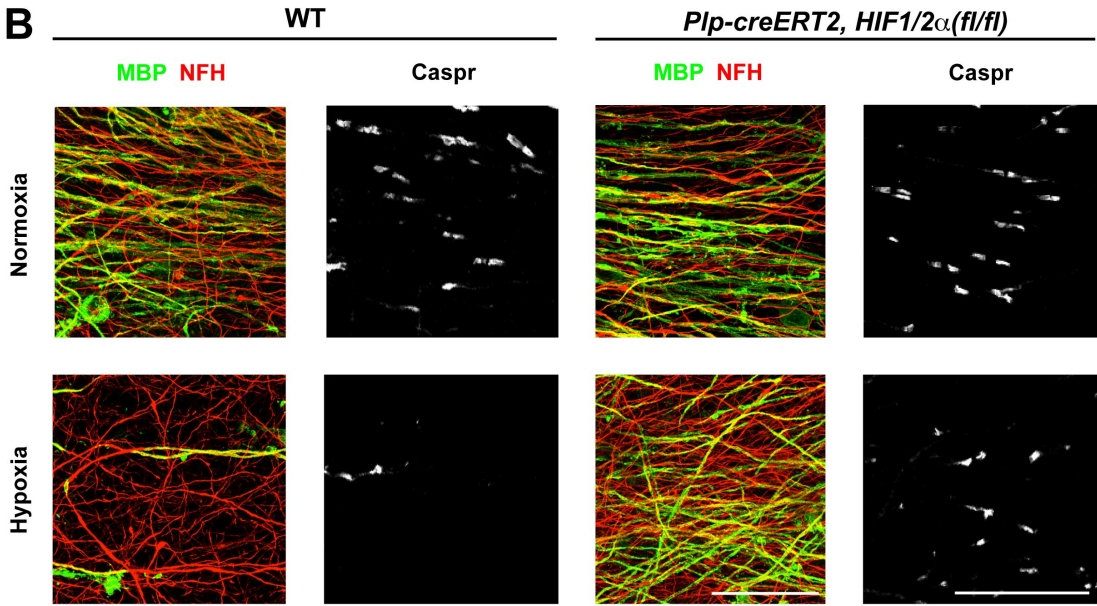
C
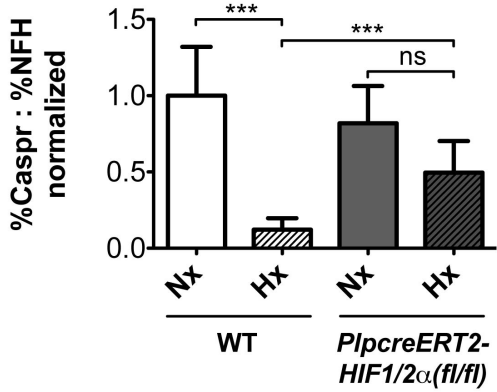
D
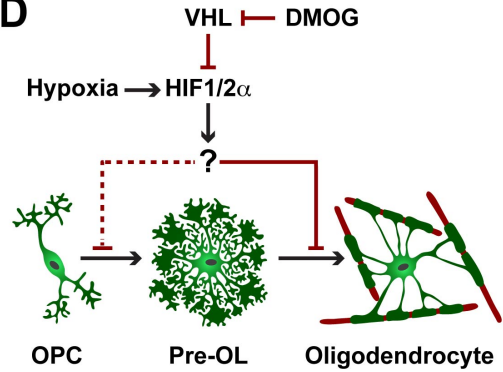
Figure 4: Additional analyses of survival, HIF expression and OPC differentiation block in cerebellar slice cultures.

(A) Addition of tamoxifen to cerebellar slice cultures did not affect survival (Casp3+ cells) in normoxic or hypoxic culture conditions. Data were analyzed by one-way ANOVA with Dunnett's multiple comparison test, and no significant differences were found. (B) *HIF1/2α* function in oligodendrocytes is required for hypoxia-induced OPC differentiation block in CSC. Data were analyzed by t-test and the significant difference (**p<0.01) is shown.

A

Casp3+ cells

Normoxia
Normoxia + Tamoxifen
Hypoxia
Hypoxia + Tamoxifen

B

24h Hypoxia

WT

PlpcreErt2, HIF1/2α(fl/fl)

Nkx2.2
Olig2
MBP

24h Hypoxia

Nkx2.2/Olig2

WT
Cre

**
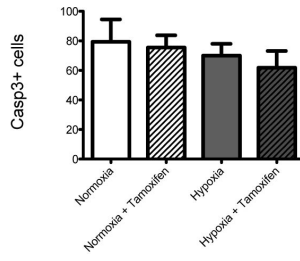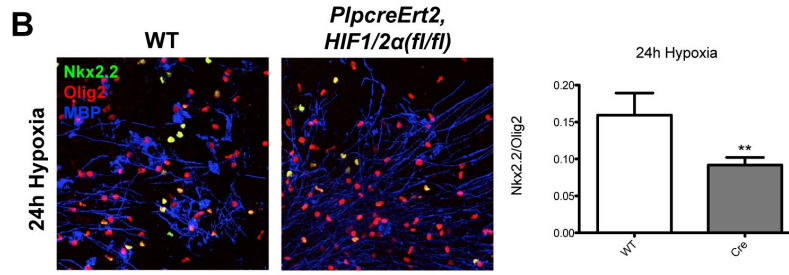
Figure 5: HIF stabilization in OPCs activates canonical Wnt signaling.

(A) Scheme showing IWP2 blockade of Wnt secretion, and inhibition of tankyrase activity by XAV939, which stabilizes Axin2 to promote β-catenin degradation. (B) Western blots of P11 white matter demonstrating upregulation of activated β-catenin and Wnt target Axin2 in wild type mice reared in hypoxia and *Sox10-cre, VHL(fl/fl)* mice. (C) IWP2 rescues hypomyelination in CSC exposed to hypoxia or from *Plp-creERT2, VHL(fl/fl)* mice; similar effects were observed with XAV939. Data were analyzed by one-way ANOVA with Dunnett's multiple comparison test, and significant differences ($*p<0.05$, $**p<0.01$, $***p<0.001$) are shown. Scale bars: 25μm (Caspr), 50μm (MBP/NFH). (D) Differentiation block in *Plp-creERT2, VHL(fl/fl)* OPCs is rescued by Wnt inhibitors IWP2 or XAV939. Data were analyzed by one-way ANOVA with Dunnett's multiple comparison test, and significant differences ($**p<0.01$, $***p<0.001$) are shown.

A

B P11 white matter

C Cerebellar slice cultures

% Caspr: % NFH

D OPC cultures

MBP/Olig2

Figure 6: Additional analyses of activation of canonical Wnt signaling upon HIF stabilization in OPCs.

(A) Western blots of P11 white matter lysates demonstrating additional Wnt targets (Naked1, Notum) are upregulated in WT mice reared in hypoxia and *Sox10-cre, VHL(fl/fl)* mice. (B) qRT-PCR data showing increase in Wnt target gene expression (*Notum, Axin2*) in OPCs following DMOG treatment. (C) Hypomyelination in CSC following DMOG treatment is reversed with XAV or IWP2 treatment. Data were analyzed by one-way ANOVA with Dunnett's multiple comparison test, and significant differences (***p<0.001) are shown. (D) Representative images of XAV treatment in CSC in WT, WT-hypoxia, and *Plp-creERT2, VHL(fl/fl)*. (E) XAV treatment of OPC cultures reverses OPC maturation arrest following hypoxia or DMOG treatment. Data were analyzed by one-way ANOVA with Dunnett's multiple comparison test, and significant differences (***p<0.001) are shown.

A P11 White Matter:

WT   *Sox10-Cre VHL(fl/fl)*

Nx   Hx   Cre- Cre+

Naked1

Notum

Actin

B OPC cultures:

Fold change in mRNA of OPCs treated with DMOG vs. vehicle

Notum   Axin2

C WT - DMOG

MBP NFH   Caspr

Vehicle

0.01uM XAV

2.5uM IWP2

% Caspr: % NFH

Vehicle   XAV   IWP2

D 0.01uM XAV

MBP NFH   Caspr

WT

WT Hypoxia

Plp-creErt2 VHL(fl/fl)

E

-DMOG   +DMOG

MBP Olig2 DAPI

Vehicle

0.01uM XAV

MBP/Olig2

Vehicle XAV   Vehicle XAV   Vehicle XAV

Normoxia   Hypoxia   DMOG
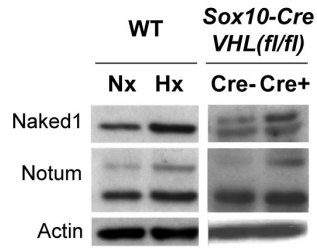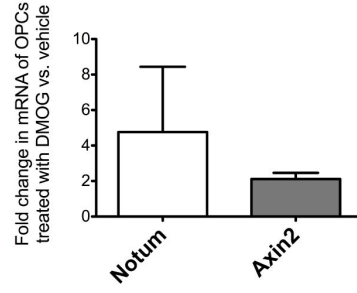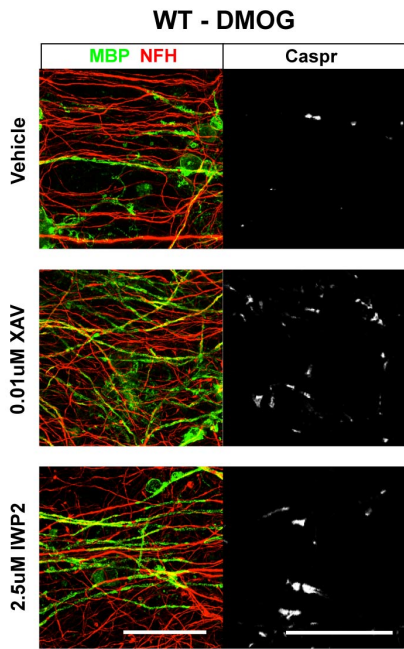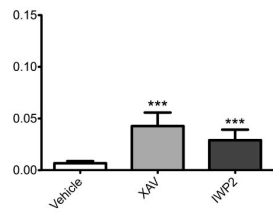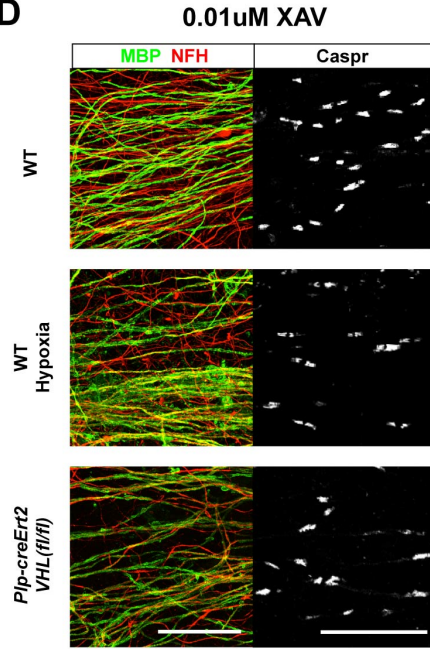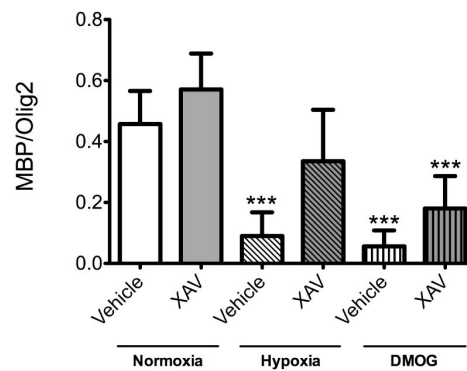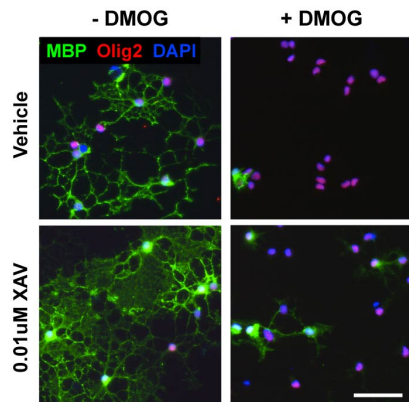
Figure 7: HIF1α directly binds and activates *Wnt7a* and *Wnt7b*.

(A) Immunopurified OPCs cultured in hypoxic conditions or exposed to DMOG specifically

upregulate *Wnt7a* and *Wnt7b* as shown by qRT-PCR.

(B) Mouse *HIF1/2α* knockout and control embryonic fibroblasts cultured with/without DMOG

(16h) were assayed by ChIP. Following immunoprecipitation with antibodies against HIF1α or

mouse IgG control, DNA extracts were assessed by qRT-PCR. HIF1α bound to the *Wnt7a* locus

at one HRE, and *Wnt7b* locus via two HREs. Binding was not observed in DMOG-treated

HIF1/2α mutant cells, or non-DMOG-treated controls.

(C) Wnt7a causes hypomyelination and OPC maturation arrest in CSC, which is reversed by

addition of XAV939. Data were analyzed by one-way ANOVA with Dunnett's multiple

comparison test, and significant differences (***p<0.001) are shown.

A OPC cultures
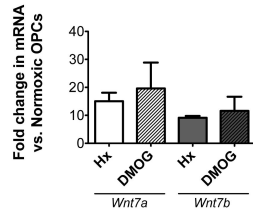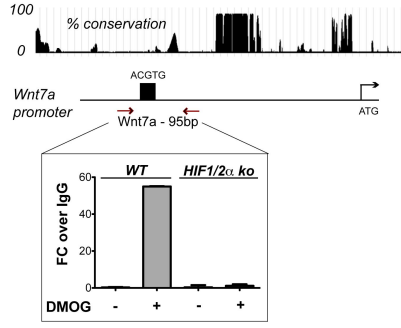
B Wnt7a locus   Wnt7b locus
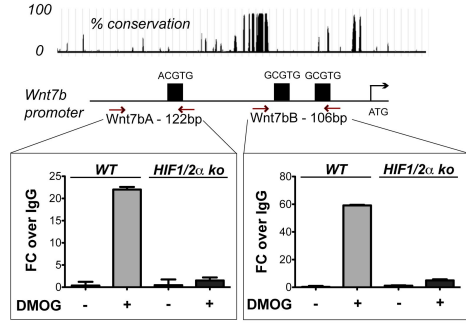
C Cerebellar slice cultures
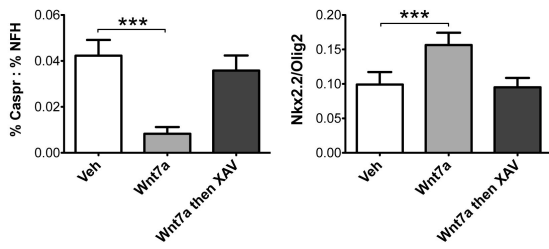
Figure 8: Additional controls for ChIP and analyses of the role of Wnt7a in causing OPC maturation arrest and hypomyelination.

(A) Graph of Wnt4, Wnt7a, and Wnt7b expression data in cultures of OPCs, oligodendrocytes, and myelinating oligodendrocytes (Cahoy et al., 2008). (B) Positive control for ChIP analysis (Epo, a known HIF target). (C) Wnt7a causes OPC maturation arrest in cultured OPCs. Data were analyzed by one-way ANOVA with Dunnett's multiple comparison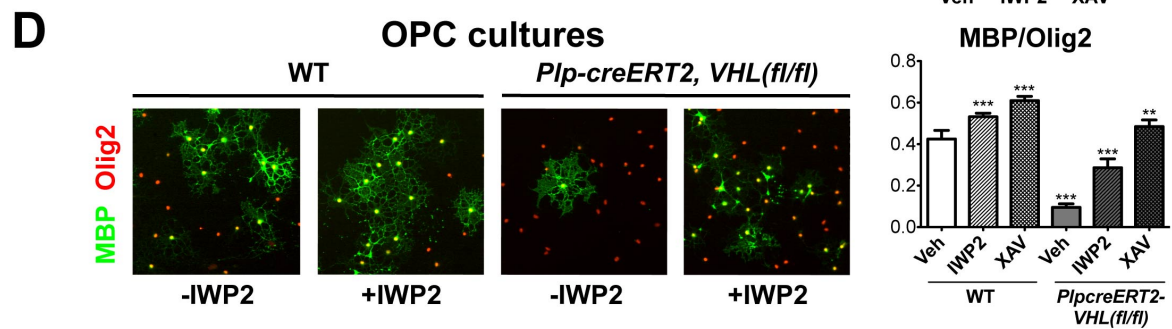 test, and significant differences (***$p<0.001$) are shown. (D) Images of CSC cultured with vehicle, 100ng/ml Wnt7a, or 100ng/ml Wnt7a followed by 0.1uM XAV.
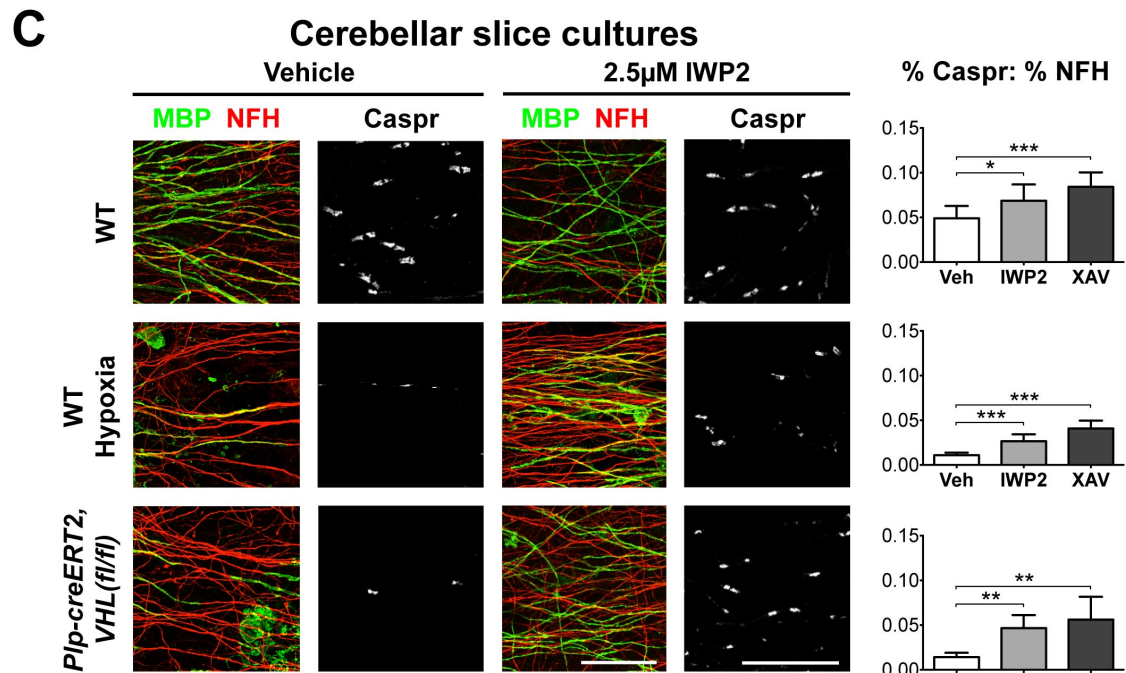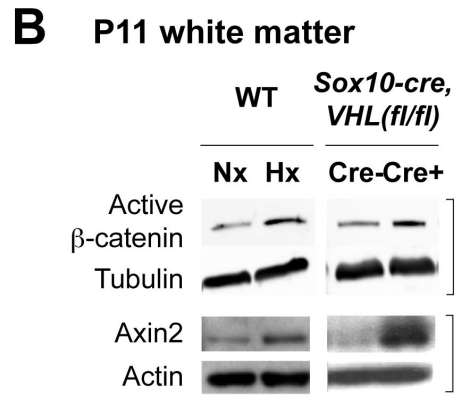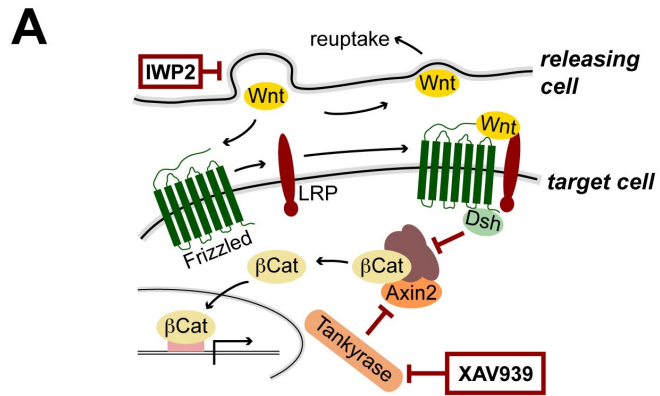
A

Expression Level vs cell type — Wnt4, Wnt7a, Wnt7b

B

Epo promoter — ACGTG — Epo - 149bp — ATG

FC over IgG (WT vs HIF1/2α ko), DMOG − / +

C *OPC cultures*

Vehicle   100ng/ml Wnt7a

MBP Olig2

MBP/Olig2 — Veh, 25ng/ml, 50ng/ml, 100ng/ml — Wnt7a — ***

D *Cerebellar slice cultures*

Vehicle   Wnt7a   Wnt7a then XAV

MBP NFH

Caspr
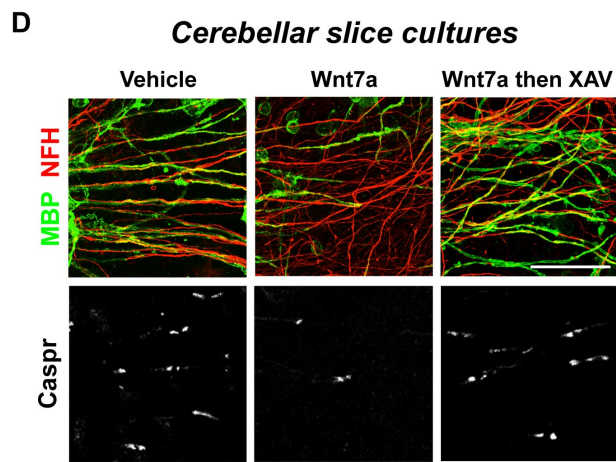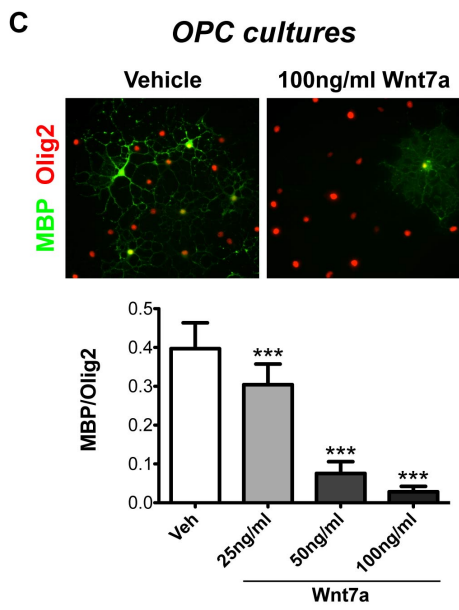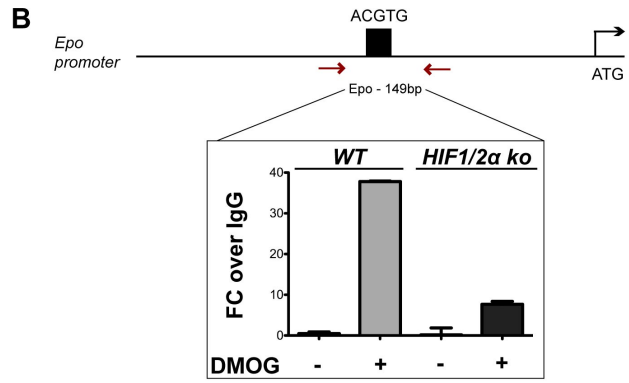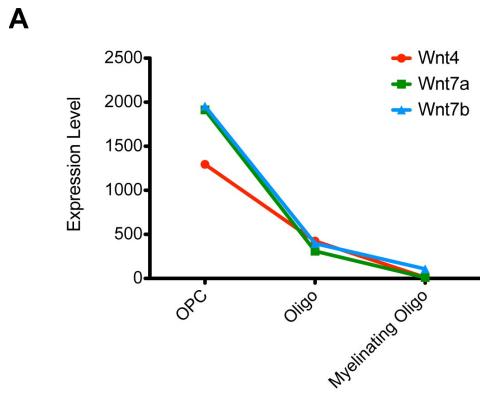
Chapter 6:

Oligodendrocyte-encoded *HIF* function couples postnatal myelination and white matter angiogenesis

Introduction: Roles for WNT7a/b in CNS vascular development

Combined *Wnt7a/7b* function and canonical Wnt signaling is essential for the formation of CNS

vasculature in the embryo (Daneman et al., 2009; Stenman et al., 2008). CNS angiogenesis

persists postnatally, through the sprouting and elongation of embryonically derived vessels,

during the first 10 days of murine life (Harb et al., 2013), which coincides with the onset of

myelination in the corpus callosum (Foran and Peterson, 1992). Although angiogenic roles for

OPCs are unprecedented, these findings raise the possibility that production of *Wnt7a/7b* (or

other HIF targets) from OPCs might also have paracrine effects on late CNS angiogenesis.

Given the extraordinary nutritive and metabolic demands of producing myelin, such a

mechanism would provide an elegant means to constrain myelination in brain

microenvironments that do not have adequate blood supply and oxygenation to support this

process.

**Wnt-mediated HIF signaling in OPCs increases CNS angiogenesis by inducing
endothelial cell proliferation.**

We first investigated whether HIF stabilization within OPCs resulted in a vascular phenotype. As

shown (Figure 1 A-B), we found dramatic increases in CNS blood vessel density of *Sox10-cre,*

VHL(fl/fl) mice, as indicated by the endothelial marker CD31, throughout the brain and

cerebellum. Similar findings were observed in *Olig1-cre, VHL(fl/fl)* mice (Figure S5A). Despite

increased vessel density, we found normal investment by pericytes and astrocyte end-feet, and

no evidence for blood-brain-barrier leakage of fibrinogen in the perivascular space (Figure 2B,

data not shown).

To assess activation of Wnt signaling in the endothelium of such ectopic vessels, we

stained for Lef1, a transcriptional target of Wnt signaling and a β-catenin binding partner

(Eastman and Grosschedl, 1999; Huber et al., 1996; Porfiri et al., 1997). As shown, we found

robust induction of Lef1 specifically in CD31+ endothelial cells of *Sox10-cre, VHL(fl/fl)* mutants

in vivo (Figure 1C). Moreover, the majority of Lef1+ endothelia co-stained with the proliferation marker Ki67 (Figure 1C), suggesting that Wnt signaling promoted vessel growth. Although members of the vascular endothelial growth factor (VEGF) family are HIF target genes expressed within the OL lineage during development (Figure 2C) (Cahoy et al., 2008), we found no evidence for increased VEGF-A expression in OPCs of *Sox10-cre, VHL(fl/fl)* mice *in vivo* (Figure 2 D-E). Together, these findings indicate that HIF stabilization in OPCs is sufficient to promote greatly elevated levels of angiogenesis, which is associated with the activation of Wnt signaling and endothelial proliferation.

OPCs directly promote Wnt-dependent endothelial cell proliferation.

The results above suggested a novel role for OPCs in vascular induction and/or remodeling, but left open the question of whether such effects were direct. In cultures of the brain endothelial cell line bEnd.3 (ATCC), we found that Wnt7a induced Lef1 expression and proliferation in keeping with our findings *in vivo* (Figure 1 D-F, Figure 2F). To demonstrate direct effects of OPCs, we performed a transwell assay with bEnd.3 cells (Figure 5D). This assay allows for an exchange of diffusible factors in the medium but prevents cell-cell contact between OPCs and endothelial cells. In this assay, soluble Wnt7a and/or VEGF proteins resulted in proliferation of endothelial cells (Figure 1 D-E, Figure 2F), as expected. As shown (Figure 1D-E), tamoxifen-induced *PLP-creERT2, VHL(fl/fl)* OPCs also induced endothelial cell proliferation. Moreover, this effect was inhibited by the addition of canonical Wnt pathway inhibitor XAV939 (Figure 1D-E, Figure S5F). In contrast, VEGF inhibitor SU5416 did not inhibit OPC-induced endothelial proliferation (Figure 2G). Taken together, these results indicate that HIF-stabilized OPCs induce angiogenesis by enhancing endothelial cell proliferation in a Wnt-dependent manner that does not require cell-cell contact.

Oligodendrocyte HIF1/2α function is essential for angiogenesis and integrity of white matter tracts.

To explore if oligodendrocyte-intrinsic *HIF* function has essential roles for normal vascular and oligodendrocyte development *in vivo*, we intercrossed *HIF1/2α(fl/fl)* mice with *Sox10-cre* and *Olig1-cre* lines. *Sox10-cre, HIF1/2α(fl/fl)* only survived until P4-7. In contrast, *Olig1-cre, HIF1/2α(fl/fl)* mice were viable into adulthood as late as P90 (*n*=5), but exhibited foot clasping behavior (Figure 4A). Histological analysis demonstrated reduction in gray matter and near absence of forebrain white matter tracts, and presence of cysts in the corpus callosum accompanied by ventricular enlargement (Figure 3A).

To resolve distinct and/or overlapping contributions of *HIF1α* versus *HIF2α* in this white matter phenotype, we analyzed single, compound and double mutant animals. As shown (Figure 3 A,C, Table 1), in P4 double knockout *Sox10-cre, HIF1/2α(fl/fl)* and *Olig1-cre, HIF1/2α(fl/fl)* mice, we observed macroscopic and microscopic acellular cysts in the corpus callosum, that were typically located at the boundary with adjacent grey matter structures (neocortex, striatum). In contrast, single *HIF1α* or *HIF2α* mutants showed minimal effects, and compound mutants that were *HIF1α(fl/fl);HIF2α(fl/+)* or *HIF1α(fl/+);HIF2α(fl/fl)* showed only microcysts. Thus, OPC intrinsic *HIF1α* and *HIF2α* show partially overlapping yet essential functions in white matter development.

In order to determine the basis for white matter loss, we assessed the ontogeny of OLs and the brain vasculature at E18, P4, and P7. While the brain of E18 *Olig1-cre, HIF1/2α(fl/fl)* mice had a grossly normal appearance, by P7 we observed dysgenesis of the forebrain white matter as well as reduced volume of neocortex, striatum, and hippocampus (Figure 3 A-B). We hypothesized that the more severe white matter phenotype observed by P7 may have resulted from a failure of OPC-induced angiogenesis postnatally between P0-P7. While the E18 mutant brain had a normal density of CD31+ blood vessels, we also noted a significant reduction in

Olig2+ cell numbers (Figure 6B, Figure S6B).   However, as shown (Figure 3B), IHC for CD31

showed a significant decrease in the number of blood vessels in the white matter and cerebral

cortex at P4 in *Olig1-cre, HIF1/2α(fl/fl)* mice. Analysis of apoptotic cell death in these animals

revealed a significantly increased number of cleaved Caspase 3 (Casp3+) cells in the mutant

white matter and cortex (Figure 3C). While the majority of Casp3+ cells were activated CD68+

microglia and/or macrophages, we also observed Olig2+ and PDGFRα+ oligodendrocyte

lineage cells (Figure 3D, Figure 4C). Strikingly, in the P4 mutant, we observed catastrophic

axonal damage in the corpus callosum as shown by SMI32 staining (Figure 3E). This

progresses to an acellular "cyst," which represents a loss of the corpus callosum and other

white matter axon tracts as shown at P7 and all later stages examined (Figure 6A, data not

shown). These data demonstrate that combined *HIF1/2α* function in OPCs is necessary to

promote postnatal white matter angiogenesis (Figure 5), and is critical to maintain structural

integrity of axons of the corpus callosum. My findings thus suggest that OPC-encoded HIF-

signaling coordinates the onset of postnatal OPC differentiation and myelination with

establishment of adequate vasculature in the white matter through autocrine and paracrine Wnt

activities, respectively.

Figure 1. *HIF* **activation in oligodendrocytes results in increased angiogenesis and Wnt-mediated endothelial cell proliferation.**

(A) Angiogenesis throughout the brain of *Sox10-cre, VHL(fl/fl)* mice was dramatically increased as shown by expression of endothelial marker, CD31. Dense regions of Olig2 staining indicate white matter tracts in the corpus callosum and cerebellar white matter. (B) Quantification of vessel area demonstrates significant increases in mice reared in hypoxia and normoxic *Sox10-cre, VHL(fl/fl)* mice. Data were analyzed by one-way ANOVA with Dunnett's multiple comparison test, and significant differences (*$p<0.05$, **$p<0.05$, ***$p<0.001$) are shown. (C) Increased Lef1 expression in endothelia of *Sox10-cre, VHL(fl/fl)* mice. Of these, the majority co-labeled with the proliferation marker, Ki67. (D) Scheme showing transwell co-culture assay for OPCs and bEND.3 cells. OPCs from *Plp-creERT2, VHL(fl/fl)* mice induce endothelial cell proliferation in a Wnt-dependent manner. (E) Quantification of endothelial cell proliferation in transwell assay at 24h and 48h. Data were analyzed by one-way ANOVA with Dunnett's multiple comparison test, and significant differences (***$p<0.001$) are shown. (F) Wnt7a addition to brain endothelial cells (bEND.3) induces Lef1 expression (arrowheads).

A

Corpus Callosum   Cortex   Cerebellar WM

Olig2 CD31

WT

Sox10-cre, VHL(fl/fl)

B

%CD31+

C

Lef1 CD31   Ki67 Lef1 DAPI

WT

Sox10-cre, VHL(fl/fl)

Vessel

D

EdU CD31 DAPI

Transwell
OPCs
bEnd.3 cells

Endo alone

+ WT OPCs

+ *Plp-creERT2, VHL(fl/fl)* OPCs
-XAV   +XAV

E

EdU/DAPI

24h

48h

Endo alone
+Wnt7a/VEGF
+WT OPCs
+VHL OPCs
+VHL OPCs, XAV

Endo alone
+Wnt7a/VEGF
+WT OPCs
+VHL OPCs
+VHL OPCs XAV

F

Lef1 CD31 DAPI

+Wnt7a
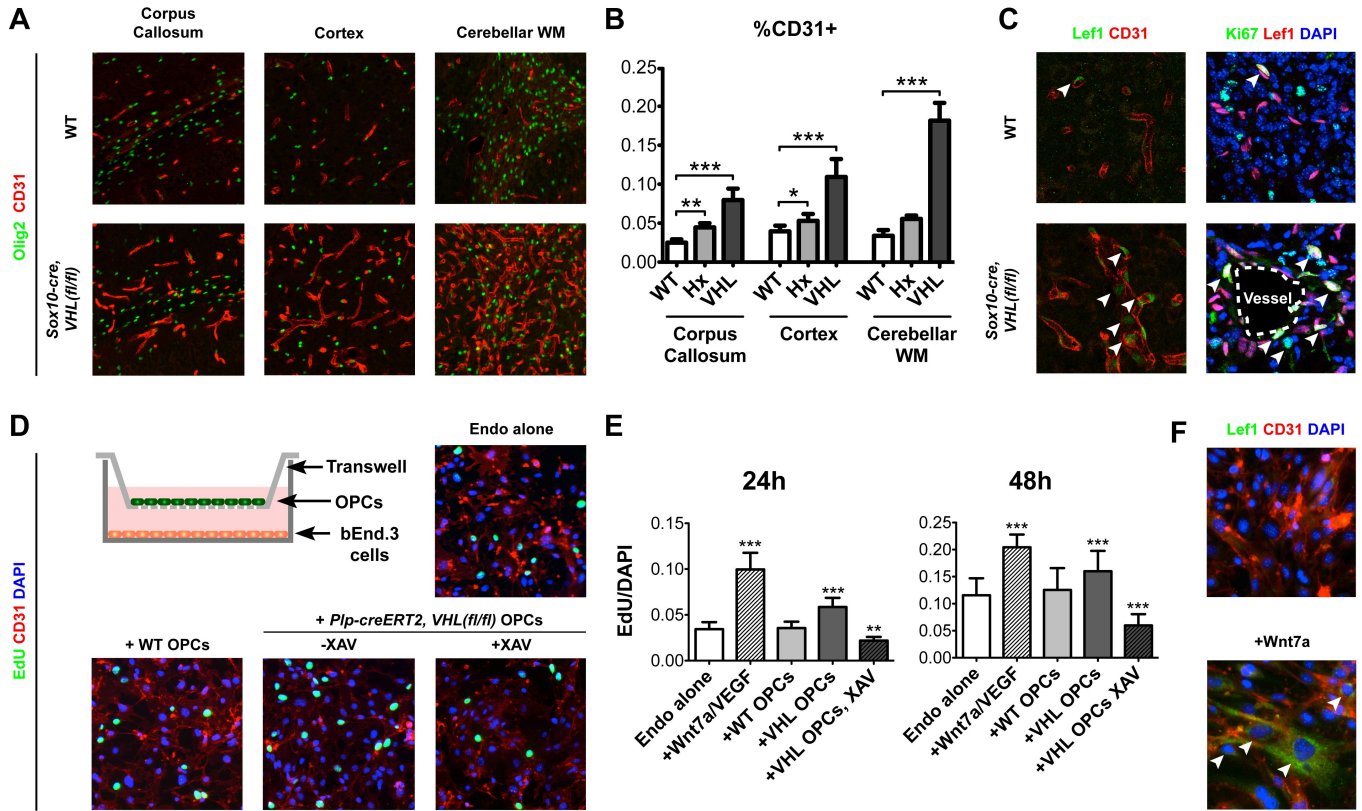
Figure 2: Additional analyses and controls demonstrating *HIF* activation in oligodendrocytes results in increased angiogenesis and Wnt-mediated endothelial cell proliferation

(A) Angiogenesis throughout the brain of *Olig1-cre, VHL(fl/fl)* mice was dramatically increased as shown by the expression of endothelial marker, CD31. (B) Normal pericyte (Zic1+) and astrocyte endfeet (Aqn4+) investment on blood vessels (CD31+) in WT-normoxia and *Sox10-cre, VHL(fl/fl)* mice. (C) Graph of VEGF-A, VEGF-B, and VEGF-C expression data in cultures of OPCs, oligodendrocytes, and myelinating oligodendrocytes (Cahoy et al., 2008). (D) Western blot of P11 white matter demonstrating no change in VEGF levels in *Sox10-cre, VHL(fl/fl)* mice. (E) Immunostaining of VEGF and Olig2 in P11 corpus callosum demonstrates no change in VEGF levels in *Sox10-cre, VHL(fl/fl)* mice. (F) Increase in endothelial cell proliferation following VEGF and/or Wnt7a addition is blocked upon subsequent addition of canonical Wnt inhibitor XAV939. Data were analyzed by one-way ANOVA with Dunnett's multiple comparison test, and significant differences (*$p < 0.05$, **$p < 0.01$, ***$p < 0.001$) are shown. (G) Increase in endothelial cell proliferation following VEGF addition is blocked with VEGFR inhibitor SU5416. However, the proliferation increase seen after transwell co-culture with *Plp-creERT2, VHL(fl/fl)* OPCs is not affected. Data were analyzed by one-way ANOVA with Dunnett's multiple comparison test, and significant differences (***$p < 0.001$) are shown.

A Olig2 CD31

WT-normoxia | *Olig1-cre, VHL(fl/fl)*

Corpus Callosum

Cortex

Cerebellar WM

P7

B P11 Corpus Callosum

WT-normoxia | *Sox10-cre, VHL(fl/fl)*

CD31 Zic1

CD31 Aqn4

CD31 Aqn4 GFAP

C

D P11 Corpus Callosum

WT VHL

45kDa
VEGF
24kDa

β–actin

E

WT | *Sox10-cre, VHL(fl/fl)*

Olig2 VEGF

P11

F Endo alone

G 48h

115
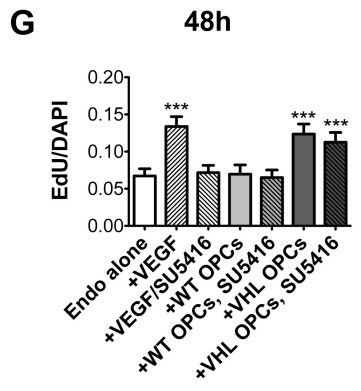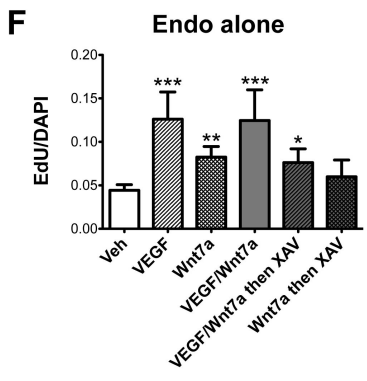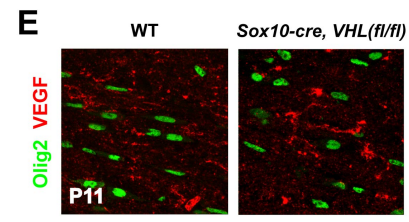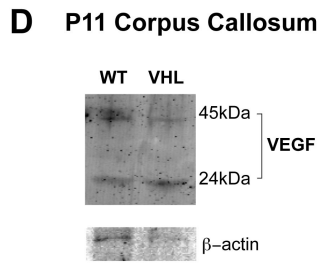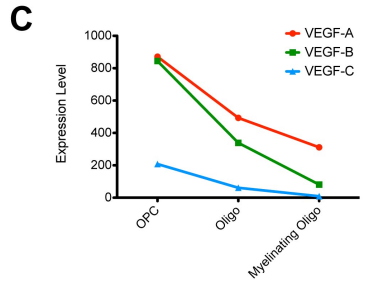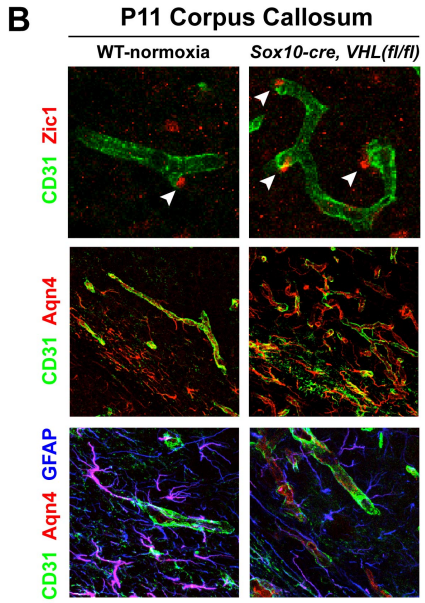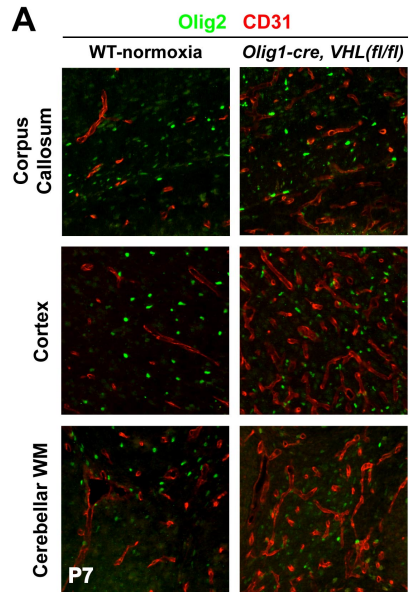
Figure 3: Oligodendrocyte *HIF1/2α* function is required for postnatal angiogenesis and maintenance of white matter integrity.

(A) Series of E18, P4, and P7 mutant and control brains show white matter cysts and dysgenesis by P7 in *Olig1-cre, HIF1/2α(fl/fl)* mice. (B) While vessel density at E18 appears normal in WT and *Olig1-cre, HIF1/2α(fl/fl)* mice, by P4, the number of Olig2+ cells and vessel area is decreased. Data were analyzed by t-test and significant differences (*p<0.05, **p<0.01) are shown. (C) White matter cysts and increased apoptotic cells (Casp3+) in P4 in *Olig1-cre, HIF1/2α(fl/fl)* mice. Data were analyzed by t-test and significant differences (*p<0.05) is shown. (D) Casp3 co-labeled CD68+ activated microglia/macrophages were frequently observed along with colabeled oligodendrocyte lineage (Olig2+) cells at P4. (E) Widespread axonal damage, indicated by SMI32+ staining, observed at P4 throughout the corpus callosum of *Olig1-cre, HIF1/2α(fl/fl)* mice.

A

WT   *Olig1-cre, HIF1/2α (fl/fl)*   E18

P4   WT   *Olig1-cre, HIF1/2α (fl/fl)*

P7   WT   *Olig1-cre, HIF1/2α (fl/fl)*

B

Olig2 CD31

E18   P4

V

P4 Corpus Callosum

Olig2+ cells

% area CD31+

WT   *Olig1-cre, HIF1/2α (fl/fl)*

*

**

C

WT   *Olig1-cre, HIF1/2α (fl/fl)*

Olig2 Casp3 DAPI

CTX   cyst   CC

P4

Casp3+ cells

WT   *Olig1-cre, HIF1/2α(fl/fl)*

*

D

CD68 Casp3   Casp3 Olig2

Olig1-cre, HIF1/2α (fl/fl)

E

WT   *Olig1-cre, HIF1/2α (fl/fl)*

SMI32 NFH

CC

P4

117
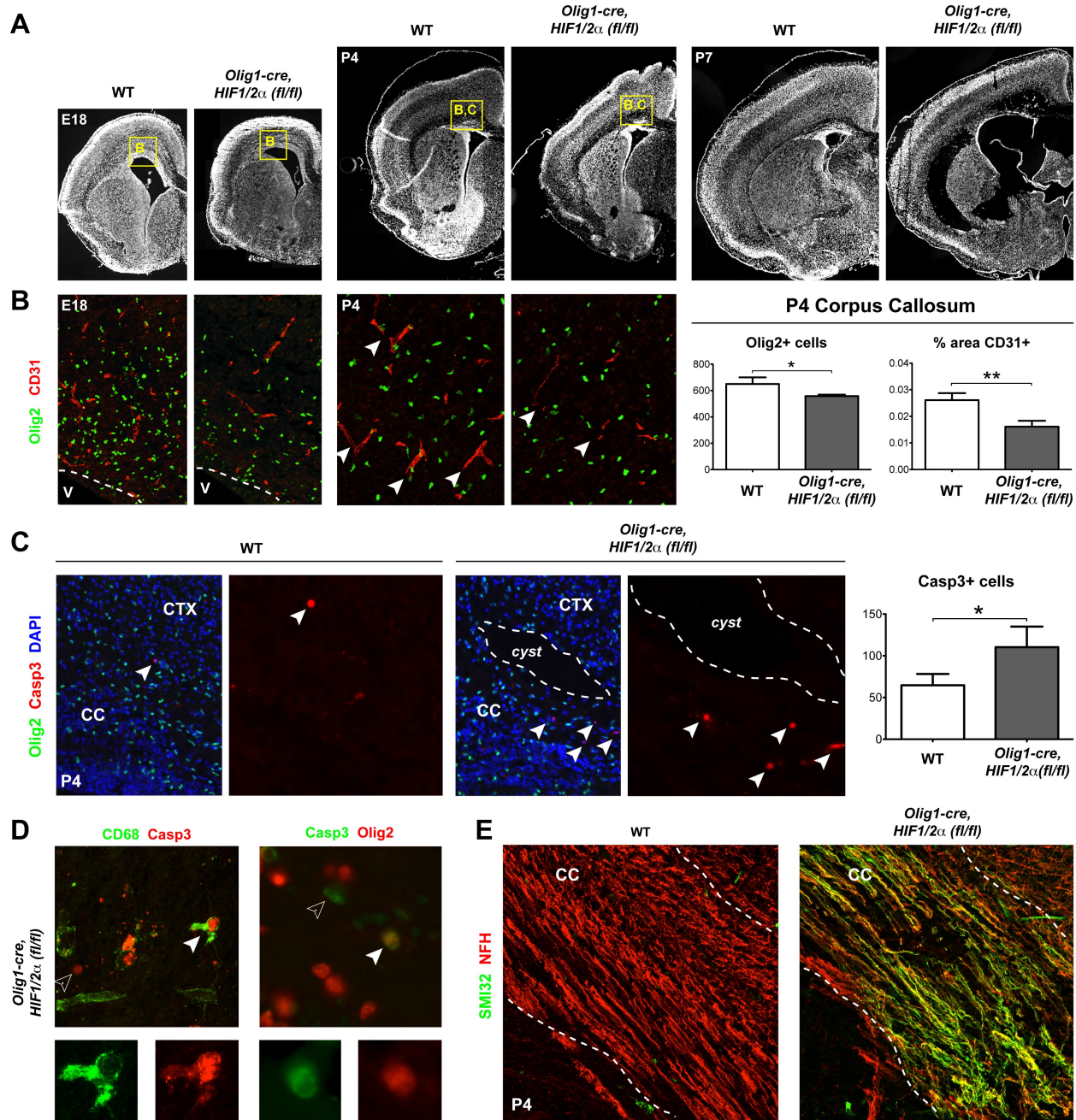
Figure 4: Additional analyses of phenotype of *Olig1-cre, HIF1/2α(fl/fl)* mice.

(A) Adult *Olig1-cre, HIF1/2α(fl/fl)* mouse exhibits foot clasping behavior. (B) Reduction in Olig2+

oligodendrocyte-lineage cells in E18 *Olig1-cre, HIF1/2α(fl/fl)* mice. (C) Immunostaining

demonstrating some apopototic cells (Casp3+) in *Olig1-cre, HIF1/2α(fl/fl)* mice are OPCs

(PDGFRa+).

A *Olig1-cre, HIF1/2α (fl/fl)*

B E18 Olig2+ cells

C PDGFRα Casp3 DAPI

P4

WT | *Olig1-cre, HIF1/2α (fl/fl)*
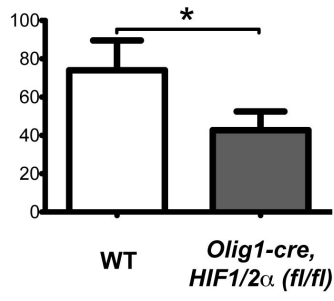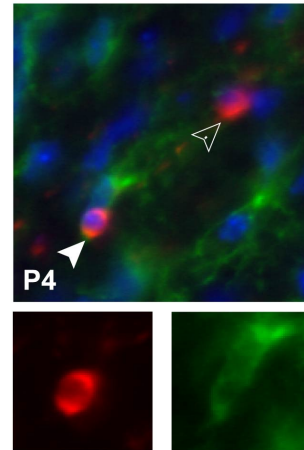
Figure 5: *HIF* pathway activation in oligodendrocytes plays an integral role in synchronizing postnatal myelination and white matter angiogenesis.

(left) Postnatal OPCs in newly forming white matter are exposed to low oxygen tension and high HIF expression levels, causing *Wnt7a/b* expression and OPC maturation arrest. Angiogenic *Wnt7a/b* expression from OPCs promotes vessel ingrowth, leading to higher oxygen levels and degradation of HIF. This dual mechanism prevents unsustainable OPC energy expenditure on myelination before there is adequate vasculature. This model does not show other substrates or metabolites that could also limit onset of myelination or the role of positive activity-dependent signals from axons.

P0   P4   P10/14

OPC Expansion   Angiogenesis/   Myelination
       OPC Differentiation

HIF expression

Wnt 7a/b   Oxygen tension
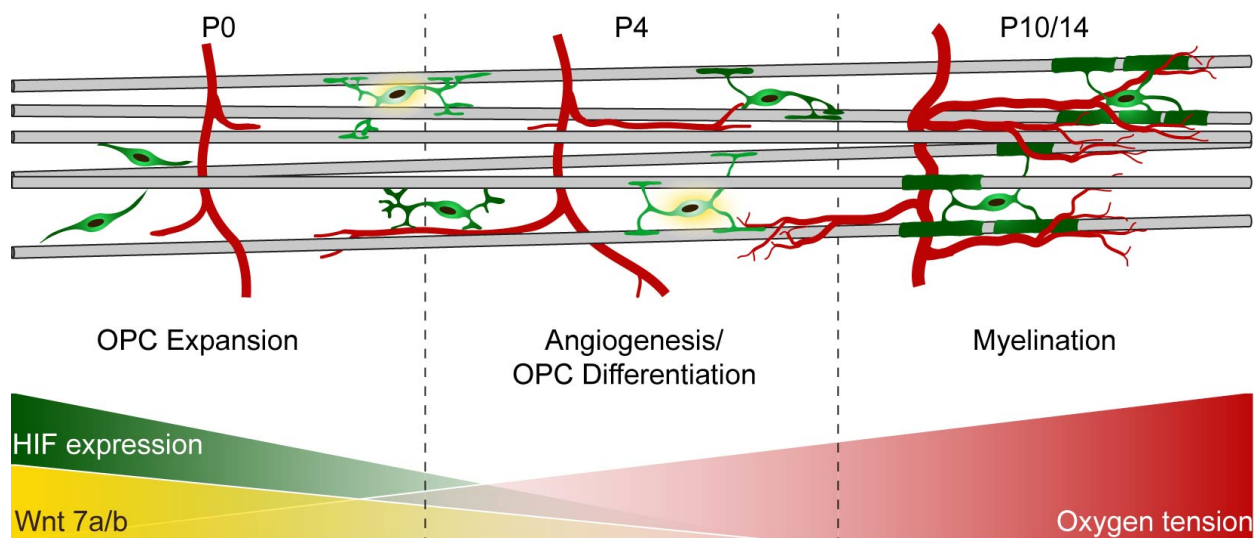
Table 1: Description of phenotypes observed in different *HIF* mutant mice.

	Genotype	Viability	White Matter Phenotype
Sox10-cre	HIF1α(fl/fl)	Normal	Reduced OPC numbers, reduced corpus callosum volume, normal MBP density
	HIF2α(fl/fl)	Normal	No apparent phenotype
	HIF1α(fl/wt); HIF2α(fl/wt)	Normal	No apparent phenotype
	HIF1α(fl/fl); HIF2α(fl/wt)	Neonatal Lethal	Reduced white matter volume at P4
	HIF1α(fl/wt); HIF2α(fl/fl)	Not Determined	Not Determined
	HIF1α(fl/fl); HIF2α(fl/fl)	Neonatal Lethal	Reduced white matter volume at E18 & P4, reduced OPC numbers at E18, appearance of cysts at P4,
Olig1-cre	HIF1α(fl/fl)	Normal	Not Determined
	HIF2α(fl/fl)	Normal	Not Determined
	HIF1α(fl/wt); HIF2α(fl/wt)	Lethality: P21 – P90	No apparent phenotype
	HIF1α(fl/fl); HIF2α(fl/wt)	Lethality: P21 – P90	Reduced brain volume & numbers at E18 and P4, appearance of WM cysts and axon damage at P4, phenotype after P4 not determined
	HIF1α(fl/wt); HIF2α(fl/fl)	Lethality: P21 – P90	Reduced brain volume & numbers at E18 and P4, appearance of WM cysts and axon damage at P4, phenotype after P4 not determined
	HIF1α(fl/fl); HIF2α(fl/fl)	Lethality: P21 – P90	Reduced brain volume & numbers at E18 and P4, appearance of WM cysts and axon damage at P4, absence of forebrain white matter by P7

Chapter 7:

General Conclusions

These studies explored several aspects of the transcriptional regulation of Oligodendrocyte ontogeny during development and their response to hypoxic brain injuries. I first focused on aspects of neuron versus OL fate specification, demonstrating that the pro-OL gene *Olig1* is also an essential inhibitor of an IN production during development and repair following hypoxia- ischemia. I then focused on the impact of hypoxia and HIFs on myelination during development and during neonatal white matter injury. These findings establish that OPC-intrinsic HIF signaling is essential for postnatal white matter angiogenesis and for synchronizing vascularization with the onset of myelination in the mammalian brain. Taken together these findings establish that there are overlapping mechanisms of the transcriptional regulation of normal OL development and repair after hypoxic white mater injury. They further establish that dysregulation of hypoxia regulated developmental signaling pathways such as WNT are an essential feature of the molecular pathology of developmental white mater injury.

Olig1 functions as an essential repressor of IN production in mammalian brain

We identified *Olig1* as a determinant of IN precursor pool size and IN numbers in the adult murine cortex. We observed a ~30% expansion of the total IN population, confined to the PV+ and CR+ IN cell types and a similar increase in PV/VGAT synapse density. This is consistent with previous findings that the maximum increase in density after transplantation of similar MGE progenitors into cortex is ~30% above normal (Baraban et al., 2009; Southwell et al., 2010; Southwell et al., 2012). Based on these studies, it was unclear whether increased endogenous generation of INs in *Olig1-/-* mice would affect inhibitory activity on pyramidal cells. Indeed, we found that increased IN cortical density in *Olig1*-null mice did not induce changes in the number of inhibitory potentials on pyramidal cells in adult mouse cortex. This may reflect the increase in CR+ cells, which make inhibitory synapses on other INs (Caputi et al., 2009; Freund and Buzsaki, 1996; Gonchar and Burkhalter, 1999). It is also notable that expression of the postsynaptic scaffolding protein Gephyrin is unaltered in *Olig1-null* mice. Gephyrin regulates the recruitment, stability and clustering of GABA receptors at the postsynapse and is

downregulated by increased inhibitory activity (Langosch et al., 1992; Poulopoulos et al., 2009; Prior et al., 1992; Saiepour et al., 2010; Tretter et al., 2008; Tretter et al., 2012; Vlachos et al., 2012). These data suggest that the increased interneuron number in *Olig1-/-* mice might result in Gephyrin-dependent postsynaptic compensation. We further demonstrated that *Olig1* is necessary to limit IN production in the cerebellum and olfactory bulb. Though numerous genes are required for IN specification and expansion, this is, to our knowledge, the first example of a transcription factor that represses cortical IN number.

Olig1 regulates neuron-glial fate choice

The expansion of cortical IN number in *Olig1-/-* animals suggested a critical role in regulating embryonic neurogenesis. *Olig1* is not robustly expressed in forebrain until E12.5 (Lu et al., 2002), a time point that coincides with the onset of oligodendrocyte specification (He et al., 2001; Kessaris et al., 2006). Indeed, several lines of evidence support the hypothesis that *Olig1* regulates the neuron-glial switch. First, *Olig1* is co-expressed in Nkx2.1+ and Nestin+ multipotent radial glia. Second, we observed upregulation of pro-IN gene expression in ventral MGE, AEP of *Olig1-/-* animals (e.g., *Lhx6*, *Dlx1/2*), coupled with decreased OPC production in the ventral telencephalon in the absence of excessive proliferation. A surprising finding of the study was that the septum appears competent to produce INs in the absence of *Olig1* function (Figure 8b). Finally, *Olig1* limits production of PV+ and CR+ cells, which are derived late in embryogenesis from progenitor domains that produce both OLs and INs, but not NPY+ and SST+ cells, which are born prior to the onset of OL specification (Kessaris et al., 2006; Miyoshi et al., 2007; Taniguchi et al., 2013; Wonders et al., 2008). In support of broad roles for Olig1 in neuron-glial fate choice, we found enhanced neurogenesis in the cerebellum and SVZ / olfactory bulb. Taken together, our findings suggest that *Olig1* acts in regions of protracted neurogenesis to limit IN production and promote OPC specification in several brain regions.

Olig1 regulates cell fate choice in multipotent progenitors through repressive interactions with *Dlx1/2*

DNA binding and luciferase assays suggest that *Olig1* is a direct repressor of the *Dlx1/2* locus acting through E-boxes in the *I12b* intergenic enhancer (Ghanem et al., 2003; Ghanem et al., 2007; Park et al., 2004; Poitras et al., 2007). This model is supported by our mouse genetic experiments in which enhanced IN genesis in *Olig1-/-* is rescued by conditional removal of *Dlx1/2* from the *Olig1* expression domain. Together, our findings indicate *Olig1* is a repressor of *Dlx1/2*. Future studies will probe interactions of *Olig1* with genes that control interneuron production in the cerebellum and other brain regions.

Despite similar structural features, Olig1 and Olig2 are functionally distinct in many respects (Meijer et al., 2012), including expression pattern, post-translational modification, cofactors, and transcriptional targets (Li et al., 2007; Li and Richardson, 2008; Lu et al., 2012). Our data show another unique role of Olig1 as an essential repressor of IN development. Prior studies show that forced *Olig1* overexpression results in ectopic OPC specification from neural progenitors (Kim et al., 2011; Lu et al., 2001; Lu et al., 2000; Maire et al., 2010) Although, *Olig2* shows more robust expression than *Olig1* in the MGE and binds E-boxes in the *Dlx I12b* enhancer (Mazzoni et al., 2011), this binding evidently is dispensable for IN genesis because we did not detect ectopic expression of *Dlx2* or *GAD67* in *Olig2-/-* animals despite upregulation of *Olig1* (Figure S4) (Petryniak et al., 2007, (Furusho et al., 2006; Ono et al., 2008). Thus, *Olig1* shows a unique function in IN repression compared to *Olig2.*

Potential roles for Olig1 in human brain development, disease and injury related to neuron versus glial specification, inhibitory tone and myelination.

In the human fetal brain, OLIG1 proteins are expressed in primitive neuroepithelia that can give rise to INs (Jakovcevski and Zecevic, 2005), consistent with our findings. *OLIG1* and *OLIG2* are colocalized to human chromosome 21 in the Down syndrome (DS) critical region and

several studies report they are overexpressed in DS (Bhattacharyya et al., 2009; Chakrabarti et al., 2010). Certain behavioral and psychiatric disorders are associated with abnormal IN numbers, including Tourette's syndrome (Kalanithi et al., 2005; Kataoka et al., 2010) and Schizophrenia (Alonso and Swadlow, 2005; Hashimoto et al., 2008; Hashimoto et al., 2003; Lewis et al., 2008). Our findings raise the possibility that *OLIG1* expression becomes dysregulated in certain pathological conditions.

Transplantation of progenitors for cortical INs deriving from the MGE can confer increased seizure threshold and alter plasticity (Baraban et al., 2009; Southwell et al., 2010). Recently, methods to derive human INs and OLs capable of transplantation, widespread migration and functional integration into mammalian brain have been established (Maroof et al., 2013; Nicholas et al., 2013). IN transplants attenuate symptoms in rodent models of epilepsy (Baraban et al., 2009; Hunt et al., 2013), Parkinson's Disease (Martinez-Cerdeno et al., 2010), and neuropathic pain (Braz et al., 2012). During repair after hypoxia-ischemia, *Olig1* promotes OL fate and represses neurogenesis suggesting it plays an important role in regulating regenerative mechanisms of neural repair*.* Based on these properties and the capacity of *Olig1* properties to repress IN formation in cultured neural progenitors, reducing *Olig1* expression (*e.g.,* siRNA) might provide a method to augment IN production for such potential therapeutic applications. Future studies will determine if increased IN number in *Olig1-/-* mice leads to differences in inhibitory tone during development, learning and memory tasks, and pathologies such as seizures.

Oxygen tension is a developmental regulator of postnatal myelination. Myelination is induced by activity-dependent neuronal signals (Demerens et al., 1996; Ishibashi et al., 2006; Makinodan et al., 2012; Stevens et al., 2002; Wake et al., 2011), and such coordination is important in part because myelin constrains axon outgrowth and synaptogenesis (Chong et al., 2012; Gyllensten and Malmfors, 1963; Hu and Strittmatter, 2004; Tauber et al., 1980; Weiss et

al., 2004). Our results suggest another level of regulation to ensure the presence of adequate blood supply, and by extension O_2 levels, that must be achieved for myelination to commence under appropriate physiological conditions. We show that OPC-encoded HIF-mediated O_2-sensing provides a regulatory cue that inhibits oligodendrocyte differentiation, but is also essential for the development of postnatal white matter vasculature (See Figure 5 of Chapter 6). We propose that this dual mechanism ensures myelination will only proceed at a time when blood supply is sufficient to meet attendant metabolic demands.

In mammals, formation of axons and specification of OPCs takes place under hypoxemic conditions *in utero* (~30-40 Torr) but myelination of the brain in both rodents and humans in the cortex is quite limited (Jakovcevski et al., 2009). After birth, oxygen tension of blood abruptly rises to 80 Torr (90-95% hemoglobin saturation) (Tina et al., 2009). In humans, cerebral blood flow and hemoglobin saturation continues to rise during the first 12-18 months of life, which is correlated with the peak time frame of cortical myelination (Franceschini et al., 2007). This suggests that greater O_2 levels themselves, which supply energy through oxidative metabolism, might comprise an important regulator of postnatal myelination. In support of this hypothesis, we show that changes in O_2, sensed by OPC-encoded HIF signaling, are necessary for the regulation of normal postnatal development of white matter tracts.

We demonstrate that stabilization of endogenous HIF proteins in OPC-directed *Sox10-cre* and *Olig1-cre* knockouts of *VHL* results in permanent maturation arrest and severe, potentially fatal hypomyelination. These results indicate that HIF proteins are normally expressed within OPCs during development and must be degraded to permit maturation. Our data and another study (Jablonska et al., 2012) show that OPCs are themselves resistant to effects of hypoxia and even abnormal HIF stabilization in conditional *VHL*-null mice. We further show that acute ablation of HIF in tamoxifen-inducible *Plp-creERT2, HIF1/2α(fl/fl)* slices rescues OPC differentiation and hypomyelination despite exposure to hypoxia. Thus, *HIF* function is necessary and sufficient for postnatal effects of oxygen levels on OPCs.

128

Autocrine Wnt signaling functions downstream of HIF to arrest oligodendrocyte maturation. Canonical Wnt signaling has been shown to regulate normal timing of OPC maturation (Fancy et al., 2009; Fancy et al., 2011; He and Lu, 2013; Hu et al., 2003; Wang et al., 1998). Our studies show that hypoxia and HIF stabilization promote Wnt production and canonical activity in OPCs. We further demonstrate that HIF1α directly binds conserved HREs at the *Wnt7a* and *Wnt7b* loci, and that stabilization of HIF in OPCs results in specific upregulation of *Wnt7a/7b.* Pharmacologically blocking porcupine-mediated Wnt secretion in OPCs with IWP2 promoted maturation suggesting an autocrine mechanism of Wnt activation.

Although HIF stabilization in OPCs prevented postnatal maturation, in preliminary analysis we do not observe precocious myelination (e.g., with prenatal onset) in *Olig1-cre, HIF1/2α(fl/fl)* animals. This might reflect the fact that down-regulation of HIF signaling must also integrate with positive cues, such as axonal activity-dependent signals for myelination to commence (see discussion above). Alternatively, it is possible that loss of *HIF* function results in the rapid death and removal of precociously maturing pre-myelinating OLs.

A new role for oligodendrocytes in the regulation of postnatal white matter angiogenesis. Oligodendrocytes and myelinated white matter tracts appear during evolution in vertebrates above the jawless fishes (Hartline and Colman, 2007; Zalc et al., 2008), which enabled growth and increased complexity of the mammalian brain (Freeman and Rowitch, 2013). Given our findings, we speculate that oligodendrocytes evolved as a cellular source of signals to recruit necessary vascular support for white matter. Postnatal angiogenesis is characterized by sprouting/ingrowth of blood vessels towards white matter regions deep in the brain from P0-P14 in mice (Harb et al., 2013; Michaloudi et al., 2006; Sapieha, 2012). Conditional OPC knockout of *HIF1/2α* resulted in deficient angiogenesis at P4 and ensuing necrosis of large white matter

tracts, such as the corpus callosum by P7. Conversely, HIF stabilization resulted in remarkable overproduction of brain blood vessels and increased expression of the pro-angiogenic genes *Wnt7a/7b.* Indeed, our findings suggest dual roles for HIF-mediated Wnt signaling that synchronize OPC maturation and white matter vascular development.

Although VEGF is expressed by neurons, astrocytes and microglia in response to hypoxia (Argaw et al., 2012; Boer et al., 2008; Ijichi et al., 1995; Ogunshola et al., 2002; Ogunshola et al., 2000; Rosenstein et al., 2010), VEGF proteins were not induced by OPC-specific HIF stabilization in our studies. One likely possibility is that Wnt production from OPCs synergizes with VEGF from other white matter cell types. Indeed, both canonical and non-canonical Wnt signaling are known to promote VEGF activity through enhanced transcription and phosphorylation of VEGF receptors.

Are there direct contacts between oligodendrocytes and developing vasculature? Our findings in the transwell assay indicate that contact-mediated signaling is not necessarily required to stimulate proliferation of endothelial precursors. Further studies are needed to determine whether Wnt signaling is sufficient within a limited postnatal developmental window to affect vascular induction into white matter *in vivo* as well as to examine potential roles for oligodendrocytes in blood vessel maintenance.

Oligodendrocyte *HIF* signaling is essential for white matter formation and axon survival. Mature oligodendrocytes provide metabolic support for axons by supplying them with ATP, glycolytic substrates and nutrients throughout life (Chrast et al., 2011; Funfschilling et al., 2012; Harris and Attwell, 2012; Lee et al., 2012b; Nave, 2010; Rinholm et al., 2011). Here, we demonstrate that loss of *HIF* in OPCs results in cell death, axon damage and the appearance of cysts in white matter at an early postnatal stage (P4). This is followed by a catastrophic loss of axons at P7 in the corpus callosum, and preliminary analysis indicates this is also the case in white matter tracts throughout the forebrain (data not shown). Evolution of corpus callosum

cysts from P4-7 is associated with a significant decrease in vessel density, suggesting that they result from a failure of adequate angiogenesis and vascular investment during a critical window. Alternatively, *HIF* signaling within oligodendrocytes might be required to promote trophic factors that are integral for support of axons. While one might argue that such lesions result from failure of myelination, we think that this is unlikely because we observed this phenotype throughout the corpus callosum at a stage where many axons are unmyelinated. In addition, myelin mutant mice (e.g. *Shiverer*) do not display markers of axon damage at these early developmental stages (Griffiths et al., 1998; Smith et al., 2013).

Potential novel roles of oligodendrocytes in CNS injury. Oligodendrocytes are early responders to a broad spectrum of brain pathologies including demyelinating disorders (e.g., Multiple Sclerosis, MS), stroke and even stab wounds (Arai and Lo, 2009; Biname et al., 2013; Chang et al., 2002; Hampton et al., 2004; Kuhlmann et al., 2008; Tanaka et al., 2001). The notion that OPCs might produce angiogenic factors to encourage revascularization of injured CNS tissue is consistent with recent studies (Cayre et al., 2013; Jiang et al., 2011; Pham et al., 2012). White matter injury induced by experimental autoimmune encephalomyelitis (EAE) results in local tissue hypoxia (Davies et al., 2013), which is consistent with observations of oligodendrocyte HIF1α expression in a subset of MS lesions (Aboul-Enein et al., 2003). Further studies are needed to determine roles for OPCs as general mediators of vascular induction after injury and, conversely, how metabolic sensors might limit remyelination after white matter injuries. In summary, our findings demonstrate that cell intrinsic *HIF* pathway function in OPCs is a key regulator of postnatal myelination and angiogenesis during a critical window of early postnatal development. Further, they suggest novel roles for OPCs in the maintenance of white matter structural integrity and in the response to injury.

Concluding Remarks

In conclusion, the oligodendrocyte lineage is exquisitely sensitive to hypoxic injury, but is also unique in its capacity for regeneration. Following injury, upregulation of genes that are essential for OL ontogeny during development enables OPCs to proliferate robustly and give rise to OLs capable of making new myelin sheaths. Myelin and white matter tracts thus have a unique capacity to repair the CNS after injury and in demyelinating disorders such us MS. Despite this regenerative capacity, remyelination is insufficient in chronic progressive MS. Similarly, white matter injuries during development lead to static lesions that underlie chronic conditions such as Cerebral Palsy. My results suggest that for myelination to proceed OLs require access to an adequate vascular supply and appropriate oxidative and nutritive support. The HIF pathway acts upstream of the WNT pathway to prevent OL maturation in microenvironments that do not meet the metabolic demands of myelination, while also promoting angiogenesis. Future studies are needed to evaluate the HIF / WNT signaling axis as a therapeutic target for remyelination and to discover additional O_2 and nutrient regulated mechanisms that control oligodendrocyte ontogeny.

Chapter 8:

References

Aboul-Enein, F., Rauschka, H., Kornek, B., Stadelmann, C., Stefferl, A., Bruck, W., Lucchinetti, C., Schmidbauer, M., Jellinger, K., and Lassmann, H. (2003). Preferential loss of myelin-associated glycoprotein reflects hypoxia-like white matter damage in stroke and inflammatory brain diseases. Journal of neuropathology and experimental neurology *62*, 25-33.

Alonso, J.M., and Swadlow, H.A. (2005). Thalamocortical specificity and the synthesis of sensory cortical receptive fields. J Neurophysiol *94*, 26-32.

Alvarez-Buylla, A., Seri, B., and Doetsch, F. (2002). Identification of neural stem cells in the adult vertebrate brain. Brain Res Bull *57*, 751-758.

Alvarez-Dolado, M., Calcagnotto, M.E., Karkar, K.M., Southwell, D.G., Jones-Davis, D.M., Estrada, R.C., Rubenstein, J.L., Alvarez-Buylla, A., and Baraban, S.C. (2006). Cortical inhibition modified by embryonic neural precursors grafted into the postnatal brain. J Neurosci *26*, 7380-7389.

Anderson, S.A., Eisenstat, D.D., Shi, L., and Rubenstein, J.L. (1997). Interneuron migration from basal forebrain to neocortex: dependence on Dlx genes. Science *278*, 474-476.

Arai, K., and Lo, E.H. (2009). Experimental models for analysis of oligodendrocyte pathophysiology in stroke. Experimental & translational stroke medicine *1*, 6.

Argaw, A.T., Asp, L., Zhang, J., Navrazhina, K., Pham, T., Mariani, J.N., Mahase, S., Dutta, D.J., Seto, J., Kramer, E.G.*, et al.* (2012). Astrocyte-derived VEGF-A drives blood-brain barrier disruption in CNS inflammatory disease. J Clin Invest *122*, 2454-2468.

Arnett, H.A., Fancy, S.P., Alberta, J.A., Zhao, C., Plant, S.R., Kaing, S., Raine, C.S., Rowitch, D.H., Franklin, R.J., and Stiles, C.D. (2004). bHLH transcription factor Olig1 is required to repair demyelinated lesions in the CNS. Science *306*, 2111-2115.

Baraban, S.C., Southwell, D.G., Estrada, R.C., Jones, D.L., Sebe, J.Y., Alfaro-Cervello, C., Garcia-Verdugo, J.M., Rubenstein, J.L., and Alvarez-Buylla, A. (2009). Reduction of seizures by transplantation of cortical GABAergic interneuron precursors into Kv1.1 mutant mice. Proc Natl Acad Sci U S A *106*, 15472-15477.

Baron, W., and Hoekstra, D. (2010). On the biogenesis of myelin membranes: sorting, trafficking and cell polarity. FEBS letters *584*, 1760-1770.

Baumann, N., and Pham-Dinh, D. (2001). Biology of oligodendrocyte and myelin in the mammalian central nervous system. Physiological reviews *81*, 871-927.

Beck, I., Ramirez, S., Weinmann, R., and Caro, J. (1991). Enhancer element at the 3'-flanking region controls transcriptional response to hypoxia in the human erythropoietin gene. J Biol Chem *266*, 15563-15566.

Beck, I., Weinmann, R., and Caro, J. (1993). Characterization of hypoxia-responsive enhancer in the human erythropoietin gene shows presence of hypoxia-inducible 120-Kd nuclear DNA-binding protein in erythropoietin-producing and nonproducing cells. Blood *82*, 704-711.

Bhattacharyya, A., McMillan, E., Chen, S.I., Wallace, K., and Svendsen, C.N. (2009). A critical period in cortical interneuron neurogenesis in down syndrome revealed by human neural progenitor cells. Dev Neurosci *31*, 497-510.

Billiards, S.S., Haynes, R.L., Folkerth, R.D., Borenstein, N.S., Trachtenberg, F.L., Rowitch, D.H., Ligon, K.L., Volpe, J.J., and Kinney, H.C. (2008). Myelin abnormalities without oligodendrocyte loss in periventricular leukomalacia. Brain Pathol *18*, 153-163.

Biname, F., Sakry, D., Dimou, L., Jolivel, V., and Trotter, J. (2013). NG2 regulates directional migration of oligodendrocyte precursor cells via Rho GTPases and polarity complex proteins. J Neurosci *33*, 10858-10874.

Boer, K., Troost, D., Spliet, W.G., van Rijen, P.C., Gorter, J.A., and Aronica, E. (2008). Cellular distribution of vascular endothelial growth factor A (VEGFA) and B (VEGFB) and VEGF receptors 1 and 2 in focal cortical dysplasia type IIB. Acta neuropathologica *115*, 683-696.

Bradl, M., and Lassmann, H. (2010). Oligodendrocytes: biology and pathology. Acta neuropathologica *119*, 37-53.

Bragina, L., Candiracci, C., Barbaresi, P., Giovedi, S., Benfenati, F., and Conti, F. (2007). Heterogeneity of glutamatergic and GABAergic release machinery in cerebral cortex. Neuroscience *146*, 1829-1840.

Braz, J.M., Sharif-Naeini, R., Vogt, D., Kriegstein, A., Alvarez-Buylla, A., Rubenstein, J.L., and Basbaum, A.I. (2012). Forebrain GABAergic neuron precursors integrate into adult spinal cord and reduce injury-induced neuropathic pain. Neuron *74*, 663-675.

Briscoe, J., Sussel, L., Serup, P., Hartigan-O'Connor, D., Jessell, T.M., Rubenstein, J.L., and Ericson, J. (1999). Homeobox gene Nkx2.2 and specification of neuronal identity by graded Sonic hedgehog signalling. Nature *398*, 622-627.

Bulfone, A., Puelles, L., Porteus, M.H., Frohman, M.A., Martin, G.R., and Rubenstein, J.L. (1993). Spatially restricted expression of Dlx-1, Dlx-2 (Tes-1), Gbx-2, and Wnt-3 in the embryonic day 12.5 mouse forebrain defines potential transverse and longitudinal segmental boundaries. J Neurosci *13*, 3155-3172.

Butt, S.J., Fuccillo, M., Nery, S., Noctor, S., Kriegstein, A., Corbin, J.G., and Fishell, G. (2005). The temporal and spatial origins of cortical interneurons predict their physiological subtype. Neuron *48*, 591-604.

Butt, S.J., Sousa, V.H., Fuccillo, M.V., Hjerling-Leffler, J., Miyoshi, G., Kimura, S., and Fishell, G. (2008). The requirement of Nkx2-1 in the temporal specification of cortical interneuron subtypes. Neuron *59*, 722-732.

Cahoy, J.D., Emery, B., Kaushal, A., Foo, L.C., Zamanian, J.L., Christopherson, K.S., Xing, Y., Lubischer, J.L., Krieg, P.A., Krupenko, S.A.*, et al.* (2008). A transcriptome database for astrocytes, neurons, and oligodendrocytes: a new resource for understanding brain development and function. J Neurosci *28*, 264-278.

Caputi, A., Rozov, A., Blatow, M., and Monyer, H. (2009). Two calretinin-positive GABAergic cell types in layer 2/3 of the mouse neocortex provide different forms of inhibition. Cereb Cortex *19*, 1345-1359.

Cayre, M., Courtes, S., Martineau, F., Giordano, M., Arnaud, K., Zamaron, A., and Durbec, P. (2013). Netrin 1 contributes to vascular remodeling in the subventricular zone and promotes progenitor emigration after demyelination. Development *140*, 3107-3117.

Chakrabarti, L., Best, T.K., Cramer, N.P., Carney, R.S., Isaac, J.T., Galdzicki, Z., and Haydar, T.F. (2010). Olig1 and Olig2 triplication causes developmental brain defects in Down syndrome. Nat Neurosci *13*, 927-934.

Chang, A., Tourtellotte, W.W., Rudick, R., and Trapp, B.D. (2002). Premyelinating oligodendrocytes in chronic lesions of multiple sclerosis. N Engl J Med *346*, 165-173.

Chapman, H., Waclaw, R.R., Pei, Z., Nakafuku, M., and Campbell, K. (2013). The homeobox gene Gsx2 controls the timing of oligodendroglial fate specification in mouse lateral ganglionic eminence progenitors. Development *140*, 2289-2298.

Charles, P., Hernandez, M.P., Stankoff, B., Aigrot, M.S., Colin, C., Rougon, G., Zalc, B., and Lubetzki, C. (2000). Negative regulation of central nervous system myelination by polysialylated-neural cell adhesion molecule. Proc Natl Acad Sci U S A *97*, 7585-7590.

Chen, B., Dodge, M.E., Tang, W., Lu, J., Ma, Z., Fan, C.W., Wei, S., Hao, W., Kilgore, J., Williams, N.S.*, et al.* (2009a). Small molecule-mediated disruption of Wnt-dependent signaling in tissue regeneration and cancer. Nature chemical biology *5*, 100-107.

Chen, Y., Wu, H., Wang, S., Koito, H., Li, J., Ye, F., Hoang, J., Escobar, S.S., Gow, A., Arnett, H.A.*, et al.* (2009b). The oligodendrocyte-specific G protein-coupled receptor GPR17 is a cell-intrinsic timer of myelination. Nat Neurosci *12*, 1398-1406.

Chong, S.Y., Rosenberg, S.S., Fancy, S.P., Zhao, C., Shen, Y.A., Hahn, A.T., McGee, A.W., Xu, X., Zheng, B., Zhang, L.I.*, et al.* (2012). Neurite outgrowth inhibitor Nogo-A establishes spatial segregation and extent of oligodendrocyte myelination. Proceedings of the National Academy of Sciences of the United States of America *109*, 1299-1304.

Chrast, R., Saher, G., Nave, K.A., and Verheijen, M.H. (2011). Lipid metabolism in myelinating glial cells: lessons from human inherited disorders and mouse models. Journal of lipid research *52*, 419-434.

Corbin, J.G., Nery, S., and Fishell, G. (2001). Telencephalic cells take a tangent: non-radial migration in the mammalian forebrain. Nat Neurosci *4 Suppl*, 1177-1182.

Daneman, R., Agalliu, D., Zhou, L., Kuhnert, F., Kuo, C.J., and Barres, B.A. (2009). Wnt/beta-catenin signaling is required for CNS, but not non-CNS, angiogenesis. Proceedings of the National Academy of Sciences of the United States of America *106*, 641-646.

Davies, A.L., Desai, R.A., Bloomfield, P.S., McIntosh, P.R., Chapple, K.J., Linington, C., Fairless, R., Diem, R., Kasti, M., Murphy, M.P.*, et al.* (2013). Neurological deficits caused by tissue hypoxia in neuroinflammatory disease. Annals of neurology.

Demerens, C., Stankoff, B., Logak, M., Anglade, P., Allinquant, B., Couraud, F., Zalc, B., and Lubetzki, C. (1996). Induction of myelination in the central nervous system by electrical activity. Proc Natl Acad Sci U S A *93*, 9887-9892.

Doerflinger, N.H., Macklin, W.B., and Popko, B. (2003). Inducible site-specific recombination in myelinating cells. Genesis *35*, 63-72.

Dunwoodie, S.L. (2009). The role of hypoxia in development of the Mammalian embryo. Developmental cell *17*, 755-773.

Eastman, Q., and Grosschedl, R. (1999). Regulation of LEF-1/TCF transcription factors by Wnt and other signals. Current opinion in cell biology *11*, 233-240.

Elias, L.A., Potter, G.B., and Kriegstein, A.R. (2008). A time and a place for nkx2-1 in interneuron specification and migration. Neuron *59*, 679-682.

Emery, B., Agalliu, D., Cahoy, J.D., Watkins, T.A., Dugas, J.C., Mulinyawe, S.B., Ibrahim, A., Ligon, K.L., Rowitch, D.H., and Barres, B.A. (2009). Myelin gene regulatory factor is a critical transcriptional regulator required for CNS myelination. Cell *138*, 172-185.

Emery, B., and Dugas, J.C. (2013). Purification of oligodendrocyte lineage cells from mouse cortices by immunopanning. Cold Spring Harbor protocols *2013*, 854-868.

Fagel, D.M., Ganat, Y., Silbereis, J., Ebbitt, T., Stewart, W., Zhang, H., Ment, L.R., and Vaccarino, F.M. (2006). Cortical neurogenesis enhanced by chronic perinatal hypoxia. Experimental neurology *199*, 77-91.

Fancy, S.P., Baranzini, S.E., Zhao, C., Yuk, D.I., Irvine, K.A., Kaing, S., Sanai, N., Franklin, R.J., and Rowitch, D.H. (2009). Dysregulation of the Wnt pathway inhibits timely myelination and remyelination in the mammalian CNS. Genes Dev *23*, 1571-1585.

Fancy, S.P., Harrington, E.P., Yuen, T.J., Silbereis, J.C., Zhao, C., Baranzini, S.E., Bruce, C.C., Otero, J.J., Huang, E.J., Nusse, R.*, et al.* (2011). Axin2 as regulatory and therapeutic target in newborn brain injury and remyelination. Nat Neurosci *14*, 1009-1016.

Fogal, B., McClaskey, C., Yan, S., Yan, H., and Rivkees, S.A. (2010). Diazoxide promotes oligodendrocyte precursor cell proliferation and myelination. PLoS One *5*, e10906.

Fogarty, M., Richardson, W.D., and Kessaris, N. (2005). A subset of oligodendrocytes generated from radial glia in the dorsal spinal cord. Development *132*, 1951-1959.

Foran, D.R., and Peterson, A.C. (1992). Myelin acquisition in the central nervous system of the mouse revealed by an MBP-Lac Z transgene. J Neurosci *12*, 4890-4897.

Forsythe, J.A., Jiang, B.H., Iyer, N.V., Agani, F., Leung, S.W., Koos, R.D., and Semenza, G.L. (1996). Activation of vascular endothelial growth factor gene transcription by hypoxia-inducible factor 1. Mol Cell Biol *16*, 4604-4613.

Franceschini, M.A., Thaker, S., Themelis, G., Krishnamoorthy, K.K., Bortfeld, H., Diamond, S.G., Boas, D.A., Arvin, K., and Grant, P.E. (2007). Assessment of infant brain development with frequency-domain near-infrared spectroscopy. Pediatric research *61*, 546-551.

Freeman, M.R., and Rowitch, D.H. (2013). Evolving concepts of gliogenesis: a look way back and ahead to the next 25 years. Neuron *80*, 613-623.

Freund, T.F., and Buzsaki, G. (1996). Interneurons of the hippocampus. Hippocampus *6*, 347-470.

Fruttiger, M., Karlsson, L., Hall, A.C., Abramsson, A., Calver, A.R., Bostrom, H., Willetts, K., Bertold, C.H., Heath, J.K., Betsholtz, C*., et al.* (1999). Defective oligodendrocyte development and severe hypomyelination in PDGF-A knockout mice. Development *126*, 457-467.

Funfschilling, U., Supplie, L.M., Mahad, D., Boretius, S., Saab, A.S., Edgar, J., Brinkmann, B.G., Kassmann, C.M., Tzvetanova, I.D., Mobius, W*., et al.* (2012). Glycolytic oligodendrocytes maintain myelin and long-term axonal integrity. Nature *485*, 517-521.

Furusho, M., Ono, K., Takebayashi, H., Masahira, N., Kagawa, T., Ikeda, K., and Ikenaka, K. (2006). Involvement of the Olig2 transcription factor in cholinergic neuron development of the basal forebrain. Developmental biology *293*, 348-357.

Ghanem, N., Jarinova, O., Amores, A., Long, Q., Hatch, G., Park, B.K., Rubenstein, J.L., and Ekker, M. (2003). Regulatory roles of conserved intergenic domains in vertebrate Dlx bigene clusters. Genome Res *13*, 533-543.

Ghanem, N., Yu, M., Long, J., Hatch, G., Rubenstein, J.L., and Ekker, M. (2007). Distinct cis-regulatory elements from the Dlx1/Dlx2 locus mark different progenitor cell populations in the ganglionic eminences and different subtypes of adult cortical interneurons. J Neurosci *27*, 5012-5022.

Goldman, J.E., Zerlin, M., Newman, S., Zhang, L., and Gensert, J. (1997). Fate determination and migration of progenitors in the postnatal mammalian CNS. Dev Neurosci *19*, 42-48.

Gomes, W.A., Mehler, M.F., and Kessler, J.A. (2003). Transgenic overexpression of BMP4 increases astroglial and decreases oligodendroglial lineage commitment. Dev Biol *255*, 164-177.

Gonchar, Y., and Burkhalter, A. (1999). Connectivity of GABAergic calretinin-immunoreactive neurons in rat primary visual cortex. Cereb Cortex *9*, 683-696.

Griffiths, I., Klugmann, M., Anderson, T., Yool, D., Thomson, C., Schwab, M.H., Schneider, A., Zimmermann, F., McCulloch, M., Nadon, N*., et al.* (1998). Axonal swellings and degeneration in mice lacking the major proteolipid of myelin. Science *280*, 1610-1613.

Gruber, M., Hu, C.J., Johnson, R.S., Brown, E.J., Keith, B., and Simon, M.C. (2007). Acute postnatal ablation of Hif-2alpha results in anemia. Proc Natl Acad Sci U S A *104*, 2301-2306.

Gyllensten, L., and Malmfors, T. (1963). Myelinization of the optic nerve and its dependence on visual function--a quantitative investigation in mice. Journal of embryology and experimental morphology *11*, 255-266.

Hagberg, H., and Mallard, C. (2005). Effect of inflammation on central nervous system development and vulnerability. Curr Opin Neurol *18*, 117-123.

Hampton, D.W., Rhodes, K.E., Zhao, C., Franklin, R.J., and Fawcett, J.W. (2004). The responses of oligodendrocyte precursor cells, astrocytes and microglia to a cortical stab injury, in the brain. Neuroscience *127*, 813-820.

Harb, R., Whiteus, C., Freitas, C., and Grutzendler, J. (2013). In vivo imaging of cerebral microvascular plasticity from birth to death. Journal of cerebral blood flow and metabolism : official journal of the International Society of Cerebral Blood Flow and Metabolism *33*, 146-156.

Harrington, E.P., Zhao, C., Fancy, S.P., Kaing, S., Franklin, R.J., and Rowitch, D.H. (2010). Oligodendrocyte PTEN is required for myelin and axonal integrity, not remyelination. Annals of neurology *68*, 703-716.

Harris, J.J., and Attwell, D. (2012). The energetics of CNS white matter. J Neurosci *32*, 356-371.

Harris, J.J., and Attwell, D. (2013). Is myelin a mitochondrion? Journal of cerebral blood flow and metabolism : official journal of the International Society of Cerebral Blood Flow and Metabolism *33*, 33-36.

Hartline, D.K., and Colman, D.R. (2007). Rapid conduction and the evolution of giant axons and myelinated fibers. Current biology : CB *17*, R29-35.

Hashimoto, T., Arion, D., Unger, T., Maldonado-Aviles, J.G., Morris, H.M., Volk, D.W., Mirnics, K., and Lewis, D.A. (2008). Alterations in GABA-related transcriptome in the dorsolateral prefrontal cortex of subjects with schizophrenia. Mol Psychiatry *13*, 147-161.

Hashimoto, T., Volk, D.W., Eggan, S.M., Mirnics, K., Pierri, J.N., Sun, Z., Sampson, A.R., and Lewis, D.A. (2003). Gene expression deficits in a subclass of GABA neurons in the prefrontal cortex of subjects with schizophrenia. J Neurosci *23*, 6315-6326.

He, L., and Lu, Q.R. (2013). Coordinated control of oligodendrocyte development by extrinsic and intrinsic signaling cues. Neurosci Bull *29*, 129-143.

He, W., Ingraham, C., Rising, L., Goderie, S., and Temple, S. (2001). Multipotent stem cells from the mouse basal forebrain contribute GABAergic neurons and oligodendrocytes to the cerebral cortex during embryogenesis. J Neurosci *21*, 8854-8862.

He, Y., Dupree, J., Wang, J., Sandoval, J., Li, J., Liu, H., Shi, Y., Nave, K.A., and Casaccia-Bonnefil, P. (2007). The transcription factor Yin Yang 1 is essential for oligodendrocyte progenitor differentiation. Neuron *55*, 217-230.

Hirose, K., Morita, M., Ema, M., Mimura, J., Hamada, H., Fujii, H., Saijo, Y., Gotoh, O., Sogawa, K., and Fujii-Kuriyama, Y. (1996). cDNA cloning and tissue-specific expression of a novel basic helix-loop-helix/PAS factor (Arnt2) with close sequence similarity to the aryl hydrocarbon receptor nuclear translocator (Arnt). Mol Cell Biol *16*, 1706-1713.

Hu, F., and Strittmatter, S.M. (2004). Regulating axon growth within the postnatal central nervous system. Semin Perinatol *28*, 371-378.

Hu, Q.D., Ang, B.T., Karsak, M., Hu, W.P., Cui, X.Y., Duka, T., Takeda, Y., Chia, W., Sankar, N., Ng, Y.K.*, et al.* (2003). F3/contactin acts as a functional ligand for Notch during oligodendrocyte maturation. Cell *115*, 163-175.

Huang, S.M., Mishina, Y.M., Liu, S., Cheung, A., Stegmeier, F., Michaud, G.A., Charlat, O., Wiellette, E., Zhang, Y., Wiessner, S.*, et al.* (2009). Tankyrase inhibition stabilizes axin and antagonizes Wnt signalling. Nature *461*, 614-620.

Huber, O., Korn, R., McLaughlin, J., Ohsugi, M., Herrmann, B.G., and Kemler, R. (1996). Nuclear localization of beta-catenin by interaction with transcription factor LEF-1. Mechanisms of development *59*, 3-10.

Hunt, R.F., Girskis, K.M., Rubenstein, J.L., Alvarez-Buylla, A., and Baraban, S.C. (2013). GABA progenitors grafted into the adult epileptic brain control seizures and abnormal behavior. Nat Neurosci.

Ijichi, A., Sakuma, S., and Tofilon, P.J. (1995). Hypoxia-induced vascular endothelial growth factor expression in normal rat astrocyte cultures. Glia *14*, 87-93.

Ishibashi, T., Dakin, K.A., Stevens, B., Lee, P.R., Kozlov, S.V., Stewart, C.L., and Fields, R.D. (2006). Astrocytes promote myelination in response to electrical impulses. Neuron *49*, 823-832.

Ivan, M., Kondo, K., Yang, H., Kim, W., Valiando, J., Ohh, M., Salic, A., Asara, J.M., Lane, W.S., and Kaelin, W.G., Jr. (2001). HIFalpha targeted for VHL-mediated destruction by proline hydroxylation: implications for O2 sensing. Science *292*, 464-468.

Iyer, N.V., Kotch, L.E., Agani, F., Leung, S.W., Laughner, E., Wenger, R.H., Gassmann, M., Gearhart, J.D., Lawler, A.M., Yu, A.Y.*, et al.* (1998). Cellular and developmental control of O2 homeostasis by hypoxia-inducible factor 1 alpha. Genes Dev *12*, 149-162.

Jaakkola, P., Mole, D.R., Tian, Y.M., Wilson, M.I., Gielbert, J., Gaskell, S.J., von Kriegsheim, A., Hebestreit, H.F., Mukherji, M., Schofield, C.J.*, et al.* (2001). Targeting of HIF-alpha to the von Hippel-Lindau ubiquitylation complex by O2-regulated prolyl hydroxylation. Science *292*, 468-472.

Jablonska, B., Aguirre, A., Raymond, M., Szabo, G., Kitabatake, Y., Sailor, K.A., Ming, G.L., Song, H., and Gallo, V. (2010). Chordin-induced lineage plasticity of adult SVZ neuroblasts after demyelination. Nat Neurosci *13*, 541-550.

Jablonska, B., Scafidi, J., Aguirre, A., Vaccarino, F., Nguyen, V., Borok, E., Horvath, T.L., Rowitch, D.H., and Gallo, V. (2012). Oligodendrocyte regeneration after neonatal hypoxia requires FoxO1-mediated p27Kip1 expression. J Neurosci *32*, 14775-14793.

Jakovcevski, I., Filipovic, R., Mo, Z., Rakic, S., and Zecevic, N. (2009). Oligodendrocyte development and the onset of myelination in the human fetal brain. Frontiers in neuroanatomy *3*, 5.

Jakovcevski, I., and Zecevic, N. (2005). Olig transcription factors are expressed in oligodendrocyte and neuronal cells in human fetal CNS. J Neurosci *25*, 10064-10073.

Jeong, J., Li, X., McEvilly, R.J., Rosenfeld, M.G., Lufkin, T., and Rubenstein, J.L. (2008). Dlx genes pattern mammalian jaw primordium by regulating both lower jaw-specific and upper jaw-specific genetic programs. Development *135*, 2905-2916.

Jiang, F., Frederick, T.J., and Wood, T.L. (2001). IGF-I synergizes with FGF-2 to stimulate oligodendrocyte progenitor entry into the cell cycle. Dev Biol *232*, 414-423.

Jiang, L., Shen, F., Degos, V., Schonemann, M., Pleasure, S.J., Mellon, S.H., Young, W.L., and Su, H. (2011). Oligogenesis and Oligodendrocyte Progenitor Maturation Vary in Different Brain Regions and Partially Correlate with Local Angiogenesis after Ischemic Stroke. Transl Stroke Res *2*, 366-375.

Johnston, M.V., Ferriero, D.M., Vannucci, S.J., and Hagberg, H. (2005). Models of cerebral palsy: which ones are best? J Child Neurol *20*, 984-987.

Kaelin, W.G., Jr., and Ratcliffe, P.J. (2008). Oxygen sensing by metazoans: the central role of the HIF hydroxylase pathway. Molecular cell *30*, 393-402.

Kalanithi, P.S., Zheng, W., Kataoka, Y., DiFiglia, M., Grantz, H., Saper, C.B., Schwartz, M.L., Leckman, J.F., and Vaccarino, F.M. (2005). Altered parvalbumin-positive neuron distribution in basal ganglia of individuals with Tourette syndrome. Proc Natl Acad Sci U S A *102*, 13307-13312.

Kataoka, Y., Kalanithi, P.S., Grantz, H., Schwartz, M.L., Saper, C., Leckman, J.F., and Vaccarino, F.M. (2010). Decreased number of parvalbumin and cholinergic interneurons in the striatum of individuals with Tourette syndrome. J Comp Neurol *518*, 277-291.

Kenney, A.M., and Rowitch, D.H. (2000). Sonic hedgehog promotes G(1) cyclin expression and sustained cell cycle progression in mammalian neuronal precursors. Molecular and cellular biology *20*, 9055-9067.

Kessaris, N., Fogarty, M., Iannarelli, P., Grist, M., Wegner, M., and Richardson, W.D. (2006). Competing waves of oligodendrocytes in the forebrain and postnatal elimination of an embryonic lineage. Nat Neurosci *9*, 173-179.

Khwaja, O., and Volpe, J.J. (2008). Pathogenesis of cerebral white matter injury of prematurity. In Arch Dis Child Fetal Neonatal Ed, pp. F153-161.

Kim, H.M., Hwang, D.H., Choi, J.Y., Park, C.H., Suh-Kim, H., Kim, S.U., and Kim, B.G. (2011). Differential and cooperative actions of Olig1 and Olig2 transcription factors on immature proliferating cells after contusive spinal cord injury. Glia *59*, 1094-1106.

Kim, J.Y., Sun, Q., Oglesbee, M., and Yoon, S.O. (2003). The role of ErbB2 signaling in the onset of terminal differentiation of oligodendrocytes in vivo. J Neurosci *23*, 5561-5571.

Kimura, N., Ueno, M., Nakashima, K., and Taga, T. (1999). A brain region-specific gene product Lhx6.1 interacts with Ldb1 through tandem LIM-domains. J Biochem *126*, 180-187.

Kuhlmann, T., Miron, V., Cui, Q., Wegner, C., Antel, J., and Bruck, W. (2008). Differentiation block of oligodendroglial progenitor cells as a cause for remyelination failure in chronic multiple sclerosis. Brain : a journal of neurology *131*, 1749-1758.

Langosch, D., Hoch, W., and Betz, H. (1992). The 93 kDa protein gephyrin and tubulin associated with the inhibitory glycine receptor are phosphorylated by an endogenous protein kinase. FEBS letters *298*, 113-117.

Langseth, A.J., Munji, R.N., Choe, Y., Huynh, T., Pozniak, C.D., and Pleasure, S.J. (2010). Wnts influence the timing and efficiency of oligodendrocyte precursor cell generation in the telencephalon. J Neurosci *30*, 13367-13372.

Laursen, L.S., and Ffrench-Constant, C. (2007). Adhesion molecules in the regulation of CNS myelination. Neuron glia biology *3*, 367-375.

Le Dreau, G., Garcia-Campmany, L., Rabadan, M.A., Ferronha, T., Tozer, S., Briscoe, J., and Marti, E. (2012). Canonical BMP7 activity is required for the generation of discrete neuronal populations in the dorsal spinal cord. Development *139*, 259-268.

Lee, S., Leach, M.K., Redmond, S.A., Chong, S.Y., Mellon, S.H., Tuck, S.J., Feng, Z.Q., Corey, J.M., and Chan, J.R. (2012a). A culture system to study oligodendrocyte myelination processes using engineered nanofibers. Nat Methods *9*, 917-922.

Lee, S.K., Lee, B., Ruiz, E.C., and Pfaff, S.L. (2005). Olig2 and Ngn2 function in opposition to modulate gene expression in motor neuron progenitor cells. Genes Dev *19*, 282-294.

Lee, Y., Morrison, B.M., Li, Y., Lengacher, S., Farah, M.H., Hoffman, P.N., Liu, Y., Tsingalia, A., Jin, L., Zhang, P.W*., et al.* (2012b). Oligodendroglia metabolically support axons and contribute to neurodegeneration. Nature *487*, 443-448.

Lewis, D.A., Hashimoto, T., and Morris, H.M. (2008). Cell and receptor type-specific alterations in markers of GABA neurotransmission in the prefrontal cortex of subjects with schizophrenia. Neurotox Res *14*, 237-248.

Li, H., Lu, Y., Smith, H.K., and Richardson, W.D. (2007). Olig1 and Sox10 interact synergistically to drive myelin basic protein transcription in oligodendrocytes. J Neurosci *27*, 14375-14382.

Li, H., and Richardson, W.D. (2008). The evolution of Olig genes and their roles in myelination. Neuron glia biology *4*, 129-135.

Liem, K.F., Jr., Tremml, G., and Jessell, T.M. (1997). A role for the roof plate and its resident TGFbeta-related proteins in neuronal patterning in the dorsal spinal cord. Cell *91*, 127-138.

Little, W.J. (1861). On the influence of abnormal parturition, difficult labor, premature birth, and asphyxia neonatorum, on the mental and physical condition of the child, especially in relation to deformities. Transactions of the London Obstetrical Society *3*, 293-344.

Liu, Y., Cox, S.R., Morita, T., and Kourembanas, S. (1995). Hypoxia regulates vascular endothelial growth factor gene expression in endothelial cells. Identification of a 5' enhancer. Circulation research *77*, 638-643.

Long, J.E., Garel, S., Alvarez-Dolado, M., Yoshikawa, K., Osumi, N., Alvarez-Buylla, A., and Rubenstein, J.L. (2007). Dlx-dependent and -independent regulation of olfactory bulb interneuron differentiation. J Neurosci *27*, 3230-3243.

Lu, J., Lian, G., Zhou, H., Esposito, G., Steardo, L., Delli-Bovi, L.C., Hecht, J.L., Lu, Q.R., and Sheen, V. (2012). OLIG2 over-expression impairs proliferation of human Down syndrome neural progenitors. Hum Mol Genet *21*, 2330-2340.

Lu, Q.R., Cai, L., Rowitch, D., Cepko, C.L., and Stiles, C.D. (2001). Ectopic expression of Olig1 promotes oligodendrocyte formation and reduces neuronal survival in developing mouse cortex. Nat Neurosci *4*, 973-974.

Lu, Q.R., Sun, T., Zhu, Z., Ma, N., Garcia, M., Stiles, C.D., and Rowitch, D.H. (2002). Common developmental requirement for Olig function indicates a motor neuron/oligodendrocyte connection. Cell *109*, 75-86.

Lu, Q.R., Yuk, D., Alberta, J.A., Zhu, Z., Pawlitzky, I., Chan, J., McMahon, A.P., Stiles, C.D., and Rowitch, D.H. (2000). Sonic hedgehog--regulated oligodendrocyte lineage genes encoding bHLH proteins in the mammalian central nervous system. Neuron *25*, 317-329.

Maire, C.L., Wegener, A., Kerninon, C., and Nait Oumesmar, B. (2010). Gain-of-function of Olig transcription factors enhances oligodendrogenesis and myelination. Stem cells *28*, 1611-1622.

Majmundar, A.J., Wong, W.J., and Simon, M.C. (2010). Hypoxia-inducible factors and the response to hypoxic stress. Mol Cell *40*, 294-309.

Makinodan, M., Rosen, K.M., Ito, S., and Corfas, G. (2012). A critical period for social experience-dependent oligodendrocyte maturation and myelination. Science *337*, 1357-1360.

Maltepe, E., Schmidt, J.V., Baunoch, D., Bradfield, C.A., and Simon, M.C. (1997). Abnormal angiogenesis and responses to glucose and oxygen deprivation in mice lacking the protein ARNT. Nature *386*, 403-407.

Maricich, S.M., and Herrup, K. (1999). Pax-2 expression defines a subset of GABAergic interneurons and their precursors in the developing murine cerebellum. J Neurobiol *41*, 281-294.

Marin, O. (2012). Brain development: The neuron family tree remodelled. Nature *490*, 185-186.

Maroof, A.M., Keros, S., Tyson, J.A., Ying, S.W., Ganat, Y.M., Merkle, F.T., Liu, B., Goulburn, A., Stanley, E.G., Elefanty, A.G*., et al.* (2013). Directed differentiation and functional maturation of cortical interneurons from human embryonic stem cells. Cell Stem Cell *12*, 559-572.

Martinez-Cerdeno, V., Noctor, S.C., Espinosa, A., Ariza, J., Parker, P., Orasji, S., Daadi, M.M., Bankiewicz, K., Alvarez-Buylla, A., and Kriegstein, A.R. (2010). Embryonic MGE precursor cells grafted into adult rat striatum integrate and ameliorate motor symptoms in 6-OHDA-lesioned rats. Cell Stem Cell *6*, 238-250.

Mazumdar, J., O'Brien, W.T., Johnson, R.S., LaManna, J.C., Chavez, J.C., Klein, P.S., and Simon, M.C. (2010). O2 regulates stem cells through Wnt/beta-catenin signalling. Nature cell biology *12*, 1007-1013.

McKinsey, G.L., Lindtner, S., Trzcinski, B., Visel, A., Pennacchio, L.A., Huylebroeck, D., Higashi, Y., and Rubenstein, J.L. (2013). Dlx1&2-dependent expression of Zfhx1b (Sip1, Zeb2) regulates the fate switch between cortical and striatal interneurons. Neuron *77*, 83-98.

Meijer, D.H., Kane, M.F., Mehta, S., Liu, H., Harrington, E., Taylor, C.M., Stiles, C.D., and Rowitch, D.H. (2012). Separated at birth? The functional and molecular divergence of OLIG1 and OLIG2. Nat Rev Neurosci *13*, 819-831.

Mekki-Dauriac, S., Agius, E., Kan, P., and Cochard, P. (2002). Bone morphogenetic proteins negatively control oligodendrocyte precursor specification in the chick spinal cord. Development *129*, 5117-5130.

Menn, B., Garcia-Verdugo, J.M., Yaschine, C., Gonzalez-Perez, O., Rowitch, D., and Alvarez-Buylla, A. (2006). Origin of oligodendrocytes in the subventricular zone of the adult brain. J Neurosci *26*, 7907-7918.

Ment, L.R., Schwartz, M., Makuch, R.W., and Stewart, W.B. (1998). Association of chronic sublethal hypoxia with ventriculomegaly in the developing rat brain. Brain research Developmental brain research *111*, 197-203.

Mi, S., Miller, R.H., Lee, X., Scott, M.L., Shulag-Morskaya, S., Shao, Z., Chang, J., Thill, G., Levesque, M., Zhang, M.*, et al.* (2005). LINGO-1 negatively regulates myelination by oligodendrocytes. Nat Neurosci *8*, 745-751.

Michailov, G.V., Sereda, M.W., Brinkmann, B.G., Fischer, T.M., Haug, B., Birchmeier, C., Role, L., Lai, C., Schwab, M.H., and Nave, K.A. (2004). Axonal neuregulin-1 regulates myelin sheath thickness. Science *304*, 700-703.

Michaloudi, H., Batzios, C., Grivas, I., Chiotelli, M., and Papadopoulos, G.C. (2006). Developmental changes in the vascular network of the rat visual areas 17, 18 and 18a. Brain Res *1103*, 1-12.

Miyoshi, G., Butt, S.J., Takebayashi, H., and Fishell, G. (2007). Physiologically distinct temporal cohorts of cortical interneurons arise from telencephalic Olig2-expressing precursors. J Neurosci *27*, 7786-7798.

Morrison, B.M., Lee, Y., and Rothstein, J.D. (2013). Oligodendroglia: metabolic supporters of axons. Trends in cell biology.

Mudhar, H.S., Pollock, R.A., Wang, C., Stiles, C.D., and Richardson, W.D. (1993). PDGF and its receptors in the developing rodent retina and optic nerve. Development *118*, 539-552.

Mukhopadhyay, A., McGuire, T., Peng, C.Y., and Kessler, J.A. (2009). Differential effects of BMP signaling on parvalbumin and somatostatin interneuron differentiation. Development *136*, 2633-2642.

Nakamura, T., Colbert, M.C., and Robbins, J. (2006). Neural crest cells retain multipotential characteristics in the developing valves and label the cardiac conduction system. Circulation research *98*, 1547-1554.

Naruse, M., Nakahira, E., Miyata, T., Hitoshi, S., Ikenaka, K., and Bansal, R. (2006). Induction of oligodendrocyte progenitors in dorsal forebrain by intraventricular microinjection of FGF-2. Dev Biol *297*, 262-273.

Nave, K.A. (2010). Myelination and support of axonal integrity by glia. Nature *468*, 244-252.

Nelson, K.B., and Lynch, J.K. (2004). Stroke in newborn infants. Lancet Neurol *3*, 150-158.

Nicholas, C.R., Chen, J., Tang, Y., Southwell, D.G., Chalmers, N., Vogt, D., Arnold, C.M., Chen, Y.J., Stanley, E.G., Elefanty, A.G.*, et al.* (2013). Functional Maturation of hPSC-Derived Forebrain Interneurons Requires an Extended Timeline and Mimics Human Neural Development. Cell Stem Cell *12*, 573-586.

Novitch, B.G., Chen, A.I., and Jessell, T.M. (2001). Coordinate regulation of motor neuron subtype identity and pan-neuronal properties by the bHLH repressor Olig2. Neuron *31*, 773-789.

Ogunshola, O.O., Antic, A., Donoghue, M.J., Fan, S.Y., Kim, H., Stewart, W.B., Madri, J.A., and Ment, L.R. (2002). Paracrine and autocrine functions of neuronal vascular endothelial growth factor (VEGF) in the central nervous system. J Biol Chem *277*, 11410-11415.

Ogunshola, O.O., Stewart, W.B., Mihalcik, V., Solli, T., Madri, J.A., and Ment, L.R. (2000). Neuronal VEGF expression correlates with angiogenesis in postnatal developing rat brain. Brain research Developmental brain research *119*, 139-153.

Ono, K., Takebayashi, H., Ikeda, K., Furusho, M., Nishizawa, T., Watanabe, K., and Ikenaka, K. (2008). Regional- and temporal-dependent changes in the differentiation of Olig2 progenitors in the forebrain, and the impact on astrocyte development in the dorsal pallium. Dev Biol *320*, 456-468.

Park, B.K., Sperber, S.M., Choudhury, A., Ghanem, N., Hatch, G.T., Sharpe, P.T., Thomas, B.L., and Ekker, M. (2004). Intergenic enhancers with distinct activities regulate Dlx gene expression in the mesenchyme of the branchial arches. Dev Biol *268*, 532-545.

Patel, S.A., and Simon, M.C. (2008). Biology of hypoxia-inducible factor-2alpha in development and disease. Cell death and differentiation *15*, 628-634.

Paz Soldan, M.M., and Pirko, I. (2012). Biogenesis and significance of central nervous system myelin. Seminars in neurology *32*, 9-14.

Petryniak, M.A., Potter, G.B., Rowitch, D.H., and Rubenstein, J.L. (2007). Dlx1 and Dlx2 control neuronal versus oligodendroglial cell fate acquisition in the developing forebrain. Neuron *55*, 417-433.

Pham, L.D., Hayakawa, K., Seo, J.H., Nguyen, M.N., Som, A.T., Lee, B.J., Guo, S., Kim, K.W., Lo, E.H., and Arai, K. (2012). Crosstalk between oligodendrocytes and cerebral endothelium contributes to vascular remodeling after white matter injury. Glia *60*, 875-881.

Poitras, L., Ghanem, N., Hatch, G., and Ekker, M. (2007). The proneural determinant MASH1 regulates forebrain Dlx1/2 expression through the I12b intergenic enhancer. Development *134*, 1755-1765.

Porfiri, E., Rubinfeld, B., Albert, I., Hovanes, K., Waterman, M., and Polakis, P. (1997). Induction of a beta-catenin-LEF-1 complex by wnt-1 and transforming mutants of beta-catenin. Oncogene *15*, 2833-2839.

Potter, G.B., Petryniak, M.A., Shevchenko, E., McKinsey, G.L., Ekker, M., and Rubenstein, J.L. (2009). Generation of Cre-transgenic mice using Dlx1/Dlx2 enhancers and their characterization in GABAergic interneurons. Mol Cell Neurosci *40*, 167-186.

Poulopoulos, A., Aramuni, G., Meyer, G., Soykan, T., Hoon, M., Papadopoulos, T., Zhang, M., Paarmann, I., Fuchs, C., Harvey, K.*, et al.* (2009). Neuroligin 2 drives postsynaptic assembly at perisomatic inhibitory synapses through gephyrin and collybistin. Neuron *63*, 628-642.

Pozo, K., and Goda, Y. (2010). Unraveling mechanisms of homeostatic synaptic plasticity. Neuron *66*, 337-351.

Pringle, N., Collarini, E.J., Mosley, M.J., Heldin, C.H., Westermark, B., and Richardson, W.D. (1989). PDGF A chain homodimers drive proliferation of bipotential (O-2A) glial progenitor cells in the developing rat optic nerve. The EMBO journal *8*, 1049-1056.

Prior, P., Schmitt, B., Grenningloh, G., Pribilla, I., Multhaup, G., Beyreuther, K., Maulet, Y., Werner, P., Langosch, D., Kirsch, J.*, et al.* (1992). Primary structure and alternative splice variants of gephyrin, a putative glycine receptor-tubulin linker protein. Neuron *8*, 1161-1170.

Rankin, E.B., Higgins, D.F., Walisser, J.A., Johnson, R.S., Bradfield, C.A., and Haase, V.H. (2005). Inactivation of the arylhydrocarbon receptor nuclear translocator (Arnt) suppresses von Hippel-Lindau disease-associated vascular tumors in mice. Molecular and cellular biology *25*, 3163-3172.

Rankin, E.B., Tomaszewski, J.E., and Haase, V.H. (2006). Renal cyst development in mice with conditional inactivation of the von Hippel-Lindau tumor suppressor. Cancer research *66*, 2576-2583.

Riddle, A., Luo, N.L., Manese, M., Beardsley, D.J., Green, L., Rorvik, D.A., Kelly, K.A., Barlow, C.H., Kelly, J.J., Hohimer, A.R.*, et al.* (2006). Spatial heterogeneity in oligodendrocyte lineage maturation and not cerebral blood flow predicts fetal ovine periventricular white matter injury. J Neurosci *26*, 3045-3055.

Rinholm, J.E., Hamilton, N.B., Kessaris, N., Richardson, W.D., Bergersen, L.H., and Attwell, D. (2011). Regulation of oligodendrocyte development and myelination by glucose and lactate. J Neurosci *31*, 538-548.

Roelink, H., Porter, J.A., Chiang, C., Tanabe, Y., Chang, D.T., Beachy, P.A., and Jessell, T.M. (1995). Floor plate and motor neuron induction by different concentrations of the amino-terminal cleavage product of sonic hedgehog autoproteolysis. Cell *81*, 445-455.

Rosenberg, S.S., Kelland, E.E., Tokar, E., De la Torre, A.R., and Chan, J.R. (2008). The geometric and spatial constraints of the microenvironment induce oligodendrocyte differentiation. Proc Natl Acad Sci U S A *105*, 14662-14667.

Rosenstein, J.M., Krum, J.M., and Ruhrberg, C. (2010). VEGF in the nervous system. Organogenesis *6*, 107-114.

Rowitch, D.H. (2004). Glial specification in the vertebrate neural tube. Nature reviews Neuroscience *5*, 409-419.

Rowitch, D.H., and Kriegstein, A.R. (2010). Developmental genetics of vertebrate glial-cell specification. Nature *468*, 214-222.

Rowitch, D.H., Lu, Q.R., Kessaris, N., and Richardson, W.D. (2002). An 'oligarchy' rules neural development. Trends Neurosci *25*, 417-422.

Rubin, A.N., Alfonsi, F., Humphreys, M.P., Choi, C.K., Rocha, S.F., and Kessaris, N. (2010). The germinal zones of the basal ganglia but not the septum generate GABAergic interneurons for the cortex. J Neurosci *30*, 12050-12062.

Ryan, H.E., Poloni, M., McNulty, W., Elson, D., Gassmann, M., Arbeit, J.M., and Johnson, R.S. (2000). Hypoxia-inducible factor-1alpha is a positive factor in solid tumor growth. Cancer research *60*, 4010-4015.

Saab, A.S., Tzvetanova, I.D., and Nave, K.A. (2013). The role of myelin and oligodendrocytes in axonal energy metabolism. Current opinion in neurobiology *23*, 1065-1072.

Saiepour, L., Fuchs, C., Patrizi, A., Sassoe-Pognetto, M., Harvey, R.J., and Harvey, K. (2010). Complex role of collybistin and gephyrin in GABAA receptor clustering. J Biol Chem *285*, 29623-29631.

Samanta, J., Burke, G.M., McGuire, T., Pisarek, A.J., Mukhopadhyay, A., Mishina, Y., and Kessler, J.A. (2007). BMPR1a signaling determines numbers of oligodendrocytes and calbindin-expressing interneurons in the cortex. J Neurosci *27*, 7397-7407.

Samanta, J., and Kessler, J.A. (2004). Interactions between ID and OLIG proteins mediate the inhibitory effects of BMP4 on oligodendroglial differentiation. Development *131*, 4131-4142.

Sapieha, P. (2012). Eyeing central neurons in vascular growth and reparative angiogenesis. Blood *120*, 2182-2194.

Schuller, U., Kho, A.T., Zhao, Q., Ma, Q., and Rowitch, D.H. (2006). Cerebellar 'transcriptome' reveals cell-type and stage-specific expression during postnatal development and tumorigenesis. Molecular and cellular neurosciences *33*, 247-259.

Scortegagna, M., Ding, K., Oktay, Y., Gaur, A., Thurmond, F., Yan, L.J., Marck, B.T., Matsumoto, A.M., Shelton, J.M., Richardson, J.A.*, et al.* (2003). Multiple organ pathology, metabolic abnormalities and impaired homeostasis of reactive oxygen species in Epas1-/- mice. Nat Genet *35*, 331-340.

Segovia, K.N., McClure, M., Moravec, M., Luo, N.L., Wan, Y., Gong, X., Riddle, A., Craig, A., Struve, J., Sherman, L.S.*, et al.* (2008). Arrested oligodendrocyte lineage maturation in chronic perinatal white matter injury. Annals of neurology *63*, 520-530.

Semenza, G.L. (2012). Hypoxia-inducible factors in physiology and medicine. Cell *148*, 399-408.

Shin, D., Shin, J.Y., McManus, M.T., Ptacek, L.J., and Fu, Y.H. (2009). Dicer ablation in oligodendrocytes provokes neuronal impairment in mice. Annals of neurology *66*, 843-857.

Silbereis, J., Cheng, E., Ganat, Y.M., Ment, L.R., and Vaccarino, F.M. (2009). Precursors with glial fibrillary acidic protein promoter activity transiently generate GABA interneurons in the postnatal cerebellum. Stem Cells *27*, 1152-1163.

Silbereis, J.C., Huang, E.J., Back, S.A., and Rowitch, D.H. (2010). Towards improved animal models of neonatal white matter injury associated with cerebral palsy. Disease models & mechanisms *3*, 678-688.

Skoff, R.P., Ghandour, M.S., and Knapp, P.E. (1994). Postmitotic oligodendrocytes generated during postnatal cerebral development are derived from proliferation of immature oligodendrocytes. Glia *12*, 12-23.

Smith, C.M., Cooksey, E., and Duncan, I.D. (2013). Myelin loss does not lead to axonal degeneration in a long-lived model of chronic demyelination. J Neurosci *33*, 2718-2727.

Southwell, D.G., Froemke, R.C., Alvarez-Buylla, A., Stryker, M.P., and Gandhi, S.P. (2010). Cortical plasticity induced by inhibitory neuron transplantation. Science *327*, 1145-1148.

Southwell, D.G., Paredes, M.F., Galvao, R.P., Jones, D.L., Froemke, R.C., Sebe, J.Y., Alfaro-Cervello, C., Tang, Y., Garcia-Verdugo, J.M., Rubenstein, J.L*., et al.* (2012). Intrinsically determined cell death of developing cortical interneurons. Nature *491*, 109-113.

Stenman, J.M., Rajagopal, J., Carroll, T.J., Ishibashi, M., McMahon, J., and McMahon, A.P. (2008). Canonical Wnt signaling regulates organ-specific assembly and differentiation of CNS vasculature. Science *322*, 1247-1250.

Stevens, B., Porta, S., Haak, L.L., Gallo, V., and Fields, R.D. (2002). Adenosine: a neuron-glial transmitter promoting myelination in the CNS in response to action potentials. Neuron *36*, 855-868.

Stolt, C.C., Schlierf, A., Lommes, P., Hillgartner, S., Werner, T., Kosian, T., Sock, E., Kessaris, N., Richardson, W.D., Lefebvre, V*., et al.* (2006). SoxD proteins influence multiple stages of oligodendrocyte development and modulate SoxE protein function. Developmental cell *11*, 697-709.

Sun, T., Dong, H., Wu, L., Kane, M., Rowitch, D.H., and Stiles, C.D. (2003). Cross-repressive interaction of the Olig2 and Nkx2.2 transcription factors in developing neural tube associated with formation of a specific physical complex. J Neurosci *23*, 9547-9556.

Taglialatela, P., Soria, J.M., Caironi, V., Moiana, A., and Bertuzzi, S. (2004). Compromised generation of GABAergic interneurons in the brains of Vax1-/- mice. Development *131*, 4239-4249.

Tanaka, K., Nogawa, S., Ito, D., Suzuki, S., Dembo, T., Kosakai, A., and Fukuuchi, Y. (2001). Activation of NG2-positive oligodendrocyte progenitor cells during post-ischemic reperfusion in the rat brain. Neuroreport *12*, 2169-2174.

Taniguchi, H., Lu, J., and Huang, Z.J. (2013). The spatial and temporal origin of chandelier cells in mouse neocortex. Science *339*, 70-74.

Tauber, H., Waehneldt, T.V., and Neuhoff, V. (1980). Myelination in rabbit optic nerves is accelerated by artificial eye opening. Neurosci Lett *16*, 235-238.

Tessitore, C., and Brunjes, P.C. (1988). A comparative study of myelination in precocial and altricial murid rodents. Brain Res *471*, 139-147.

Tina, L.G., Frigiola, A., Abella, R., Artale, B., Puleo, G., D'Angelo, S., Musmarra, C., Tagliabue, P., Li Volti, G., Florio, P.*, et al.* (2009). Near Infrared Spectroscopy in healthy preterm and term newborns: correlation with gestational age and standard monitoring parameters. Current neurovascular research *6*, 148-154.

Tomita, S., Ueno, M., Sakamoto, M., Kitahama, Y., Ueki, M., Maekawa, N., Sakamoto, H., Gassmann, M., Kageyama, R., Ueda, N.*, et al.* (2003). Defective brain development in mice lacking the Hif-1alpha gene in neural cells. Molecular and cellular biology *23*, 6739-6749.

Tretter, V., Jacob, T.C., Mukherjee, J., Fritschy, J.M., Pangalos, M.N., and Moss, S.J. (2008). The clustering of GABA(A) receptor subtypes at inhibitory synapses is facilitated via the direct binding of receptor alpha 2 subunits to gephyrin. J Neurosci *28*, 1356-1365.

Tretter, V., Mukherjee, J., Maric, H.M., Schindelin, H., Sieghart, W., and Moss, S.J. (2012). Gephyrin, the enigmatic organizer at GABAergic synapses. Frontiers in cellular neuroscience *6*, 23.

Trollmann, R., and Gassmann, M. (2009). The role of hypoxia-inducible transcription factors in the hypoxic neonatal brain. Brain & development *31*, 503-509.

Turner, C.P., Seli, M., Ment, L., Stewart, W., Yan, H., Johansson, B., Fredholm, B.B., Blackburn, M., and Rivkees, S.A. (2003). A1 adenosine receptors mediate hypoxia-induced ventriculomegaly. Proc Natl Acad Sci U S A *100*, 11718-11722.

Turrigiano, G. (2011). Too many cooks? Intrinsic and synaptic homeostatic mechanisms in cortical circuit refinement. Annual review of neuroscience *34*, 89-103.

Vlachos, A., Reddy-Alla, S., Papadopoulos, T., Deller, T., and Betz, H. (2012). Homeostatic Regulation of Gephyrin Scaffolds and Synaptic Strength at Mature Hippocampal GABAergic Postsynapses. Cereb Cortex.

Volpe, J.J. (2009). Brain injury in premature infants: a complex amalgam of destructive and developmental disturbances. Lancet Neurol *8*, 110-124.

Waclaw, R.R., Allen, Z.J., 2nd, Bell, S.M., Erdelyi, F., Szabo, G., Potter, S.S., and Campbell, K. (2006). The zinc finger transcription factor Sp8 regulates the generation and diversity of olfactory bulb interneurons. Neuron *49*, 503-516.

Wake, H., Lee, P.R., and Fields, R.D. (2011). Control of local protein synthesis and initial events in myelination by action potentials. Science *333*, 1647-1651.

Wang, G.L., Jiang, B.H., Rue, E.A., and Semenza, G.L. (1995). Hypoxia-inducible factor 1 is a basic-helix-loop-helix-PAS heterodimer regulated by cellular O2 tension. Proc Natl Acad Sci U S A *92*, 5510-5514.

Wang, S., Sdrulla, A.D., diSibio, G., Bush, G., Nofziger, D., Hicks, C., Weinmaster, G., and Barres, B.A. (1998). Notch receptor activation inhibits oligodendrocyte differentiation. Neuron *21*, 63-75.

Webster, H.D. (1971). The geometry of peripheral myelin sheaths during their formation and growth in rat sciatic nerves. The Journal of cell biology *48*, 348-367.

Weiss, J., Takizawa, B., McGee, A., Stewart, W.B., Zhang, H., Ment, L., Schwartz, M., and Strittmatter, S. (2004). Neonatal hypoxia suppresses oligodendrocyte Nogo-A and increases axonal sprouting in a rodent model for human prematurity. Experimental neurology *189*, 141-149.

Willert, K., and Nusse, R. (2012). Wnt proteins. Cold Spring Harbor perspectives in biology *4*, a007864.

Wonders, C.P., and Anderson, S.A. (2006). The origin and specification of cortical interneurons. Nature reviews Neuroscience *7*, 687-696.

Wonders, C.P., Taylor, L., Welagen, J., Mbata, I.C., Xiang, J.Z., and Anderson, S.A. (2008). A spatial bias for the origins of interneuron subgroups within the medial ganglionic eminence. Developmental biology *314*, 127-136.

Woodruff, R.H., Tekki-Kessaris, N., Stiles, C.D., Rowitch, D.H., and Richardson, W.D. (2001). Oligodendrocyte development in the spinal cord and telencephalon: common themes and new perspectives. Int J Dev Neurosci *19*, 379-385.

Wu, M., Hernandez, M., Shen, S., Sabo, J.K., Kelkar, D., Wang, J., O'Leary, R., Phillips, G.R., Cate, H.S., and Casaccia, P. (2012). Differential modulation of the oligodendrocyte transcriptome by sonic hedgehog and bone morphogenetic protein 4 via opposing effects on histone acetylation. J Neurosci *32*, 6651-6664.

Xia, X., Lemieux, M.E., Li, W., Carroll, J.S., Brown, M., Liu, X.S., and Kung, A.L. (2009). Integrative analysis of HIF binding and transactivation reveals its role in maintaining histone methylation homeostasis. Proc Natl Acad Sci U S A *106*, 4260-4265.

Xin, M., Yue, T., Ma, Z., Wu, F.F., Gow, A., and Lu, Q.R. (2005). Myelinogenesis and axonal recognition by oligodendrocytes in brain are uncoupled in Olig1-null mice. J Neurosci *25*, 1354-1365.

Ye, F., Chen, Y., Hoang, T., Montgomery, R.L., Zhao, X.H., Bu, H., Hu, T., Taketo, M.M., van Es, J.H., Clevers, H.*, et al.* (2009). HDAC1 and HDAC2 regulate oligodendrocyte differentiation by disrupting the beta-catenin-TCF interaction. Nat Neurosci *12*, 829-838.

Yuen, T.J., Johnson, K.R., Miron, V.E., Zhao, C., Quandt, J., Harrisingh, M.C., Swire, M., Williams, A., McFarland, H.F., Franklin, R.J.*, et al.* (2013). Identification of endothelin 2 as an inflammatory factor that promotes central nervous system remyelination. Brain *136*, 1035-1047.

Zalc, B., Goujet, D., and Colman, D. (2008). The origin of the myelination program in vertebrates. Curr Biol *18*, R511-512.

Zhang, L., and Goldman, J.E. (1996). Generation of cerebellar interneurons from dividing progenitors in white matter. Neuron *16*, 47-54.

Zhong, J., Kim, H.T., Lyu, J., Yoshikawa, K., Nakafuku, M., and Lu, W. (2011). The Wnt receptor Ryk controls specification of GABAergic neurons versus oligodendrocytes during telencephalon development. Development *138*, 409-419.

Zhou, Q., and Anderson, D.J. (2002). The bHLH transcription factors OLIG2 and OLIG1 couple neuronal and glial subtype specification. Cell *109*, 61-73.

Publishing Agreement

It is the policy of the University to encourage the distribution of all theses, dissertations, and manuscripts. Copies of all UCSF theses, dissertations, and manuscripts will be routed to the library via the Graduate Division. The library will make all theses, dissertations, and manuscripts accessible to the public and will preserve these to the best of their abilities, in perpetuity.

Please sign the following statement:

I hereby grant permission to the Graduate Division of the University of California, San Francisco to release copies of my thesis, dissertation, or manuscript to the Campus Library to provide access and preservation, in whole or in part, in perpetuity.

_____   2-19-14
Author Signature   Date